HHS Public Access

Author manuscript

Clin Transl Imaging. Author manuscript; available in PMC 2021 June 01.

Published in final edited form as:

Clin Transl Imaging. 2020 June ; 8(3): 167–206. doi:10.1007/s40336-020-00368-y.

Copper-Mediated Late-stage Radiofluorination: Five Years of Impact on Pre-clinical and Clinical PET Imaging

Jay S. Wright[1], **Tanpreet Kaur**[1], **Sean Preshlock**[1], **Sean S. Tanzey**[1], **Wade P. Winton**[1], **Liam S. Sharninghausen**[2], **Nicholas Wiesner**[1], **Allen F. Brooks**[1], **Melanie S. Sanford**[2], **Peter J. H. Scott**[1]

[1]Department of Radiology, University of Michigan, Ann Arbor, MI 48109, USA.

[2]Department of Chemistry, University of Michigan, Ann Arbor, MI 48109, USA.

Abstract

Purpose—Copper-mediated radiofluorination (CMRF) is emerging as the method of choice for the formation of aromatic C-^{18}F bonds. This minireview examines proof-of-concept, pre-clinical, and in-human imaging studies of new and established imaging agents containing aromatic C-^{18}F bonds synthesized with CMRF. An exhaustive discussion of CMRF methods is not provided, although key developments that have enabled or improved upon the syntheses of fluorine-18 imaging agents are discussed.

Methods—A comprehensive literature search from April 2014 onwards of the Web of Science and PubMed library databases was performed to find reports that utilize CMRF for the synthesis of fluorine-18 radiopharmaceuticals, and these represent the primary body of research discussed in this minireview. Select conference proceedings, previous reports describing alternative methods for the synthesis of imaging agents, and preceding fluorine-19 methodologies have also been included for discussion.

Conclusions—CMRF has significantly expanded the chemical space that is accessible to fluorine-18 radiolabeling with production methods that can meet the regulatory requirements for use in Nuclear Medicine. Furthermore, it has enabled novel and improved syntheses of radiopharmaceuticals and facilitated subsequent PET imaging studies. The rapid adoption of

P. J. H. Scott (pjhscott@umich.edu.) and M. S. Sanford (mssanfor@umich.edu).

Author contributions: All authors participated in literature search, literature review, manuscript writing, manuscript editing and content planning.

Dedication: This article is dedicated to the memory of Dr. Giovanni Lucignani, Editor-in-Chief of *Clinical and Translational Imaging*, who sadly passed away recently. The energy and enthusiasm he brought to this field will be greatly missed. *Ciao, amico mio*.

Conflict of interest

All authors (Jay S. Wright, Tanpreet Kaur, Sean Preshlock, Sean S. Tanzey, Wade P. Winton, Liam S. Sharninghausen, Nicholas Wiesner, Allen F. Brooks, Melanie S. Sanford and Peter J. H. Scott) declare that there is no conflict of interest regarding the publication of this article.

Ethical approval

This review article does not contain any original studies with human or animal subjects performed by any of the authors.

CMRF will undoubtedly continue to simplify the production of imaging agents and inspire the development of new radiofluorination methodologies.

Keywords

Fluorine-18; Positron Emission Tomography; Radiotracer; Radioligand; Copper; Radiofluorination

1.1 Introduction

Positron emission tomography (PET) is a functional nuclear medicine imaging technique[1] that is routinely used to: i) study, diagnose, and stage diseases in a health care setting[2] ii) predict and monitor patient response to (experimental) therapies [3, 4]; iii) enrich clinical trials[5]; and iv) support drug discovery programs in the pharmaceutical industry [6,7]. In PET imaging studies, an animal or clinical subject is injected with a bioactive molecule that has been tagged with a positron-emitting radionuclide (radiopharmaceutical). The PET image is generated via the detection of coincident pairs of 511 keV gamma rays resulting from positron annihilation events, and provides a 3-dimensional image of radiopharmaceutical concentration throughout the body for use by radiologists and scientists in clinical care and research studies.

Fluorine-18 is one of several positron-emitting radionuclides that is used to radiolabel biomolecules for PET imaging because of its excellent imaging properties (97% β+ decay), ready availability in TBq (multi-Curie) amounts from small medical cyclotrons, prevalence of fluorine in bioactive molecules [8], and a convenient half-life (109.8 min) that allows for commercial distribution to satellite imaging centers without a cyclotron.[9] In the production of [^{18}F]fluoride, a proton beam generated by the cyclotron is directed at an [^{18}O]H_2O target, which induces a ^{18}O(p,n)^{18}F nuclear reaction. Typically, the obtained aqueous [^{18}F]fluoride is loaded onto a preconditioned ion exchange resin (e.g. a quaternary methyl ammonium cartridge, QMA), eluted under basic conditions (e.g. K_2CO_3) in the presence of additives (e.g. metal chelators) and azeotropically dried for use in a radiofluorination reaction. Procedures that follow these or closely related steps are generally required in order to facilitate the handling and reactivity of [^{18}F]fluoride, although modern elution procedures with greater applicability to CMRF have been described, and some of these are discussed in this minireview.

Since the introduction of PET in the 1960s and 1970s, extensive work has been undertaken to develop fluorine-18 radiochemistry, with a particular focus on the manufacture of [^{18}F]fluorodeoxyglucose ([^{18}F]FDG), the most widely used PET radiopharmaceutical (Figure 1). However, the generation and translation of new radiofluorination methodologies suitable for labeling some substrate classes in high radiochemical conversion (RCC) and radiochemical yield (RCY) via high molar activity (A_m) [^{18}F]fluoride remains a challenge to radiochemists, particularly electronic-rich aromatic rings. To address these long-standing challenges, the last few years have seen extensive research aimed at developing new fluorine-18 radiochemistry methodology (for recent reviews see: [10–17]). Transition metal-mediated methods have been particularly effective for installing fluorine-18, and many

exciting new developments have been realized since 2014.[18–24] In particular, Cu-mediated radiofluorination (CMRF) has emerged as a powerful technique for construting C-^{18}F bonds. Developments in CMRF have benefited from the availability of synthetic methods that enable the installation of non-radioactive [^{19}F]fluoride into aromatic systems.[25–30] This minireview focuses dicussion on the key applications of fluorine-18 radiofluorination methods, including the Cu-mediated ^{18}F-fluorination of pinacol boronate (Bpin) esters reported by Gouverneur[31], and independent discloures by our laboratories on the Cu-mediated radiofluorination of iodonium salts,[32] aryl halides,[33] boronic acids and Bpin esters,[34] stannanes,[35] and aromatic C-H bonds [36,37]. Since these primary publications, we have further optimized these approaches for use with automated radiochemistry synthesis modules[38] and variants have subsequently been reported by other laboratories that are discussed throughout this review.

In these methodology papers, direct introduction of nucleophilic [^{18}F]fluoride into a variety of (hetero)arenes bearing electron-rich, -neutral, and -withdrawing groups was demonstrated, typically in proof-of-concept studies using small amounts of [^{18}F]fluoride (typically ≤185 MBq or ≤5 mCi). Scalability has also been demonstrated using clinical production levels of [^{18}F]fluoride (typically 74 GBq or ≤ 2 Ci) and automated synthesis modules compatible with current Good Manufacturing Practice (cGMP). However, the true test of a method's utility lies in its ability to both enable the synthesis of previously difficult (or not yet possible) to access PET radiopharmaceuticals and meet routine pre-clinical / clinical production demands.

What is apparent since its introduction in 2014 is that CMRF has been brought online at PET Centers worldwide for the labeling of a wide variety of complex bioactive molecules. It is an attractive approach to radiochemical facilities because, unlike some transition metal-mediated processes, CMRF can generally be conducted without the stringent exclusion of air and/or moisture. Furthermore, late-stage CMRF can offer efficiency and practicality advantages over other labeling methods, such as "prosthetic group" strategies.[39–42] In addition to being widely adopted by the PET radiochemistry community for the synthesis of new PET radiopharmaceuticals for pre-clinical research, CMRF has also been validated for production of clinical PET radiopharmaceutical doses. Products manufactured using CMRF have been translated into clinical trials following regulatory approval by both Health Canada and the Food and Drug Administration (FDA). Herein, we discuss the current state of pre-clinical and clinical radiopharmaceutical synthesis using CMRF. The impact of CMRF on the synthesis of ^{18}F-labeled radiopharmaceuticals in the years since it was introduced is also considered. Chemistry aspects of the new methods have been covered extensively in prior reviews and are therefore discussed only when they pertain to the synthesis of clinically or pharmaceutically relevant imaging agents. Copper-mediated transformations for the installation of ^{18}F[43–49] and other radionuclides such as ^{11}C,[50–57] $^{76/77}$Br,[54,55] $^{123/125/131}$I,[60–62] and ^{211}At[62] into a range of other scaffolds is also possible, although a discussion of these is beyond the scope of this review.

1.2 Copper-Mediated Radiofluorination of Carbon-Halogen Bonds

1.2.1 Iodonium Salts

Aryliodonium salts undergo nucleophilic fluorination in the absence of copper with selectivity for the more sterically congested carbon fragment.[63] However, Sanford and co-workers reported a non-radioactive [^{19}F]fluorination of diaryliodoniums with selectivity for the smaller substituent in the presence of $Cu(OTf)_2$ and KF.[25] Density Functional Theory (DFT) calculations support a mechanism in which $Cu(OTf)_2$ is reduced (either by solvent or by Cu disproportionation) to produce $[Cu(OTf)_2]^-$ (i.e. (Cu(I)), which then undergoes ligand exchange with fluoride). Subsequent oxidative addition of the iodonium salt produces a copper(III) fluoride, which undergoes C-F reductive elimination, furnishing the product and completing the catalytic cycle. A new method describing a copper-catalyzed [^{18}F]fluorination of (mesityl)(aryl)iodonium salts (mesityl = mes = 2,4,6-trimethylphenyl) was reported by our laboratories thereafter.[32] In this radiofluorination, [^{18}F]KF **2** in the presence of $(CH_3CN)_4CuOTf$ was employed in order to access ^{18}F-labeled aryl fluorides. This method was applied to the synthesis of protected 4-[^{18}F]L-fluorophenylalanine **3** (4-[^{18}F]L-FPhA, Scheme 1a), a radiopharmaceutical originally developed in the 1970s as a probe for pancreatic and cerebral protein synthesis [64], and protected 6-[^{18}F]fluoro-L-DOPA ([^{18}F]FDOPA, **5**), used for PET imaging in neuro-oncology,[46,47] Parkinson's disease,[67] and focal hyperinsulinism of infancy.[68]

Modifications to this method have broadened its utility. For example, Neumaier and co-workers applied "minimalist" and "low-base" protocols[69] for the [^{18}F]fluorination of (mesityl)(aryl)iodonium salts. In these methods, [^{18}F]fluoride is eluted using reduced quantities of K_2CO_3 from an ion exchange resin with the molecule to be functionalized (precursor) dissolved in MeOH. It was shown that conventional elution techniques, such as the use of metal chelator additives and azeotropic drying, could be omitted, and only addition of the remaining reagents following the removal of MeOH was required for the subsequent radiofluorination. This protocol was showcased with the synthesis of imaging agents in good radiochemical yields, including [^{18}F]fluorophenylalanines, such as 4-[^{18}F]L-FPhA **7** (Scheme 2a), 6-[^{18}F]fluorodopamine (6-[^{18}F]FDA) **9** (Scheme 2b), and [^{18}F]DAA1106 **11** (Scheme 2c). [^{18}F]DAA1106 was preclinically evaluated in a rat stroke model, demonstrating excellent visualization of translocator protein 18 kDa (TSPO) overexpression associated with neuroinflammation following ischemic stroke.[70] This approach is particularly attractive for use in conjunction with late-stage CMRF since it ameliorates side-reactions of copper with bases (e.g. formation of copper carbonates). An automated radiosynthesis on a Scintomics hot*box*^{three} (HB3) synthesis module of **7** and **11** was subsequently reported under minimalist conditions by the same group.[71]

Other imaging agents have been synthesized using further modifications to this protocol. Neumaier and co-workers developed a new minimalist approach that does not require evaporation of the alcohol used in the elution of [^{18}F]fluoride, and applied it to the radiosynthesis of several isomeric L-phenylalanine ([^{18}F]L-Phe) derivatives using manual and semi-automated conditions (Scheme 3a). The authors proposed that reduced base concentration mitigated the deprotonation and subsequent racemization of iodonium

precursors, affording labeled imaging agents in high enantiomeric excess (ee). Notably, clinical doses of 2-[^{18}F]fluorophenylalanine (2-[^{18}F]Phe) **12b** could be prepared in high RCY, and preliminary PET imaging experiments in mice displayed a higher uptake of this imaging agent in a number of tumor cell lines than [^{18}F]fluoroethyltyrosine ([^{18}F]FET). In addition, a greater metabolic stability of **12b** toward radiodefluorination over isomer **14b** was measured (Scheme 3b).[72]

Despite the availability of modern aryl iodonium syntheses that are applicable to radiochemistry, the synthesis, handling, and storage of the requisite I(III) precursor can in some instances be cumbersome.[73] To simplify precursor synthesis, we developed a method for generating the (mesityl)(aryl)iodonium salts *in situ*.[37] This involves an initial C(sp^2)–H functionalization of an arene with MesI(OH)OTs to form a (mesityl)(aryl)iodonium salt. The applications of this method are discussed in Section 1.6.

Since these initial reports, CMRF of iodonium precursors has been adopted by others for the synthesis of imaging agents. For example, Tsushima and co-workers utilized (mesityl)(aryl)iodonium **19** salt in a CMRF reaction to synthesize [^{18}F]4-fluoro-3-iodobenzyl)guanidine ([^{18}F]FIBG) **20** (Scheme 4a), a potential theranostic agent for the diagnosis and treatment of neuroblastomas and pheochromocytomas.[74] Furthermore, Elie and co-workers developed a radiolabeled indazole **22** for the imaging of inducible isozyme cyclooxygenase-2 (COX-2) inhibitor (Scheme 4b). This enzyme metabolizes arachidonic acid and is overexpressed in a number of cancers. Despite the efficient COX inhibition recorded for the corresponding non-radioactive fluorine-19 analog, it was concluded from PET imaging that this imaging agent possesses low *in vivo* blood-brain barrier (BBB) permeability and low specific binding.[75]

1.2.2 Organohalides

Our laboratories recently described a novel CMRF of (hetero)aryl chlorides, bromides, and iodides using *ortho*-substituted pyridine, oxazoline, and imine DGs.[33] Building on Cu-mediated [^{19}F]fluorination methodology reported by Liu and co-workers,[30] this newly optimized radiofluorination was shown to carry a wider substrate scope and could be conducted using [^{18}F]KF instead of precious metal fluoride [^{19}F]AgF. The use of an N-heterocyclic carbene 1,3-bis-(2,6-diisopropylphenyl)imidazol-2-ylidine (IPr) in this process was critical, and this could be due to rate enhancements that this ligand confers to C-Br oxidative addition at Cu as well as stabilizing effects that reduces Cu dimerization and disproportionation. This method was applied to the synthesis of radiofluorinated analogs vismodegib **23b** (anti-cancer) and PH089 **24b** (MK-2 inhibitor) (Scheme 5).

1.3 Copper-Mediated Radiofluorination of Organoborons

1.3.1 Introduction

With respect to the other strategies discussed in this review, the radiofluorination of organoborons has emerged as the most popular CMRF reaction. Two related methods for the radiofluorodeborylation of (hetero)aromatic boronic acids and Bpin esters have been described by both our laboratories [34] and Gouverneur.[31] Both employ Cu^{II} ligated with

pyridine, either as the preformed [$Cu(OTf)_2(py)_4$] complex (Gouverneur) or an *in situ* variant prepared from Cu(OTf)2 and pyridine (our laboratories), along with [^{18}F]fluoride in DMF with varying substrate and reagent stoichiometries. Gouverneur's system requires a high quantity (60 μmol) of precursor and 5.3 μmol Cu, while a significantly reduced quantity of precursor (4 μmol) can be used in our system with 20 μmol Cu. The seminal publications described the direct, automated syntheses of imaging agents scaffolds, including mGluR5 inhibitor [^{18}F]FPEB **26** (Scott and Sanford, Scheme 5a), TSPO agonist [^{18}F]DAA1106 **11**, protected 6-[^{18}F]fluoro-L-tyrosine (6-[^{18}F]FMT) **27b**, and 6-[^{18}F]fluoro-L-DOPA **28b** (Gouverneur, Scheme 5b). These methods were translated from the non-radioactive ^{19}F fluorination of aryl organoboron compounds using $Cu(OTf)_2$ and KF previously developed by Sanford.[26] In this report, it was proposed that $Cu(OTf)_2$ first undergoes ligand exchange with fluoride to form [Cu(OTf)(F)], which undergoes transmetalation with the precursor to form [Cu(F)(Ar)] (Ar = aryl). This complex subsequently undergoes disproportionation with one equivalent of $Cu(OTf)_2$ to form [Cu(F)(Ar)(OTf)], which then reductively eliminates the labeled product.

Organoboron precursors are attractive because their synthesis has been well-studied in different contexts. In particular, C-B bonds can be installed into aromatic systems from the corresponding C-X (X = F, Cl, Br, I) or C-H bonds with representative (e.g. alkyllithiums) or transition metal-based (e.g. nickel, copper, palladium, iridium) organometallic reagents.[76–82] For example, the synthesis of aryl boronates from fluoroarenes under a dual Ni/Cu catalytic system has recently been reported.[83] Notably, this method has been used in conjunction with CMRF to synthesize fluvastatin (structure not shown) analog **31**. The parent pharmaceutical is an FDA approved antilipemic which treats cardiovascular disease by inhibiting HMG-CoA reductase, reducing plasma cholesterol levels (Scheme 7).

Furthermore, the presence of boronic acids/boronates in organic molecules generally does not pose significant toxicity concerns, simplifying purification in routine production and facilitating compliance with cGMP and Q3D guidance from the International Council for Harmonisation of Technical Requirements for Pharmaceuticals for Human Use.[84] The radiofluorinations exhibit excellent functional group compatibility and are particularly efficient for the labeling of electron-rich arenes, offering complementary electronic selectivity to nucleophilic aromatic substitution (S_NAr) radiofluorinations of electron-deficient aromatics. These attributes have established CMRF of organoborons as state-of-the-art for late-stage radiofluorination, although the approach is not without limitations. For example, despite the reaction tolerating *ortho* alkyl substituents, conversions can be low for heteroatomic *ortho* substituted precursors, including alkoxy, amino, and fluoro groups. Furthermore, the labeling of densely functionalized scaffolds, (such as those prevalent in many drugs and imaging agents) can exhibit poor conversions, and it can be challenging to discern the offending functionality(s). In order to address this, Gouverneur described a study with the aim to "derisk" CMRF of organoborons that investigated reaction efficiency in the presence of different heterocyclic substrates and additives.[85] This further explored the detrimental effect of acidic N-H protons observed in previous reports, and identified heterocycles with comparable or greater performance than pyridine in some cases, including imidazo[1,2-*b*]pyridazine (impy) and isoquinoline (structures not shown), using a model

substrate. Furthermore, it was found that challenging substrates (usually containing multiple basic nitrogen atoms) could be radiolabeled by increasing the ratio of Cu to substrate. Using various direct and multi-step synthesis procedures, seven heterocycle-containing drug scaffolds **32–38a** were successfully radiolabeled by applying these insights (Scheme 8).

1.3.2 Further Developments

Like iodonium precursors, modified condition sets have been disclosed which offer reactivity improvements to some organoboron substrates. As discussed previously, carbonate can be inhibitory to CMRF due to basic sequestration of copper. We initially reduced the concentration of K_2CO_3 by eluting with a 73:1 molar ratio solution of KOTf:K_2CO_3 to mitigate this, and this additionally resulted in excellent ^{18}F fluoride recovery.[34] Later, a modified elution protocol which reduced K_2CO_3 using K_2C2O_4 was adopted by Gouverneur and co-workers.[86] Their enhanced method was showcased with the synthesis of eight clinically relevant imaging agents from free and protected precursors on three different synthesis modules (Scheme 9).

Neumaier and co-workers recorded unexpectedly elevated RCC when trace levels of aliphatic alcohols were introduced into the CMRF following their usage as ^{18}F elutants.[87] While the reasons for this accelerated reactivity are currently unclear, it is speculated that alcohols promote this process by esterifying boronic acids (introduced as precursors or generated *in situ*). Indeed, the most significant conversion enhancements are observed for boronic acid substrates. Alternatively, the authors have suggested that stabilization of the rate limiting B/Cu(III) transmetalation step by hydrogen bonding interactions between alcohol and the organoboron substrate could be responsible for this rate enhancement, rationalizing why other precursors, such as organostannanes, do not appear to benefit from this effect (see Section 1.4).

In contrast to organostannane precursors, most cross-coupling methods that employ organoboron precursors require a basic activator for transmetalation, and it is also possible that the alcoholic additives fulfil an analogous role in CMRF. This alcohol-additive protocol was employed for the synthesis of two tryptophan derivatives **44–45b**, TSPO agonist [^{18}F]F-DPA **46b**, and protected tumor imaging agents 6-[^{18}F]FDA **47b** and 6-[^{18}F]fluoro-L-DOPA **48b** (Scheme 10a). Non-azeotropically dried [^{18}F]fluoride was not required, although it should be noted that a higher substrate quantity (26.5 μmol precursor) is used in alcohol enhanced radiofluorination than in the preceding report by our laboratories (4 μmol precursor). This may contribute to the elevated reactivity of the former system. Later, Neumaier applied a modified alcohol-enhanced CMRF protocol, by replacing nBuOH with MeOH, to the synthesis of 7−[^{18}F]fluorotryptophan **50** (7-[^{18}F]FTrp). The metabolic pathways of tryptophan can be distinctly altered by various diseases (Section 1.3.3), and a proof-of-concept study using xenografts in the chick chorioallantoic membrane model demonstrated a high avidity of **50** in tumor cells relative to free [^{18}F]fluoride. Furthermore, 7-[^{18}F]FTrp displayed a superior resistance to metabolic defluorination over the corresponding 4-, 5-, and 6-radiofluorinated analogs, which was correlated with activity leakage into the bone of healthy rats (Scheme 10b).[88]

We have described elution studies undertaken to improve the synthesis of [^{18}F]4-fluorophenacylbromide **53** ([^{18}F]FPB), a potential PET imaging agent for targeting glycogen synthase kinase-3.[89] Of the organic bases investigated, the use of aqueous *N,N*-dimethylpyridin-4-amine (DMAP) as a cartridge eluent and DMAP as a replacement ligand for copper was found to promote the manual and automated synthesis of intermediate [^{18}F]fluoroacetophenone ([^{18}F]FAP) **52**. DMAP also facilitated the subsequent bromination of **52** to form [^{18}F]4-fluorophenacylbromide **53** ([^{18}F]FBP) in high RCC, which had previously been hampered by pyridine (Scheme 11a). This enabled a fully automated synthesis of **53** to be conducted for the first time. The imaging agent was obtained in 1.5% RCY, and used for preclinical PET imaging of glycogen synthase kinase 3 in rodents and nonhuman primates (NHPs). Other elution studies centered on the role of the ancillary Cu ligand have also been described. For example, Krasikova and co-workers found that extra pyridine improved the radiosynthesis of protected amino acid 4-[^{18}F]L-FPhA **55**, and an optimal pyridine:Cu ratio of 30:1 was established (Scheme 11b).[90]

In analogy to the DMAP elution protocol described by our laboratories, Krasikova and Swenson described the use of an organic solution of dimethylaminopyridinium trifluoromethanesulfonate (DMAPHOTf) in order to elute [^{18}F]fluoride. The delivered DMAPH^{+} behaves as an [^{18}F] counterion and a phase-transfer catalyst (PTC). This elutant was used for the synthesis of racemic 4-[^{18}F]phenylalanine (4-[^{18}F]FPhA) **14c**, and for an improved synthesis of benzodiazepine receptor antagonist [^{18}F]flumazenil **40b** (Scheme 11c&d). In each case, conventional azeotropic drying steps were obviated.[91, 92]

We have also identified order-of-addition as another important variable in CMRF. In particular, the use of pre-dissolved [^{18}F]fluoride is critical for the automated synthesis of [^{18}F]TRACK **58** ([^{18}F]−(±)−IPMICF17).[38] [^{18}F]TRACK targets tropomyosin receptor kinase TrkA/B/C, which is downregulated in neurological disorders such as Alzheimer's disease (AD). Another automated synthesis of [^{18}F]TRACK was reported in improved RCY with alcohol-enhanced radiofluorination (Scheme 12a).[93] Pre-clinical studies, including NHP PET imaging, established good BBB permeability, with the highest regional uptake occurring within TrKB/C-rich gray matter. Later, the first in-human PET study with was conducted, and [^{18}F]TRACK exhibited high pan-Trk selectivity, good metabolic stability, and moderate brain uptake *in vivo* (Scheme 12b).[94] Combined, CMRF of organoborons and the developments discussed in this section have facilitated the radiosynthesis of new (and known) imaging agents that have been employed in preclinical PET imaging studies, and the following sections highlight examples of these.

1.3.3 Oncological Imaging

As previously discussed, fluorine-18 labeled tryptophans are promising agents for imaging the metabolic pathways connected with various diseases. For example, the upregulation of indole- and tryptophan-2,3-dioxygenase (IDO1, TDO2) in the tumor microenvironment is associated with decreased cancer recognition by the immune system. Therefore, these enzymes carry the potential to serve as biomarkers for the development of cancer therapies. Reflecting this, the independent syntheses and preclinical assessments of 5-[^{18}F]L-fluoro-α-methyltryptophan (5-[^{18}F]AMT) **60** and L-5-[^{18}F]fluorotryptophan (5-[^{18}F]Trp) **62** (Scheme

13a&b) have been reported.[95] The association of IDO1 expression with the accumulation of **60** in tumor cell lines has been confirmed using PET, with tumor uptake observable in a B16F10 melanoma model, although it was noted that further confirmation of binding specificity is required. In contrast, the uptake of **62** could not be correlated with IDO1 or TDO2 activity *in vivo*, and this was attributed to competition with endogenous tryptophan and radiotracer metabolism.

Other tumor imaging agents have also been accessed using CMRF of organoborons, including cationic sulfonamide **61**. The imaging agent has shown promising inhibitory activity in preclinical studies with carbonic anhydrase (CA-IX), a surrogate marker for tumor hypoxia. Despite only moderate uptake in HT-29 tumor xenografts, time-activity studies revealed that a lower accumulation occurred in non-target tissues *in vivo*, permitting tumor visualisation by PET (Scheme 14a).[96] Furthermore, [^{18}F]CJ-042794 has been investigated as an antagonist of EP4, a prostanoid receptor that is overexpressed in several forms of cancer (Scheme 14b). PET imaging in mice afforded an acceptable tumor-to-muscle contrast ratio (2.73 ± 0.22, 1 h, n = 5), although no difference between the imaged LNCaP human cell lines at baseline and blocked groups was found (against non-radioactive CJ-042794). This was indicative of non-specific binding that is not due to EP4.[97]

As previously discussed, COX-2 is overexpressed in tumors and may be targeted for cancer imaging. Indazole **22** has been synthesized using CMRF of the corresponding organoboron, in addition to an iodonium salt precursor (Scheme 4) but, as noted in Section 1.2, has limited utility because of low BBB permeability [75]. Triacoxib is a structural relative of the NSAID celecoxib and the labeled analog [^{18}F]triacoxib **68** has been reported by Wuest, and assessed for uptake in colorectal tumor cells (Scheme 15). Notably, CMRF of **67** superseded other synthetic approaches, including SNAr and a prosthetic group strategy. Despite pronounced off-target binding of [^{18}F]triacoxib *in vitro* and *in vivo*, PET imaging in HCA-7 tumor-bearing mice revealed a reduction of uptake when celecoxib was employed as a blocking agent, suggesting specific binding to COX-2.[98]

A fluorine-18 labeled analog of the cancer therapeutic olaparib has been investigated by Gouverneur and co-workers . This drug inhibits poly(ADP-ribose) polymerases (PARP), a family of enzymes with various functions including DNA repair. A correlation between PARP expression and worse outcomes in some tumors has been drawn, suggesting that quantification of enzyme expression could provide a more accurate disease prognosis. To investigate the relationship between DNA damage response and tumor hypoxia, the uptake of [^{18}F]olaparib **71** by PARP has been assessed in a preclinical study. A 70% increase in uptake into PARP-expressing cell lines was recorded following external irradiation of mice PSN-1 xenografts to simulate DNA damage incurred during radiotherapy. A Western Blot study confirmed PARP-1 expression was visibly increased following irradiation (Scheme 16a), and the work showcased the potential of **71** to assess radiation damage and tumor burden.[99] An automated synthesis of **71** was recently described by the same group.[100]

[^{18}F]ABF2 **73** has been developed by Elsinga and co-workers in order to target arginase, an enzyme that is responsible for the metabolism of arginine. Upregulation of arginase is interrelated with a range of pathogenic processes, and PET imaging using **73** has been

conducted in order to study arginase expression in human prostate carcinoma cell lines. Preliminary PET studies in mice displayed tumor uptake *in vivo* which could be moderately suppressed by related inhibitors (Scheme 16b).[101]

1.3.4 Neuroimaging

CMRF of organoborons has also been implemented for the radiosynthesis of agents that image neurological and psychological disorders. For example, Ametamey and co-workers have reported studies on [^{18}F]PF-NB1 **75**, a promising antagonist for GluN2B receptors. These are a subunit of glutamatergic N-methyl-D-aspartate receptors (NMDAR), which are promising targets for the treatment of disorders such as Parkinson's disease (PD), cerebral ischemia, neuropathic pain, and depression, in which overexpression of glutamate can lead to neurotoxic effects. *In vivo* rodent imaging studies with **75** revealed a dose-dependent decrease in avidity with increasing doses of experimental GluN2B antagonist CP-101,606 (Scheme 17a). Notably, this imaging agent was developed following a study by the same group on the structural analog (R)-^{18}F-OF-Me-NB1 **77**, which was used to investigate off-target binding of ^{11}C labeled analogs via blockade studies with eliprodil (Scheme 17b). Combined, these reports showcased the potential of both imaging agents for GluN2B receptor occupancy monitoring.[102, 103]

PD may also be probed using [^{18}F]-2-(4-fluoro-2-(p-tolyloxy)phenyl)-1,2-dihydroisoquinolin-3(4H)-one ([^{18}F]FTPQ, **79**), a radioligand that can quantify TSPO overexpression by the microglia of afflicted subjects. *In vivo* pharmacokinetic data obtained from PET imaging of PD rat brains (induced with oxidopamine) displayed accumulation of **79** in the striatum (Scheme 18a), and longitudinal imaging found that brain uptake of [^{18}F]FTPQ may reflect the severity of PD.[104] TSPO may also be imaged with [^{18}F]N,N-diethyl-2-(4-methoxyphenyl)-5,7-dimethylpyrazolo[1,5-a]pyrimidine-3-acetamide ([^{18}F]-DPA-713, **81**). Preclinical [^{18}F]-DPA-713 PET studies revealed an upregulation of TSPO in microglia/macrophages and astrocytes upon pro-inflammatory stimulation with TNF-inducing adenovirus phenotypes, but no change in TSPO expression during anti-inflammatory stimulation. This could provide insight into the role of pro-inflammatory pathways in neurological disorders (Scheme 18b).[105] The structural analog [^{18}F]F-DPA may also be synthesized with CMRF from the corresponding organoboron [106] and organostannane [107] precursors (see Section 1.4).

Other neuroimaging agents have also been accessed using CMRF of organoborons. The radiolabeled chalcones [^{18}F]4-dimethylamino-4'-fluorochalcone ([^{18}F]DMFC) **83a** and [^{18}F]4-fluoro-4-methylaminochalcone ([^{18}F]FMC) **83b** have been investigated as β-amyloid plaque (Aβ) imaging probes; *in vitro* autoradiography (ARG) studies using postmortem AD human brain sections confirmed colocalization of both agents with Aβ plaques (Scheme 19a).[108]).

Synaptic vesicle glycoprotein 2A (SV2A) is an abundant synaptic protein found in the brains of vertebrates which regulates the release of neurotransmitters. SV2A has been targeted using [^{18}F]SDM-8 **85** in order to quantify *in vivo* synapse density (Scheme 19b). Since this imaging agent was most efficiently synthesized from an organostannane precursor, a discussion on its imaging properties is provided in Section 1.4.[109] The adenosine A_{2A}

receptor ($A_{2A}R$) receptor may also be targeted in order to provide insight into the diagnosis of neurodegenerative (and neurooncological) diseases. CMRF of organoborons **86a** and **86b** was described by Brust, and a preliminary assessment was conducted with *in vitro* ARG using mice brain slices. *ortho*-Fluorinated isomer **87b** was efficiently blocked by its non-radioactive analog and by known $A_{2A}R$ antagonist ZM241385, suggesting specific uptake in the striatum where receptor expression is localized (Scheme 20). Further studies are anticipated to explain the marked difference in brain uptake exhibited by these two isomeric imaging agents.[110]

CMRF can also be used to synthesize imaging agents for psychological disorders. For example, [^{18}F]AZ10419096 **89**, a 5-hydroxytryptamine receptor 1B (5-HT_{1B}) receptor antagonist, has been developed as this subtype of serotonin receptor has been linked with depression and anxiety. Baseline NHP PET studies displayed rapid uptake of **89** into brain regions corresponding to the distribution of 5-HT_{1B} receptors. Pretreatment using AR-A000002 (a 5-HT_{1B} antagonist) led to an 80% decrease in avidity in all regions, suggesting binding of **89** is highly specific (Scheme 21a).[111] Lastly, azaindole **92** may be used as a radioligand for dopamine D_4-receptor subtype, which is implicated in the development of disorders such as schizophrenia. A prosthetic group strategy for the radiosynthesis of this imaging agent was described by Ermert, involving initial synthesis of labeled intermediate **91** (Scheme 21b). Unfortunately, *in vitro* ARG studies using mice brains displayed low specific binding, which was attributed in part to the low A_m (<30 GBq/ μmol) of **92**. This is a problem that can frequently challenge the use of indirect, multi-step labelling strategies.[112]

1.3.5 Myocardial Imaging

CMRF of organoboron precursors has been used to synthesize a number of radiopharmaceuticals for imaging cardiovascular myocardial tissue and associated diseases. For instance, [^{18}F]darapladib **94** has been investigated in order to image lipoprotein-associated phospholipase A2 (Lp-PLA_2), an enzyme associated with atherosclerotic plaques of arterial disease. Initially, an automated synthesis was conducted in a GE TRACERLab FX_{FN} module under vacuum, affording poor (<1%) RCY. The injection of air into the reactor led to an improved RCY of 6%, demonstrating the essential role of O_2 in certain situations and when less equivalents of copper are used. *Ex vivo* imaging showed aortic uptake of the PET imaging agent into apolipoprotein E-deficient (ApoE) or knockout mice (known to develop atherosclerotic plaques). Accumulation of [^{18}F]darapladib was also observed *ex vivo* in the culprit and noncomplicated plaques of human atherosclerotic carotid samples with a ten-fold greater uptake in comparison to [^{18}F]FDG (Scheme 22a).[113]

A direct synthesis of 4−[^{18}F]fluorobenzyltriphenylphosphonium cation ([^{18}F]FBnTP) has been reported from boronate **95**. The synthesis adopted the reaction stoichiometries (i.e. 4 μmol precursor, 20 μmol Cu) described by Scott and Sanford [34], outperforming the related system described by Gouverneur [31], and improving on previous multi-step procedures. [^{18}F]FBnTP is utilized for myocardial imaging and has been investigated in a preclinical mouse study. Dynamic PET imaging produced high contrast images displaying good and

sustained myocardium uptake *in vivo*, shown in the coronal slices centered at the heart apex (Scheme 22b), and corroborated previous findings.[114]

Imaging agents that can probe the pharmacokinetic profile of glycomimetics have also been synthesized with CMRF of organoboron precursors. These compounds resemble endogenous carbohydrates but are structurally altered in order to modulate different properties, such as metabolic stability. Glycomimetics including disaccharide **98** and monosaccharide **100** have been labeled via CMRF and imaged with PET in order to elucidate *in vivo* biodistribution and systemic efficacy. Rodent images displayed rapid excretion of **98** and good uptake of **100** in the blood (characterized by accumulation in the heart) suggesting that the latter imaging agent may be useful in systemic studies (Scheme 23a&b).[115]

1.3.6 Endocrinology Imaging

Type-2 diabetes may be treated with agents such as FDA approved pharmaceutical canagliflozin, which reduces plasma glucose concentration by inhibiting sodium glucose co-transporter 2 (SGLT-2). However, treatment response between patients can be variable, and Attia and co-workers have hypothesized that a correlation between patient response and drug biodistribution may be used to understand this observation. Preliminary studies investigated this by developing an automated radiosynthesis of analog [^{18}F]canagliflozin **102**. Biodistribution was investigated in an ARG study on a human kidney section and selective avidity to SGLT-2 was observed, which could be blocked with excess canagliflozin (Scheme 24). These results warrant further clinical studies in order to ascertain the relationship between patient response and drug biodistribution.[116]

1.3.7 Other Imaging Agents

The production of fluorine-18 containing imaging agents such as **104** (nNOS-inhibitor),[117] protected [^{18}F]-Boc-CM198 **106** (potential 5-HT2A receptor agonist),[118] radiolabeled amino acids including [^{18}F]FMT **43b**,[119] [^{18}F]MDL100907 **109** (5−HT2a receptor ligand),[120] BMS-986205 **111** (IDO1 inhibitor),[121] 5-[^{18}F]fluoro-L-tryptophan **62** (*vide supra*),[122] 6-[^{18}F]fluoro-L-tryptophan **114** (*vide supra*),[123] [^{18}F]2-({2-[(dimethylamino)methyl]phenyl}thio)-5-[^{18}F]fluoroaniline **116** ([^{18}F]ADAM, imaging agent for serotonin transporter),[124] [^{18}F]atorvastatin **118** (dyslipidemia and cardiovascular disease therapeutic),[125] protected 6-[^{18}F]fluoro-L-DOPA **120** (*vide supra*),[126] 4(4-[^{18}F]fluorophenyl)piracetam **122** (potential PD imaging agent),[127, 128] 2-[^{18}F]fluoro-4-boronophenylalanine **124** ([^{18}F]FBPA, *vide supra*),[129] azaindole **126** (Sigma 2 receptor radioligand),[130] and α-amino tetrazole **128**[131] have been studied in the context of synthesis/purification optimization, methodology investigation, and purity quantification. A detailed discussion on the findings of these studies is beyond the scope of this review, although their syntheses are illustrated in Schemes 25, 26, and 27.

1.4 Copper-Mediated Radiofluorination of Organostannanes

Organostannanes are attractive precursors for the formation of aromatic C-[^{18}F]F bonds owing to their good reactivity in CMRF and bench-top stability. Typically, aromatic carbon-tin bonds are conveniently accessed from their corresponding haloarene precursors using a

representative (e.g. organolithium) or transition metal (e.g. Pd) organometallic reagent,[132, 133] and are often intermediates in the synthesis of iodonium salts. Therefore, in some cases the use of organostannanes can offer a more direct alternative for CMRF than the use of iodonium salts. To address challenges such as the low A_m of imaging agents obtained with electrophilic fluorodestannyalation,[134–138] we developed the first Cu-mediated nucleophilic radiofluorination of (hetero)aryl organostannanes using [^{18}F]KF and Cu(OTf)$_2$/pyridine in DMA or DMF.[35] Notably, in several cases ^{18}F fluorodestannylation gives superior performance compared to fluorodeboronation of the analogous boronate precursor. A concurrent report by Murphy described a non-radioactive [^{19}F]fluorination of stannanes under a related condition set. The authors proposed a mechanism for this process that is similar to the fluorination of organoborons described in Section 1.3, with the aryl stannane instead undergoing transmetalation with a putative [Cu(II)(OTf)(F)] intermediate.[27]

The labeling of clinically relevant organostannane precursors, including protected [^{18}F]fluorophenylalanines **129b-c**, protected 6-[^{18}F]fluoro-L-DOPA **130b**, [^{18}F]FPEB **26**, and serotonin radioligand 2′-methoxyphenyl-(N-2′-pyridinyl)-*p*-^{18}F-fluorobenzamidoethylpiperazine ([^{18}F]MPPF) **132b** was conducted using this approach (Scheme 28). Noteworthy is that an automated variant of this method for the synthesis of **132b** outperformed an automated commercial SNAr strategy (Scheme 29a,b).[139] Later, Maurer and co-workers developed a statistical design-of-experiments approach in order to guide optimizations of the methodology, and applied it to the synthesis of [^{18}F]4-fluorobenzylalcohol **132** (4-[^{18}F]BnOH), a precursor to alkyltransferase radioligand [^{18}F]*O*^{6}-[(4-fluoro)benzyl]guanine (Scheme 29c).[140, 141]

The reaction parameters of the CMRF of organostannanes have been investigated by Neumaier and co-workers, who conducted a systematic investigation of radioactivity recovery and fluorine-18 incorporation under various temperatures, solvents, and in the presence of different salts. Among the salts screened, Et_4NHCO_3, Et_4NOTf, $KOTf/K_{222}$, and Bu_4POMs in nBuOH, all improved RCCs. It was also found that CMRF of organostannanes does not receive the same rate enhancement as the CMRF of organoborons in the presence of aliphatic alcohol additives (see also Section 1.3.2). Their approach was used to synthesize 6-[^{18}F]fluoro-L-DOPA **42b**, 6-[^{18}F]FMT **43b**, and 3-O-methyl-6-[^{18}F]FDOPA **135b**, ([^{18}F]F-OMFD), in moderate to excellent RCCs (Scheme 30). Furthermore, pyrazole analog [^{18}F]anle186b **136b**, which binds to pathological protein aggregates in α-synucleinopathies found in prion disease, was synthesized for the first time using this method.[142]

Kirjavainen and co-workers utilized CMRF or organostannanes for the synthesis of exo−3−[(6−[^{18}F]fluoro−2−pyridyl)oxy]8−azabicyclo[3.2.1]octane **138**, ([^{18}F]NS12137) a highly selective norepinephrine transporter (NET) imaging agent (Scheme 31a). NETs maintain reuptake of the neurotransmitters norepinephrine and dopamine, which are associated with many neurogenerative disorders. Notably, the previous methods to access this imaging agent resulted in lower RCYs. Furthermore, tin and copper levels of 0.25 μg were measured in ICP-MS analyses of **138**, permitting the translation of this radiosynthesis to a clinical production method compliant with cGMP.[143]

The same group also developed an alternative CMRF of precursors including organostannanes using $Cu(OTf)_2$ and LiOTf as [^{18}F]fluoride elutants, and obviating the need for azeotropic drying. With this modified protocol, monoamine transporter imaging agent [^{18}F]CFT **140** could be synthesized in an RCY of 6.5% (Scheme 31b).[144] [^{18}F]F-DPA **46b** (see Section 1.3) has been synthesized via CMRF of the corresponding tributyl stannane **138**, and this method offered superior Am to an analogous synthesis using [^{18}F]selectfluor bis(triflate), an electrophilic radiofluorination reagent (Scheme 31c). A 1.5-fold higher uptake of radioactivity in the brains of APP/PS1–21 animals using the high A_m imaging agent was recorded. This was attributed to reduced TSPO blocking due to lower levels of competing nonradioactive F-DPA,[107] and clearly demonstrates the benefits of using high A_m nucleophilic [^{18}F]fluoride over electrophilic methods.

As previously discussed, the synthesis of [^{18}F]SDM-8 **85** has been conducted for the imaging and quantification of SV2A in NHPs and humans (see Section 1.3.4). SV2A is a synaptic protein found in the brain which regulates the release of neurotransmitters, and a reduction of SV2A has recently been correlated with schizophrenia.[145] The radiofluorination of boronates (Scheme 19), iodoniums, and trialkyl tin (Scheme 32a) precursors has been investigated under various conditions, with tin precursor **142** exhibiting the highest reactivity. PET images displayed high uptake in the gray matter of NHP brain, and blocking studies with levetiracetam indicated high specific binding.[109] Recently, the same group conducted a human brain imaging study with **85** and recorded high specific binding, rapid and high uptake, and appropriate tissue kinetics relative to the prototypical SV2A agent [^{11}C]UCB-J (Scheme 32a).[146] Compound **85** (also known as [^{18}F]MNI-1126) has also been synthesized from the stannane using related conditions and imaged in NHP brains.[147]

Lastly, an improved synthesis of 4-(4-[^{18}F]fluorophenyl)piracetam **122** has been described by Osborne and co-workers by replacing organoboron precursor **121** (see Section 1.3.7) with stannane precursor **143** (Scheme 33). This is a fluorine-18 analog of phenylpiracetam, an experimental nootropic stimulant.[148]

1.6 Copper-Mediated Radiofluorination of sp^2 C-H Bonds

Relatively few examples for the direct CMRF of aromatic C-H bonds exist. Non-radioactive fluorobenzene may be produced from the reaction of benzene with CuF_2, which occurs in >95% selectivity. However, the requirement for a large excess of fluoride salt and harsh reaction conditions (450–550 °C) has so far restricted the translation of this method to C-H radiofluorination. Milder fluorination conditions have since been developed by using pre-functionalized (hetero)arenes installed with appropriate directing groups (DG) which can coordinate to Cu, facilitating C-H activation.

For example, azacalix[1]arene[3]pyridines are amenable to regiospecific C-H fluorination through $Cu(ClO_4)_2$-mediated aryl C-H cleavage.[149] Gouverneur has shown that one of these structurally well-defined Cu(III) complexes [150, 151] reacts with carrier added [^{18}F]KF/$K_{2.2.2}$ to reductively eliminate the corresponding ^{18}F-labeled arene.[85] Dauglulis described the oxidative copper-catalyzed auxiliary-assisted C-H [^{19}F]fluorination of arenes

in the presence of AgF.[152] We successfully developed a related method for C-H radiofluorination, and found that [^{18}F]KF outperformed [^{18}F]AgF.[19] A series of analogs **144–147a** of the carboxylic acid containing drug molecules probenecid, ataluren, tamibarotene, and AC261066 containing 8-aminoquinoline (quin) benzamide auxiliaries, were radiolabeled using this method (Scheme 34). Removal of the directing group can be achieved via amide hydrolysis, which was demonstrated in the radiosynthesis of the RARβ2 agonist **147b**.

Finally, CMRF of electron-rich (hetero)aryl C-H bonds has been demonstrated by stepwise C-H functionalization and radiofluorination of activated intermediates. We optimized electrophilic aromatic substitution reaction conditions for the site selective oxidative C-H iodination of aromatics using the electrophilic iodination reagent MesI(OH)OTs **152** in the presence of TMSOTf as an activator. The intermediary (mesityl)(aryl)iodonium salts formed can be used directly without purification as precursors for CMRF under conditions also reported by our laboratories.[32] The addition of iPr_2NEt and quinaldic acid to the post C-H activation Cu-mediated radiolabeling step further improved compatibility with the (mesityl)(aryl)iodonium salt solutions. This two-step strategy was applied to radiolabel benzyl-protected propofol **148b**, a tianeptine fragment **149b**, a *N,N*-dimethyluracil **150b** derivative and *N*-Bn-protected nimesulide **151b** from the corresponding C-H precursors (Scheme 35). As a proof-of-concept, the radiosynthesis of **151b** was automated on a TRACERLab FXFN radiosynthesis module.

Conclusions and Future Perspectives

CMRF permits the late-stage installation of aromatic C-[^{18}F] bonds using iodonium, organoboron, organostannane, C-H, and haloarene precursors. The simplicity and efficiency of these methods has facilitated access to both new and established PET imaging agents that have historically been difficult to synthesize using traditional fluorine-18 radiochemistry. CMRF has been rapidly adopted by the PET radiochemistry community and, as the diverse spectrum of radiotracers showcased in this article demonstrate, the methods are continually being adapted, customized, and optimized in order to synthesize new PET imaging agents. We expect CMRF to continue to expedite access to new fluorine-18 imaging agents, and ultimately accelerate their evaluation and translation for use in clinical care and to support drug discovery. Lastly, the growing use of CMRF to label more diverse chemical space with fluorine-18 will also continue to improve our understanding of functional group tolerance and substrate scope compatibility. These lessons will provide input on what other radiofluorination methods are required to label scaffolds currently incompatible with CMRF, and spur development of such reactions in the future. Reflecting the developments and progresses made in the last five years, such as the recently disclosed protocols for describing the radiosynthesis of [^{18}F]olaparib[100] and 6-[^{18}F]fluoro-L-DOPA [126, 153] for clinical use, CMRF has altered the way that fluorine-18 imaging agents are designed and synthesized for proof-of-concept, pre-clinical, and in-human research studies, and we expect this to continue in the future.

Acknowledgments

Funding: Funding from the National Institutes of Health (R01EB021155 to P.J.H.S and M.S.S; F32GM136022 to L.S.S) is gratefully acknowledged.

5 References

1. Ametamey SM, Honer M, and Schubiger PA (2008) Molecular Imaging with PET. Chem Rev 108:1501–1516. 10.1021/cr0782426 [PubMed: 18426240]
2. Pither R (2003) PET and the role of in vivo molecular imaging in personalized medicine. Expert Rev Mol Diagn 3:703–713. 10.1586/14737159.3.6.703 [PubMed: 14628899]
3. Van Der Veldt AAM, Lubberink M, Greuter HN, Comans EFI, Herder GJM, Yaqub M, Schuit RC, Van Lingen A, Rizvi SN, Mooijer MPJ, Rijnders AY, Windhorst AD, Smit EF, Hendrikse NH, and Lammertsma AA (2011) Absolute Quantification of [^{11}C]docetaxel Kinetics in Lung Cancer Patients using Positron Emission Tomography. Clin Cancer Res 17:4814–4824. 10.1158/1078-0432.CCR-10-2933 [PubMed: 21750197]
4. Avril NE, and Weber WA (2005) Monitoring Response to Treatment in Patients Utilizing PET. Radiol Clin North Am 43:189–204. 10.1016/j.rcl.2004.09.006 [PubMed: 15693656]
5. Sevigny J, Suhy J, Chiao P, Chen T, Klein G, Purcell D, Oh J, Verma A, Sampat M, and Barakos J (2016) Amyloid PET Screening for Enrichment of Early-Stage Alzheimer Disease Clinical Trials: Experience in a Phase 1b Clinical Trial. Alzheimer Dis Assoc Disord 30:1–7. 10.1097/WAD.0000000000000144 [PubMed: 26885819]
6. Matthews PM, Rabiner EA, Passchier J, and Gunn RN (2012) Positron Emission Tomography Molecular Imaging for Drug Development. Br J Clin Pharmacol 73:175–186. 10.1111/j.1365-2125.2011.04085.x [PubMed: 21838787]
7. Elsinga P, van Waarde A, Paans A, and Dierckx R (2012) Trends on the Role of PET in Drug Development. Worldwide Scientific
8. Gillis EP, Eastman KJ, Hill MD, Donnelly DJ, and Meanwell NA (2015) Applications of Fluorine in Medicinal Chemistry. J Med Chem 58:8315–8359. 10.1021/acs.jmedchem.5b00258 [PubMed: 26200936]
9. Ducharme J, Goertzen AL, Patterson J, and Demeter S (2009) Practical Aspects of ^{18}F-FDG PET when Receiving ^{18}F-FDG from a Distant Supplier. J Nucl Med Technol 37:164–169. 10.2967/jnmt.109.062950 [PubMed: 19692456]
10. Deng X, Rong J, Wang L, Vasdev N, Zhang L, Josephson L, and Liang SH (2019) Chemistry for Positron Emission Tomography: Recent Advances in 11C-, 18F-, 13 N-, and 15O-Labeling Reactions. Angew Chemie - Int Ed 58:2580–2605. 10.1002/anie.201805501
11. Brooks AF, Drake LR, Stewart MN, Cary BP, Jackson IM, Mallette D, Mossine AV, and Scott PJH (2016) Fluorine-18 Patents (2009–2015). Part 1: Novel Radiotracers. Pharm Pat Anal 5:17–47. 10.4155/ppa.15.36 [PubMed: 26670619]
12. Mossine AV, Thompson S, Brooks AF, Sowa AR, Miller JM, and Scott PJH (2016) Fluorine-18 Patents (2009–2015). Part 2: New Radiochemistry. Pharm Pat Anal 5:319–349. 10.4155/ppa-2016-0028 [PubMed: 27610753]
13. Brooks AF, Topczewski JJ, Ichiishi N, Sanford MS, and Scott PJH (2014) Late-Stage [18F]Fluorination: New Solutions to Old Problems. Chem Sci 5:4545–4553. 10.1039/C4SC02099E [PubMed: 25379166]
14. Tredwell M, and Gouverneur V (2012) 18F Labeling of Arenes. Angew Chemie - Int Ed 51:11426–11437. 10.1002/anie.201204687
15. Van Der Born D, Pees A, Poot AJ, Orru RVA, Windhorst AD, and Vugts DJ (2017) Fluorine-18 Labelled Building Blocks for PET Tracer Synthesis. Chem Soc Rev 46:4709–4773. 10.1039/c6cs00492j [PubMed: 28608906]
16. Sanford MS, and Scott PJH (2016) Moving Metal-Mediated 18F-fluorination from Concept to Clinic. ACS Cent Sci 2:128–130. 10.1021/acscentsci.6b00061 [PubMed: 27163039]

17. Preshlock S, Tredwell M, and Gouverneur V (2016) ^{18}F-Labeling of Arenes and Heteroarenes for Applications in Positron Emission Tomography. Chem Rev 116:719–766. 10.1021/acs.chemrev.5b00493 [PubMed: 26751274]
18. Thompson S, Lee SJ, Jackson IM, Ichiishi N, Brooks AF, Sanford MS, and Scott PJH (2019) Synthesis of [^{18}F]-γ-Fluoro-α,β-unsaturated Esters and Ketones via Vinylogous ^{18}F-Fluorination of α-Diazoacetates with [^{18} F]AgF. Synth 51:4401–4407. 10.1055/s-0039-1690012
19. Lee SJ, Brooks AF, Ichiishi N, Makaravage KJ, Mossine AV, Sanford MS, and Scott PJH (2019) C–H ^{18}F-Fluorination of 8-Methylquinolines with Ag[^{18}F]F. Chem Commun 55:2976–2979. 10.1039/C9CC00641A
20. Gray EE, Nielsen MK, Choquette KA, Kalow JA, Graham TJA, and Doyle AG (2016) Nucleophilic (Radio)Fluorination of α-Diazocarbonyl Compounds Enabled by Copper-Catalyzed H-F Insertion. J Am Chem Soc 138:10802–10805. 10.1021/jacs.6b06770 [PubMed: 27500313]
21. Beyzavi MH, Mandal D, Strebl MG, Neumann CN, D'Amato EM, Chen J, Hooker JM, Ritter T, D'Amato EM, Chen J, Hooker JM, and Ritter T (2017) ^{18}F-Deoxyfluorination of Phenols via Ru π-Complexes. ACS Cent Sci 3:944–948. 10.1021/acscentsci.7b00195 [PubMed: 28979935]
22. Hoover AJ, Lazari M, Ren H, Narayanam MK, Murphy JM, Van Dam RM, Hooker JM, and Ritter T (2016) A Transmetalation Reaction Enables the Synthesis of [^{18}F]5-Fluorouracil from [^{18}F]Fluoride for Human PET Imaging. Organometallics 35:1008–1014. 10.1021/acs.organomet.6b00059 [PubMed: 27087736]
23. Brandt JR, Lee E, Boursalian GB, and Ritter T (2014) Mechanism of Electrophilic Fluorination with Pd(IV): Fluoride Capture and Subsequent Oxidative Fluoride Transfer. Chem Sci 5:169–179. 10.1039/c3sc52367e
24. Verhoog S, Brooks AF, Winton WP, Viglianti BL, Sanford MS, and Scott PJH (2019) Ring Opening of Epoxides with [^{18}F]FeF Species to Produce [^{18}F]Fluorohydrin PET Imaging Agents. Chem Commun 2–6. 10.1039/C9CC02779C
25. Ichiishi N, Canty AJ, Yates BF, and Sanford MS (2013) Cu-Catalyzed Fluorination of Diaryliodonium Salts with KF. Org Lett 15:5134–5137. 10.1021/ol4025716 [PubMed: 24063629]
26. Ye Y, Schimler SD, Hanley PS, and Sanford MS (2013) Cu(OTf)2-Mediated Fluorination of Aryltrifluoroborates with Potassium Fluoride. J Am Chem Soc 135:16292–16295. 10.1021/ja408607r [PubMed: 24160267]
27. Gamache RF, Waldmann C, and Murphy JM (2016) Copper-Mediated Oxidative Fluorination of Aryl Stannanes with Fluoride. Org Lett 18:4522–4525. 10.1021/acs.orglett.6b02125 [PubMed: 27571319]
28. Fier PS, Luo J, and Hartwig JF (2013) Copper-mediated Fluorination of Arylboronate Esters. Identification of a Copper(III) Fluoride Complex. J Am Chem Soc 135:2552–2559. 10.1021/ja310909q [PubMed: 23384209]
29. Fier PS, and Hartwig JF (2012) Copper-mediated Fluorination of Aryl Iodides. J Am Chem Soc 134:10795–10798. 10.1021/ja304410x [PubMed: 22709145]
30. Mu X, Zhang H, Chen P, and Liu G (2014) Copper-catalyzed Fluorination of 2-pyridyl Aryl Bromides. Chem Sci 5:275–280. 10.1039/c3sc51876k
31. Tredwell M, Preshlock SM, Taylor NJ, Gruber S, Huiban M, Passchier J, Mercier J, Génicot C, and Gouverneur V (2014) A General Copper-Mediated Nucleophilic ^{18}F Fluorination of Arenes. Angew Chemie - Int Ed 53:7751–7755. 10.1002/anie.201404436
32. Ichiishi N, Brooks AF, Topczewski JJ, Rodnick ME, Sanford MS, and Scott PJH (2014) Copper-Catalyzed [^{18}F]Fluorination of (Mesityl)(aryl)iodonium Salts. Org Lett 16:3224–3227. 10.1021/ol501243g [PubMed: 24890658]
33. Sharninghausen LS, Brooks AF, Winton W, Makaravage J, Scott PJH, Sanford MS, Sharninghausen LS, Brooks AF, Winton W, Makaravage KJ, and Scott PJH (2020) NHC-Copper Mediated Ligand-Directed Radiofluorination of Aryl Halides NHC-Copper Mediated Ligand-Directed Radiofluorination of Aryl Halides. Accepted: 10.1021/jacs.0c02637
34. Mossine AV, Brooks AF, Makaravage KJ, Miller JM, Ichiishi N, Sanford MS, and Scott PJHH (2015) Synthesis of [^{18}F]Arenes via the Copper-Mediated [^{18}F]Fluorination of Boronic Acids. Org Lett 17:5780–5783. 10.1021/acs.orglett.5b02875 [PubMed: 26568457]

35. Makaravage KJ, Brooks AF, Mossine AV, Sanford MS, and Scott PJH (2016) Copper-Mediated Radiofluorination of Arylstannanes with [^{18}F]KF. Org Lett 18:5440–5443. 10.1021/acs.orglett.6b02911 [PubMed: 27718581]
36. Lee SJ, Makaravage KJ, Brooks AF, Scott PJH, and Sanford MS (2019) Copper−Mediated Aminoquinoline−Directed Radiofluorination of Aromatic C−H Bonds with K^{18}F. Angew Chemie 131:3151–3154. 10.1002/ange.201812701
37. McCammant MS, Thompson S, Brooks AF, Krska SW, Scott PJH, and Sanford MS (2017) Cu-Mediated C–H ^{18}F-Fluorination of Electron-Rich (Hetero)arenes. Org Lett 19:3939–3942. 10.1021/acs.orglett.7b01902 [PubMed: 28665619]
38. Mossine AV, Brooks AF, Bernard-Gauthier V, Bailey JJ, Ichiishi N, Schirrmacher R, Sanford MS, and Scott PJH (2018) Automated Synthesis of PET Radiotracers by Copper-Mediated ^{18}F-Fluorination of Organoborons: Importance of the Order of Addition and Competing Protodeborylation. J Label Compd Radiopharm 61:228–236. 10.1002/jlcr.3583
39. Jacobson O, Kiesewetter DO, and Chen X (2015) Fluorine-18 Radiochemistry, Labeling Strategies and Synthetic Routes. Bioconjug Chem 26:1–18. 10.1021/bc500475e [PubMed: 25473848]
40. Block D, Coenen HH, and Stacklin G (1988) 18F-Fluoroalkylation of H-Acidic Compounds. J Label Compd Rodiopharmceuticals 1:
41. Kilbourn MR, Dence CS, Welch MJ, and Mathias CJ (1987) Fluorine-18 Labeling of Proteins. J Nucl Med 28:462–471 [PubMed: 3494825]
42. Shai Y, Kirk KL, Channing MA, Dunn BB, Lesniak MA, Eastman RC, Finn RD, Roth J, and Jacobson KA (1989) ^{18}F-Labeled Insulin: A Prosthetic Group Methodology for Incorporation of a Positron Emitter into Peptides and Proteins. Biochemistry 28:4801–4806. 10.1021/bi00437a042 [PubMed: 2669963]
43. Ivashkin P, Lemonnier G, Cousin J, Grégoire V, Labar D, Jubault P, and Pannecoucke X (2014) $CuCF_3$: A [^{18}F]trifluoromethylating Agent for Arylboronic Acids and Aryl Iodides. Chem - A Eur J 20:9514–9518. 10.1002/chem.201403630
44. Rühl T, Rafique W, Lien VT, and Riss PJ (2014) Cu(I)-Mediated 18F-Trifluoromethylation of Arenes: Rapid Synthesis of 18F-Labeled Trifluoromethyl Arenes. Chem Commun 50:6056–6059. 10.1039/C4CC01641F
45. Yang BY, Telu S, Haskali MB, Morse CL, and Pike VW (2019) A Gas Phase Route to [^{18}F]fluoroform with Limited Molar Activity Dilution. Sci Rep 9:1–10. 10.1038/s41598-019-50747-3 [PubMed: 30626917]
46. Vanderborn D, Sewing C, Herscheid JDMKDM, Windhorst AD, Orru RVAA, Vugts DJ, van der Born D, Sewing C, Herscheid JDMKDM, Windhorst AD, Orru RVAA, and Vugts DJ (2014) A Universal Procedure for the [^{18}F]trifluoromethylation of Aryl Iodides and Aryl Boronic acids with Highly Improved Specific Activity. Angew Chemie - Int Ed 53:11046–11050. 10.1002/anie.201406221
47. Zheng J, Cheng R, Lin J-HH, Yu D-HH, Ma L, Jia L, Zhang L, Wang L, Xiao J-CC, and Liang SH (2017) An Unconventional Mechanistic Insight into SCF3 Formation from Difluorocarbene: Preparation of ^{18}F-Labeled α-SCF3 Carbonyl Compounds. Angew Chemie - Int Ed 56:3196–3200. 10.1002/anie.201611761
48. Huiban M, Tredwell M, Mizuta S, Wan Z, Zhang X, Collier TL, Gouverneur V, and Passchier J (2013) A Broadly Applicable [^{18}F]trifluoromethylation of Aryl and Heteroaryl Iodides for PET imaging. Nat Chem 5:941–944. 10.1038/nchem.1756 [PubMed: 24153372]
49. Kim HY, Lee JY, Lee YS, and Jeong JM (2019) Design and Synthesis of Enantiopure 18F-labelled [18F]trifluoromethyltryptophan from 2-halotryptophan Derivatives via Copper(I)-mediated [18F]trifluoromethylation and Evaluation of its in vitro Characterization for the Ser. J Label Compd Radiopharm 62:566–579. 10.1002/jlcr.3772
50. Ponchant M, Hinnen F, Demphel S, and Crouzel C (1997) [11C] Copper(I) Cyanide : A New Radioactive Precursor for 11C-cyanation and Functionalization of Haloarenes. Appl Radiat Isot 48:755–762
51. Makaravage KJ, Shao X, Brooks AF, Yang L, Sanford MS, and Scott PJH (2018) Copper(II)-Mediated [11C]Cyanation of Arylboronic Acids and Arylstannanes. Org Lett 20:1530–1533. 10.1021/acs.orglett.8b00242 [PubMed: 29484880]

52. Rotstein BH, Hooker JM, Woo J, Collier TL, Brady TJ, Liang SH, and Vasdev N (2014) Synthesis of [^{11}C]bexarotene by Cu-mediated [^{11}C]carbon Dioxide Fixation and Preliminary PET Imaging. ACS Med Chem Lett 5:668–672. 10.1021/ml500065q [PubMed: 24944741]
53. Riss PJ, Lu S, Telu S, Aigbirhio FI, and Pike VW (2012) Cu^{I}-Catalyzed ^{11}C Carboxylation of Boronic Acid Esters: A Rapid and Convenient Entry to ^{11}C-labeled Carboxylic Acids, Esters, and Amides. Angew Chemie - Int Ed 51:2698–2702. 10.1002/anie.201107263
54. Yang L, Brooks AF, Makaravage KJ, Zhang H, Sanford MS, Scott PJHH, and Shao X (2018) Radiosynthesis of [^{11}C]LY2795050 for Preclinical and Clinical PET Imaging Using Cu(II)-Mediated Cyanation. ACS Med Chem Lett 9:1274–1279. 10.1021/acsmedchemlett.8b00460 [PubMed: 30613339]
55. Matthews WB, Monn JA, Ravert HT, Holt DP, Schoepp DD, and Dannals RF (2006) Synthesis of a mGluR5 Antagonist using [^{11}C]Copper(I) Cyanide. J Label Compd Radiopharm 49:829–834. 10.1002/jlcr
56. Haskali MB, and Pike VW (2017) [^{11}C]Fluoroform, a Breakthrough for Versatile Labeling of PET Radiotracer Trifluoromethyl Groups in High Molar Activity. Chem - A Eur J 23:8156–8160. 10.1002/chem.201701701
57. Ma L, Placzek MS, Hooker JM, Vasdev N, and Liang SH (2017) Cyanation of Arylboronic Acids in Aqueous Solutions. Chem Commun 53:6597–6600. 10.1039/c7cc02886e
58. Zhou D, Chu W, Voller T, and Katzenellenbogen JA (2018) Copper-mediated Nucleophilic Radiobromination of Aryl Boron Precursors: Convenient Preparation of a Radiobrominated PARP-1 Inhibitor. Tetrahedron Lett 59:1963–1967. 10.1016/j.tetlet.2018.04.024 [PubMed: 30349147]
59. Ordonez AA, Carroll LS, Abhishek S, Mota F, Ruiz-Bedoya CA, Klunk MH, Singh AK, Freundlich JS, Mease RC, and Jain SK (2019) Radiosynthesis and PET Bioimaging of 76Br-Bedaquiline in a Murine Model of Tuberculosis. ACS Infect Dis 5:1996–2002. 10.1021/acsinfecdis.9b00207 [PubMed: 31345032]
60. Zhang P, Zhuang R, Guo Z, Su X, Chen X, and Zhang X (2016) A Highly Efficient Copper-Mediated Radioiodination Approach Using Aryl Boronic Acids. Chem - A Eur J 22:16783–16786. 10.1002/chem.201604105
61. Wilson TC, McSweeney G, Preshlock S, Verhoog S, Tredwell M, Cailly T, and Gouverneur V (2016) Radiosynthesis of SPECT Tracers: via a Copper Mediated 123I Iodination of (hetero)aryl Boron Reagents. Chem Commun 52:13277–13280. 10.1039/c6cc07417k
62. Reilly SW, Makvandi M, Xu K, and Mach RH (2018) Rapid Cu-Catalyzed [^{211}At]Astatination and [^{125}I]Iodination of Boronic Esters at Room Temperature. Org Lett 20:1752–1755. 10.1021/acs.orglett.8b00232 [PubMed: 29561158]
63. Chun J-H, Lu S, Lee Y-S, and Pike VW (2010) Fast and High-Yield Microreactor Syntheses of ortho-Substituted [^{18}F]Fluoroarenes from Reactions of [^{18}F]Fluoride Ion with Diaryliodonium Salts. J Org Chem 75:3332–3338. 10.1021/jo100361d [PubMed: 20361793]
64. Goulding RW, and Palmer AJ (1972) The Preparation of Fluorine-18 Labelled *p*-fluorophenylalanine for Clinical Use. Int J Appl Radiat Isot 23:133–137. 10.1016/0020-708X(72)90085-3 [PubMed: 5015657]
65. Calabria F, and Cascini GL (2015) Current Status of ^{18}F-DOPA PET Imaging. Hell J Nucl Med 18:152–156
66. Nandu H, Wen PY, and Huang RY (2018) Imaging in Neuro-oncology. Ther Adv Neurol Disord 11:1–19. 10.1177/1756286418759865
67. Darcourt J, Schiazza A, Sapin N, Dufour M, Ouvrier M, Benisvy D, X F, and Koulibaly PM (2014) ^{18}F-FDOPA PET for the Diagnosis of Parkinsonian Syndromes. Q J Nucl Med Mol Imaging 58:355–65 [PubMed: 25366711]
68. Shah P, Demirbilek H, and Hussain K (2014) Persistent Hyperinsulinaemic Hypoglycaemia in Infancy. Semin Pediatr Surg 23:76–82. 10.1053/j.sempedsurg.2014.03.005 [PubMed: 24931352]
69. Richarz R, Krapf P, Zarrad F, Urusova EA, Neumaier B, and Zlatopolskiy BD (2014) Neither Azeotropic drying, nor Base nor Other Additives: A Minimalist Approach to ^{18}F-labeling. Org Biomol Chem 12:8094–8099. 10.1039/c4ob01336k [PubMed: 25190038]

70. Zlatopolskiy BD, Zischler J, Krapf P, Zarrad F, Urusova EA, Kordys E, Endepols H, and Neumaier B (2015) Copper-Mediated Aromatic Radiofluorination Revisited: Efficient Production of PET Tracers on a Preparative Scale. Chem - A Eur J 21:5972–5979. 10.1002/chem.201405586
71. Zischler J, Krapf P, Richarz R, Zlatopolskiy BD, and Neumaier B (2016) Automated Synthesis of 4-[18F]fluoroanisole, [18F]DAA1106 and 4-[18F]FPhe using Cu-Mediated Radiofluorination under “Minimalist” Conditions. Appl Radiat Isot 115:133–137. 10.1016/j.apradiso.2016.04.030 [PubMed: 27372807]
72. Modemann DJ, Zlatopolskiy BD, Urusova EA, Zischler J, Craig A, Ermert J, Guliyev M, Endepols H, and Neumaier B (2019) 2-[18F]Fluorophenylalanine: Synthesis by Nucleophilic 18F-Fluorination and Preliminary Biological Evaluation. Synth 51:664–676. 10.1055/s-0037-1611370
73. Yuan Z, Cheng R, Chen P, Liu G, and Liang SH (2016) Efficient Pathway for the Preparation of Aryl(isoquinoline)iodonium(III) Salts and Synthesis of Radiofluorinated Isoquinolines. Angew Chemie Int Ed 55:11882–11886. 10.1002/anie.201606381
74. Yamaguchi A, Hanaoka H, Higuchi T, and Tsushima Y (2018) Radiolabeled (4-fluoro-3-iodobenzyl)guanidine Improves Imaging and Targeted Radionuclide Therapy of Norepinephrine Transporter-Expressing Tumors. J Nucl Med 59:815–821. 10.2967/jnumed.117.201525 [PubMed: 29217738]
75. Elie J, Vercouillie J, Arlicot N, Lemaire L, Bidault R, Bodard S, Hosselet C, Deloye JB, Chalon S, Emond P, Guilloteau D, Buron F, and Routier S (2019) Design of Selective COX-2 Inhibitors in the (aza)indazole series. Chemistry, in vitro Studies, Radiochemistry and Evaluations in Rats of a [18F] PET Tracer. J Enzyme Inhib Med Chem 34:1–7. 10.1080/14756366.2018.1501043
76. Ishiyama T, Takagi J, Ishida K, Miyaura N, Anastasi NR, and Hartwig JF (2002) Mild Iridium-Catalyzed Borylation of Arenes. High Turnover Numbers, Room Temperature Reactions, and Isolation of a Potential Intermediate. J Am Chem Soc 124:390–391. 10.1021/ja0173019 [PubMed: 11792205]
77. Cho J-Y, Tse MK, Holmes D, Maleczka RE, and Smith MR (2002) Remarkably Selective Iridium Catalysts for the Elaboration of Aromatic C-H Bonds. Science (80-) 295:305–308. 10.1126/science.1067074
78. Malapit CA, Bour JR, Laursen SR, and Sanford MS (2019) Mechanism and Scope of Nickel-Catalyzed Decarbonylative Borylation of Carboxylic Acid Fluorides. J Am Chem Soc 141:17322–17330. 10.1021/jacs.9b08961 [PubMed: 31617708]
79. Wulff G, and Lauer M (1983) Arylboronic Acids with Intramolecular B-N Interaction: Convenient Synthesis Through *ortho*-Lithiation of Subsituted Benzylamines. J Organomet Chem 256:1–9
80. Kuehn L, Huang M, Radius U, and Marder TB (2019) Copper-Catalysed Borylation of Aryl Chlorides. Org Biomol Chem 17:6601–6606. 10.1039/c9ob01244c [PubMed: 31225579]
81. Wright JS, Scott PJH, and Steel PG (2020) Iridium Catalysed C-H Borylation of Heteroarenes: Balancing Steric and Electronic Regiocontrol. Angew Chemie Accepted:
82. Ishiyama T, Murata M, and Miyaura N (1995) Palladium(0)-Catalyzed Cross-Coupling Reaction of Alkoxydiboron with Haloarenes: A Direct Procedure for Arylboronic Esters. J Org Chem 60:7508– 7510. 10.1021/jo00128a024
83. Niwa T, Ochiai H, Watanabe Y, and Hosoya T (2015) Ni/Cu-Catalyzed Defluoroborylation of Fluoroarenes for Diverse C-F Bond Functionalizations. J Am Chem Soc 137:14313–14318. 10.1021/jacs.5b10119 [PubMed: 26488683]
84. Teasdale A, and Thompson S (2017) ICH Q3D Elemental Impurities. In: ICH Quality Guidelines: An Implementation Guide. pp 233–280
85. Taylor NJ, Emer E, Preshlock S, Schedler M, Tredwell M, Verhoog S, Mercier J, Genicot C, and Gouverneur V (2017) Derisking the Cu-Mediated ^{18}F-Fluorination of Heterocyclic Positron Emission Tomography Radioligands. J Am Chem Soc 139:8267–8276. 10.1021/jacs.7b03131 [PubMed: 28548849]
86. Preshlock S, Calderwood S, Verhoog S, Tredwell M, Huiban M, Hienzsch A, Gruber S, Wilson TC, Taylor NJ, Cailly T, Schedler M, Collier TL, Passchier J, Smits R, Mollitor J, Hoepping A, Mueller M, Genicot C, Mercier J, and Gouverneur V (2016) Enhanced Copper-Mediated ^{18}F-Fluorination of Aryl Boronic Esters Provides Eight Radiotracers for PET Applications. Chem Commun 52:8361–8364. 10.1039/C6CC03295H

87. Zischler J, Kolks N, Modemann D, Neumaier B, and Zlatopolskiy BD (2017) Alcohol-Enhanced Cu-Mediated Radiofluorination. Chem - A Eur J 23:3251–3256. 10.1002/chem.201604633

88. Zlatopolskiy BD, Zischler J, Schäfer D, Urusova EA, Guliyev M, Bannykh O, Endepols H, and Neumaier B (2018) Discovery of 7-[18F]Fluorotryptophan as a Novel Positron Emission Tomography (PET) Probe for the Visualization of Tryptophan Metabolism in Vivo. J Med Chem 61:189–206. 10.1021/acs.jmedchem.7b01245 [PubMed: 29053271]

89. Mossine AV, Brooks AF, Ichiishi N, Makaravage KJ, Sanford MS, and Scott PJH (2017) Development of Customized [18F] Fluoride Elution Techniques for the Enhancement of Copper-Mediated Late-Stage Radiofluorination. Sci Rep 7:233. 10.1038/s41598-017-00110-1 [PubMed: 28331174]

90. Antuganov D, Zykov M, Timofeeva K, Antuganova Y, Orlovskaya V, and Krasikova R (2017) Effect of Pyridine Addition on the Efficiency of Copper-Mediated Radiofluorination of Aryl Pinacol Boronates. ChemistrySelect 2:7909–7912. 10.1002/slct.201701628

91. Antuganov D, Zykov M, Timofeev V, Timofeeva K, Antuganova Y, Orlovskaya V, Fedorova O, and Krasikova R (2019) Copper-Mediated Radiofluorination of Aryl Pinacolboronate Esters: A Straightforward Protocol by Using Pyridinium Sulfonates. European J Org Chem 2019:918–922. 10.1002/ejoc.201801514

92. Zhang X, Basuli F, and Swenson RE (2019) An Azeotropic Drying-Free Approach for Copper-Mediated Radiofluorination without Addition of Base. J Label Compd Radiopharm 62:139–145. 10.1002/jlcr.3705

93. Bernard-Gauthier V, Mossine AV, Mahringer A, Aliaga A, Bailey JJ, Shao X, Stauff J, Arteaga J, Sherman P, Grand'Maison M, Rochon P-LL, Wängler B, Wängler C, Bartenstein P, Kostikov A, Kaplan DR, Fricker G, Rosa-Neto P, Scott PJHH, Schirrmacher R, Grand'Maison M, Rochon P-LL, Wängler B, Wängler C, Bartenstein P, Kostikov A, Kaplan DR, Fricker G, Rosa-Neto P, Scott PJHH, and Schirrmacher R (2018) Identification of [18F]TRACK, a Fluorine-18-Labeled Tropomyosin Receptor Kinase (Trk) Inhibitor for PET Imaging. J Med Chem 61:1737–1743. 10.1021/acs.jmedchem.7b01607 [PubMed: 29257860]

94. Bailey JJ, Kaiser L, Lindner S, Wüst M, Thiel A, Soucy JP, Rosa-Neto P, Scott PJH, Unterrainer M, Kaplan DR, Wängler C, Wängler B, Bartenstein P, Bernard-Gauthier V, and Schirrmacher R (2019) First-in-Human Brain Imaging of [18F]TRACK, a PET tracer for Tropomyosin Receptor Kinases. ACS Chem Neurosci 10:2697–2702. 10.1021/acschemneuro.9b00144 [PubMed: 31017386]

95. Giglio BC, Fei H, Wang M, Wang H, He L, Feng H, Wu Z, Lu H, and Li Z (2017) Synthesis of 5-[^{18}F]fluoro-alpha-methyl Tryptophan: New Trp Based PET Agents. Theranostics 7:1524–1530. 10.7150/thno.19371 [PubMed: 28529635]

96. Zhang Z, Lau J, Zhang C, Colpo N, Nocentini A, Supuran CT, Bénard F, and Lin KS (2017) Design, Synthesis and Evaluation of 18F-labeled Cationic Carbonic Anhydrase IX Inhibitors for PET Imaging. J Enzyme Inhib Med Chem 32:722–730. 10.1080/14756366.2017.1308928 [PubMed: 28385087]

97. Zhang Z, Lau J, Kuo HT, Zhang C, Colpo N, Bénard F, and Lin KS (2017) Synthesis and Evaluation of ^{18}F-labeled CJ-042794 for Imaging Prostanoid EP4 Receptor Expression in Cancer with Positron Emission Tomography. Bioorganic Med Chem Lett 27:2094–2098. 10.1016/j.bmcl.2017.03.078

98. Litchfield M, Wuest M, Glubrecht D, and Wuest F (2020) Radiosynthesis and Biological Evaluation of [^{18}F]Triacoxib: A New Radiotracer for PET Imaging of COX-2. Mol Pharm 17:251–261. 10.1021/acs.molpharmaceut.9b00986 [PubMed: 31816246]

99. Wilson TC, Xavier MA, Knight J, Verhoog S, Torres JB, Mosley M, Hopkins SL, Wallington S, Allen PD, Kersemans V, Hueting R, Smart S, Gouverneur V, and Cornelissen B (2019) PET Imaging of PARP Expression using 18F-olaparib. J Nucl Med 60:504–510. 10.2967/jnumed.118.213223 [PubMed: 30389822]

100. Guibbal F, Isenegger PG, Wilson TC, Pacelli A, Mahaut D, Sap JBI, Taylor NJ, Verhoog S, Preshlock S, Hueting R, Cornelissen B, and Gouverneur V (2020) Manual and automated Cu-mediated radiosynthesis of the PARP inhibitor [18F]olaparib. Nat Protoc ASAP. 10.1038/s41596-020-0295-7

101. Clemente GS, Antunes I, Kurade S, Waarde A Van, Dömling A, and Elsinga PH (2019) Synthesis and Preliminary Preclinical Evaluation of a 18F-fluorinated Quaternary Alpha-Amino Acid-Based Arginase Inhibitor. J Label Compd Radiopharm, 62(Suppl 1):p S214.
102. Haider A, Iten I, Ahmed H, Herde AM, Gruber S, Krämer SD, Keller C, Schibli R, Wünsch B, Mu L, and Ametamey SM (2019) Identification and Preclinical Evaluation of a Radiofluorinated Benzazepine Derivative for Imaging the GluN2B Subunit of the Ionotropic NMDA Receptor. J Nucl Med 60:259–266. 10.2967/jnumed.118.212134
103. Ahmed H, Haider A, Varisco J, Stanković M, Wallimann R, Gruber S, Iten I, Häne S, Müller Herde A, Keller C, Schibli R, Schepmann D, Mu L, Wünsch B, and Ametamey SM (2019) Structure-Affinity Relationships of 2,3,4,5-Tetrahydro-1 H-3-benzazepine and 6,7,8,9-Tetrahydro-5 H-benzo[7]annulen-7-amine Analogues and the Discovery of a Radiofluorinated 2,3,4,5-Tetrahydro-1 H-3-benzazepine Congener for Imaging GluN2B Subunit-Containi. J Med Chem. 10.1021/acs.jmedchem.9b00812
104. Wu CY, Chen YY, Lin JJ, Li JP, Chen JK, Hsieh TC, and Kao CH (2019) Development of a Novel Radioligand for Imaging 18-kD Translocator Protein (TSPO) in a Rat Model of Parkinson's Disease. BMC Med Imaging 19:1–9. 10.1186/s12880-019-0375-8 [PubMed: 30611240]
105. Pannell M, Economopoulos V, Wilson TC, Kersemans V, Isenegger PG, Larkin JR, Smart S, Gilchrist S, Gouverneur V, and Sibson NR (2020) Imaging of Translocator Protein Upregulation is Selective for Pro-Inflammatory Polarized Astrocytes and Microglia. Glia 68:280–297. 10.1002/glia.23716 [PubMed: 31479168]
106. Keller T, Krzyczmonik A, Forsback S, Kirjavainen A, López-Picón FR, Takkinen JS, Dollé F, Rinne JO, Haaparanta-Solin M, and Solin O (2017) Nucleophilic and Electrophilic Syntheses of [18F]F-DPA. J Label Compd Radiopharm, 62(Suppl 1):p S423.
107. Keller T, López-Picón FR, Krzyczmonik A, Forsback S, Takkinen JS, Rajander J, Teperi S, Dollé F, Rinne JO, Haaparanta-Solin M, and Solin O (2019) Comparison of High and Low Molar Activity TSPO Tracer [^{18}F]F-DPA in a Mouse Model of Alzheimer's Disease. J Cereb Blood Flow Metab. 10.1177/0271678X19853117
108. Kaide S, Ono M, Watanabe H, Shimizu Y, Nakamoto Y, Togashi K, Yamaguchi A, Hanaoka H, and Saji H (2018) Conversion of Iodine to Fluorine-18 Based on Iodinated Chalcone and Evaluation for β-Amyloid PET Imaging. Bioorganic Med Chem 26:3352–3358. 10.1016/j.bmc.2018.05.001
109. Li S, Cai Z, Wu X, Holden D, Pracitto R, Kapinos M, Gao H, Labaree D, Nabulsi N, Carson RE, and Huang Y (2019) Synthesis and in vivo Evaluation of a Novel PET Radiotracer for Imaging of Synaptic Vesicle Glycoprotein 2A (SV2A) in Nonhuman Primates. ACS Chem Neurosci 10:1544–1554. 10.1021/acschemneuro.8b00526 [PubMed: 30396272]
110. Lai TH, Schroeder S, Ludwig F-A, Fischer S, Moldovan R, Scheunemann M, Dukic-Stefanovic S, Deuther-Conrad W, Steinbach J, and Brust P (2019) Development of High Affinity 18F-labelled Radiotracers for PET Imaging of the Adenosine A2A Receptor. J Label Compd Radiopharm, 62(Suppl 1):p S23.
111. Lindberg A, Nag S, Schou M, Arakawa R, Nogami T, Moein MM, Elmore CS, Pike VW, and Halldin C (2019) Development of a 18F-labeled PET Radioligand for Imaging 5-HT1B Receptors: [18F]AZ10419096. Nucl Med Biol 78–79:11–16. 10.1016/j.nucmedbio.2019.10.003
112. Willmann M, Neumaier B, and Johannes Ermert (2019) A Novel 18F-labeled D4-receptor Ligand. J Label Compd Radiopharm, 62(Suppl 1): pp S410–S411.
113. Guibbal F, Meneyrol V, Ait-Arsa I, Diotel N, Patché J, Veeren B, Bénard S, Gimié F, Yong-Sang J, Khantalin I, Veerapen R, Jestin E, and Meilhac O (2019) Synthesis and Automated Labeling of [18F]Darapladib, a Lp-PLA 2 Ligand, as Potential PET Imaging Tool of Atherosclerosis. ACS Med Chem Lett 10:743–748. 10.1021/acsmedchemlett.8b00643 [PubMed: 31097993]
114. Zhang Z, Zhang C, Lau J, Colpo N, Bénard F, and Lin K-S (2016) One-Step Synthesis of 4-[^{18}F]Fluorobenzyltriphenylphosphonium Cation for Imaging with Positron Emission Tomography. J Label Compd Radiopharm 59:467–471. 10.1002/jlcr.3436
115. Bratteby K, Torkelsson E, L'Estrade ET, Peterson K, Shalgunov V, Xiong M, Leffler H, Zetterberg FR, Olsson TG, Gillings N, Nilsson UJ, Herth MM, and Erlandsson M (2020) In Vivo Veritas: 18F-Radiolabeled Glycomimetics Allow Insights into the Pharmacological Fate of Galectin-3 Inhibitors. J Med Chem. 10.1021/acs.jmedchem.9b01692

116. Attia K, Visser T, Steven J, Slart R, Antunes I, van der Hoek S, Elsinga PH, and Heerspink H (2019) Synthesis and Evaluation of [18F]Canagliflozin for Imaging SGLT-2-transporters in Diabetic Patients. J Label Compd Radiopharm, 62(Suppl 1):p S27.

117. Drerup C, Ermert J, and Coenen HH (2016) Synthesis of a Potent Aminopyridine-based nNOS-inhibitor by Two Recent No-Carrier-Added 18F-labelling Methods. Molecules 21:. 10.3390/molecules21091160

118. Petersen IN, Kristensen JL, and Herth MM (2017) Nucleophilic ^{18}F-Labeling of Spirocyclic Iodonium Ylide or Boronic Pinacol Ester Precursors: Advantages and Disadvantages. European J Org Chem 2017:453–458. 10.1002/ejoc.201601448

119. Craig A, Kolks N, Urusova E, Zischler J, Neumaier B, and Zlatopolskiy BD (2019) The Efficient Preparation of Radiolabeled Aromatic Amino Acids via Cu-Mediated Radiofluorination of Ni-Complexes. J Label Compd Radiopharm, 62(Suppl 1):p S118.

120. Zhang X, Dunlow R, Blackman BN, and Swenson RE (2018) Optimization of ^{18}F-Syntheses using ^{19}F-Reagents at Tracer-Level Concentrations and Liquid Chromatography/Tandem Mass Spectrometry Analysis: Improved Synthesis of [^{18}F]MDL100907. J Label Compd Radiopharm 61:427–437. 10.1002/jlcr.3606

121. Cole E, Donnelly D, Wallace M, Tran T, Burrell R, Turley W, Allentoff A, Huang A, Balog A, and Bonacorsi S (2018) Radiochemistry Challenges and Progression for Incorporation of ^{18}F into a Complex Substituted 6-^{18}F-Fluoroquinoline BMS-986205 for IDO Imaging. In: The Journal of Nuclear Medicine

122. Schäfer D, Zlatopolskiy BD, Johannes Ermert, and Neumaier B (2017) A Practical Two-Step Synthesis of 5-[^{18}F]fluoro-L-tryptophan (5-[18F]FTrp) via Alcohol-Enhanced Cu-Mediated Radiofluorination. J Label Compd Radiopharm, 60(Suppl 1): p S105.

123. Schäfer D, Weiß P, Ermert J, Castillo Meleán J, Zarrad F, and Neumaier B (2016) Preparation of No-Carrier-Added 6-[^{18}F]Fluoro-l-tryptophan via Cu-Mediated Radiofluorination. European J Org Chem 2016:4621–4628. 10.1002/ejoc.201600705

124. Milicevic Sephton S, Zhou X, Thompson S, and Aigbirhio FI (2019) Preparation of the Serotonin Transporter PET Radiotracer 2-({2-[(Dimethylamino)methyl]phenyl}thio)-5-[18F]fluoroaniline (4-[18F]ADAM): Probing Synthetic and Radiosynthetic Methods. Synth 51:4374–4384. 10.1055/s-0039-1690522

125. Clemente GS, Zarganes-tzitzikas T, Dömling A, and Elsinga PH (2019) Late-Stage Copper-Catalyzed Radiofluorination of an Arylboronic Ester Derivative of Atorvastatin. Molecules 24:4210– 4218. 10.3390/molecules24234210

126. Mossine AV, Tanzey SS, Brooks AF, Makaravage KJ, Ichiishi N, Miller JM, Henderson BD, Skaddan MB, Sanford MS, and Scott PJH (2019) One-Pot Synthesis of High Molar Activity 6-[18F]fluoro-l-DOPA by Cu-Mediated Fluorination of a Bpin Precursor. Org Biomol Chem 17:8701– 8705. 10.1039/c9ob01758e [PubMed: 31536095]

127. Blevins DW, Kabalka GW, Osborne DR, and Akula MR (2018) Effect of Added Cu(OTf)2 on the Cu(OTf)2(Py)4-Mediated Radiofluorination of Benzoyl and Phthaloylglycinates. Nat Sci 10:125–133. 10.4236/ns.2018.103013

128. Blevins DW, Akula MR, Kabalka GW, and Osborne DR (2017) Synthesis of 4(4-[18F]Fluorophenyl)piracetam, a Potential PET Agent for Parkinson's Disease. In: 22nd International Symposium on Radiopharmaceutical Sciences. p S256

129. Honda N, Yoshimoto M, Mizukawa Y, Katsuhiko O, Kanai Y, Kurihara H, Tateishi H, and Takahashi K (2017) Radiosynthesis of 2-[^{18}F]Fluoro-4-boronophenylalanine ([^{18}F]FBPA using Copper Mediated Oxidative Aromatic Nucleophilic [^{18}F]Fluorination. In: 22nd International Symposium on Radiopharmaceutical Sciences. p S512

130. Ludwig F-A, Fischer S, Moldovan R, Deuther-Conrad W, Kranz M, Schepmann D, Jia H, Wünsch B, and Brust P (2019) Development of a New 18F-labeled Radioligand for Imaging Sigma2 Receptors by Positron Emission Tomography. J Label Compd Radiopharm, 62(Suppl 1):pp S181– S182

131. Zarganes-Tzitzikas T, Clemente GS, Elsinga PH, and Dömling A (2019) MCR Scaffolds get Hotter with 18F-Labeling. Molecules 24:1–15. 10.3390/molecules24071327

132. Gribanov PS, Golenko YD, Topchiy MA, Minaeva LI, Asachenko AF, and Nechaev MS (2018) Stannylation of Aryl Halides, Stille Cross-Coupling, and One-Pot, Two-Step Stannylation/Stille Cross-Coupling Reactions under Solvent-Free Conditions. European J Org Chem 2018:120–125. 10.1002/ejoc.201701463

133. Gilman H, and Rosenberg SD (1953) Reaction of Triphenyltin-Lithium with Organic Halides. J Org Chem 18:680–685. 10.1021/jo01134a012

134. Furuya T, Strom AE, and Ritter T (2009) Silver-Mediated Fluorination of Functionalized Aryl Stannanes. J Am Chem Soc 131:1662–1663. 10.1021/ja8086664 [PubMed: 19191693]

135. Teare H, Robins EG, Kirjavainen A, Forsback S, Sandford G, Solin O, Luthra SK, and Gouverneur V (2010) Radiosynthesis and Evaluation of [18F]Selectfluor bis(triflate). Angew Chemie - Int Ed 49:6821–6824. 10.1002/anie.201002310

136. Adam MJ, Pate BD, Ruth TJ, Berry JM, and Hall LD (1981) Cleavage of Aryl-Tin Bonds with Elemental Fluorine: Rapid Synthesis of [^{18}F]Fluorobenzene. J Chem Soc Chem Commun 733. 10.1039/C39810000733

137. Eskola O, Grönroos T, Bergman J, Haaparanta M, Marjamäki P, Lehikoinen P, Forsback S, Langer O, Hinnen F, Dollé F, Halldin C, and Solin O (2004) A Novel Electrophilic Synthesis and Evaluation of Medium Specific Radioactivity (1R,2S)-4-[18F]fluorometaraminol, a Tracer for the Assessment of Cardiac Sympathetic Nerve Integrity with PET. Nucl Med Biol 31:103–110. 10.1016/S0969-8051(03)00098-2 [PubMed: 14741575]

138. Ye Y, and Sanford MS (2013) Mild Copper-Mediated Fluorination of Aryl Stannanes and Aryl Trifluoroborates. J Am Chem Soc 135:9. 10.1021/ja400300g

139. Alvarez M, and Le Bars D (2012) Synthesis of 4−(2′−Methoxyphenyl)−1−[2′−(N−2″Pyridinyl)−p−[18F]Fluorobenzamido]Ethylpiperazine [18F]MPPF. In: Radiochemical Syntheses. John Wiley & Sons, Ltd, p 87–94

140. Bowden GD, Franke A, Pichler BJ, and Maurer A (2019) Automated Synthesis of [18F]O6-[(4-[18F]fluoro)benzyl]guanine ([18F]pFBG) via [18F]-fluorobenzyl Alcohol ([18F]4FBnOH) from an Optimized Copper Mediated Radiofluorination (CMRF). J Label Compd Radiopharm, 62(Suppl 1): pp S329–330

141. Bowden GD, Pichler BJ, and Maurer A (2019) A Design of Experiments (DoE) Approach Accelerates the Optimization of Copper-Mediated 18F-Fluorination Reactions of Arylstannanes. Sci Rep 9:1–10. 10.1038/s41598-019-47846-6 [PubMed: 30626917]

142. Zarrad F, Zlatopolskiy B, Krapf P, Zischler J, and Neumaier B (2017) A Practical Method for the Preparation of 18F-Labeled Aromatic Amino Acids from Nucleophilic [18F]Fluoride and Stannyl Precursors for Electrophilic Radiohalogenation. Molecules 22:2231. 10.3390/molecules22122231

143. Lahdenpohja S, Keller T, Rajander J, and Kirjavainen AK (2019) Radiosynthesis of the Norepinephrine Transporter Tracer [^{18}F]NS12137 via Copper-Mediated ^{18}F-labelling. J Label Compd Radiopharm 62:259–264. 10.1002/jlcr.3717

144. Lahdenpohja SO, Rajala NA, Rajander J, and Kirjavainen AK (2019) Fast and Efficient Copper-Mediated 18F-fluorination of Arylstannanes, Aryl Boronic Acids, and Aryl Boronic Esters without Azeotropic Drying. EJNMMI Radiopharm Chem 4:. 10.1186/s41181-019-0079-y

145. Onwordi EC, Halff EF, Whitehurst T, Mansur A, Cotel MC, Wells L, Creeney H, Bonsall D, Rogdaki M, Shatalina E, Reis Marques T, Rabiner EA, Gunn RN, Natesan S, Vernon AC, and Howes OD (2020) Synaptic Density Marker SV2A is Reduced in Schizophrenia Patients and Unaffected by Antipsychotics in Rats. Nat Commun 11:. 10.1038/s41467-019-14122-0

146. Li S, Naganawa M, Zheng M, Pracitto R, Henry S, Matuskey D, Kapinos M, Emery P, Cai Z, Ropchan J, Labaree D, Nabulsi N, Carson R, and Huang Y (2019) First-In-Human Evaluation of ^{18}F-SDM-8, A Novel Radiotracer for PET Imaging of Synaptic Vesicle Glycoprotein 2A. J Nucl Med 60:49

147. Constantinescu CC, Tresse C, Zheng MQ, Gouasmat A, Carroll VM, Mistico L, Alagille D, Sandiego CM, Papin C, Marek K, Seibyl JP, Tamagnan GD, and Barret O (2019) Development and In Vivo Preclinical Imaging of Fluorine-18-Labeled Synaptic Vesicle Protein 2A (SV2A) PET Tracers. Mol Imaging Biol 21:509–518. 10.1007/s11307-018-1260-5 [PubMed: 30084043]

148. Blevins DW, Akula MR, Kabalka GW, and Osborne DR (2019) An Improved Synthesis of 4-(4-[18F]fluorophenyl)pircetam a PET Agent for Parkinson's Disease. J Label Compd Radiopharm, 62(Suppl 1):p S171.

149. Yao B, Wang ZL, Zhang H, Wang DX, Zhao L, and Wang MX (2012) Cu(ClO4)2-mediated Arene C-H Bond Halogenations of Azacalixaromatics Using Alkali Metal Halides as Halogen Sources. J Org Chem 77:3336–3340. 10.1021/jo300152u [PubMed: 22420606]

150. Yao B, Wang DX, Huang ZT, and Wang MX (2009) Room Temperature Aerobic Formation of a Stable Aryl-Cu(III) Complex and its Reactions with Nucleophiles: Highly Efficient and Diverse Arene C-H Functionalizations of Azacalix[1]arene[3]pyridine. Chem Commun 2899–2901. 10.1039/b902946j

151. Zhang H, Yao B, Zhao L, Wang DX, Xu BQ, and Wang MX (2014) Direct Synthesis of High-Valent Aryl-Cu(II) and Aryl-Cu(III) Compounds: Mechanistic Insight into Arene C-H Bond Metalation. J Am Chem Soc 136:6326–6332. 10.1021/ja412615h [PubMed: 24730979]

152. Truong T, Klimovica K, and Daugulis O (2013) Copper-Catalyzed, Directing Group-Assisted Fluorination of Arene and Heteroarene C–H Bonds. J Am Chem Soc 135:9342–9345. 10.1021/ja4047125 [PubMed: 23758609]

153. Mossine A, Tanzey S, Brooks A, Makaravage K, Ichiishi N, Miller J, Henderson B, Erhard T, Bruetting C, Skaddan M, Sanford M, and Scott P (2020) Synthesis of High Molar Activity [18F]6-Fluoro-L-DOPA Suitable for Human Use by Cu-Mediated Fluorination of a BPin Precursor. Nat Protoc doi: 10.1038/s41596-020-0305-9.

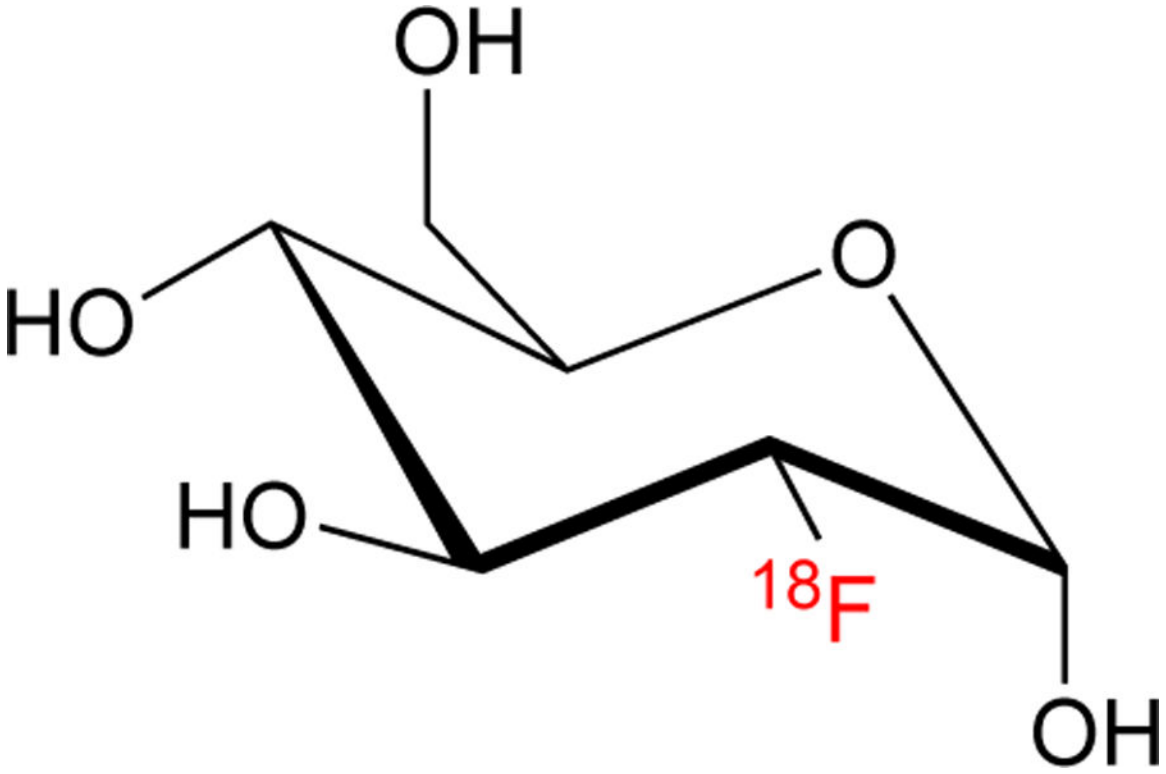

Figure 1:
[^{18}F]Fluorodeoxyglucose.

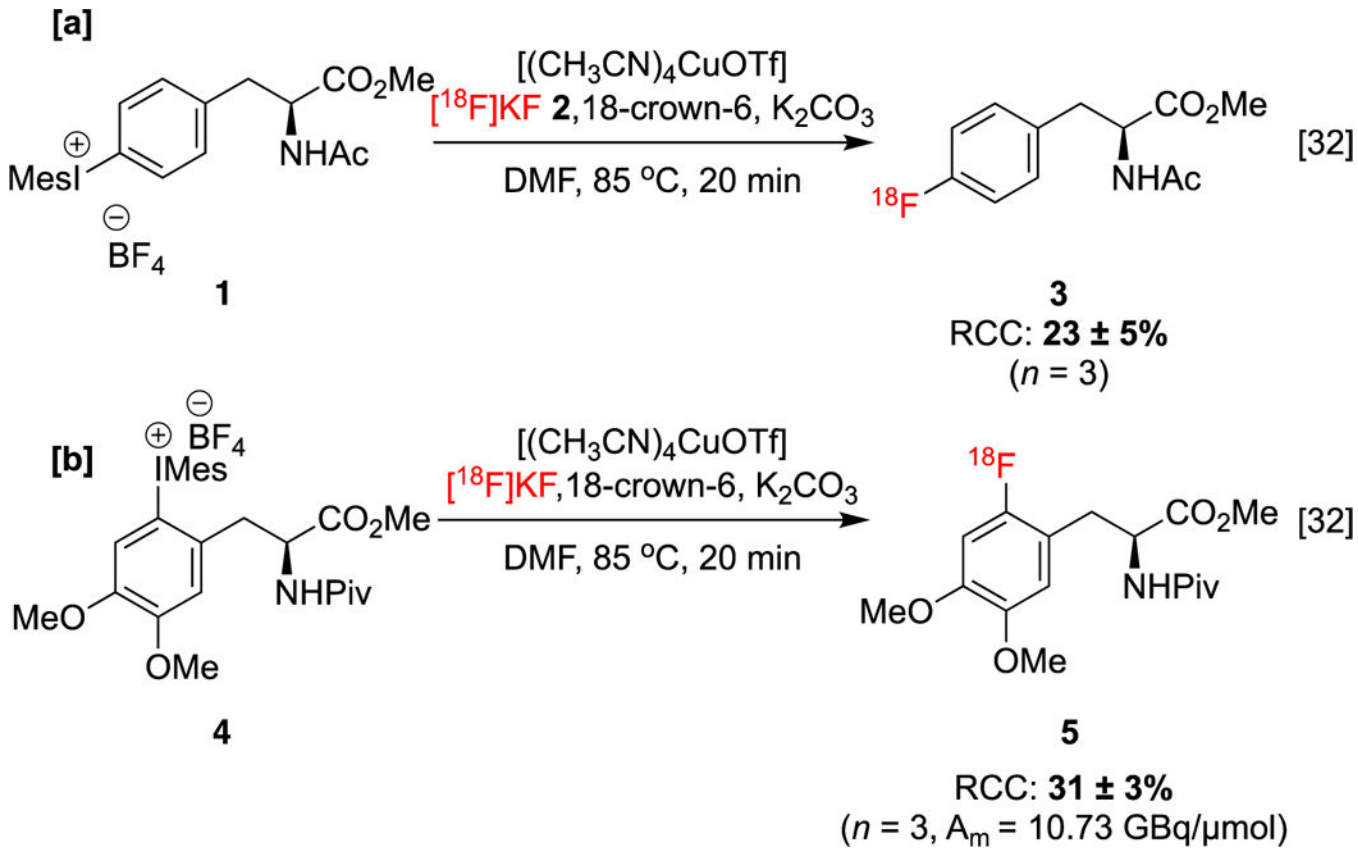

Scheme 1:
Synthesis of **[a]** Protected 4-[^{18}F]L-PhA and **[b]** Protected 6-[^{18}F]Fluoro-L-DOPA.

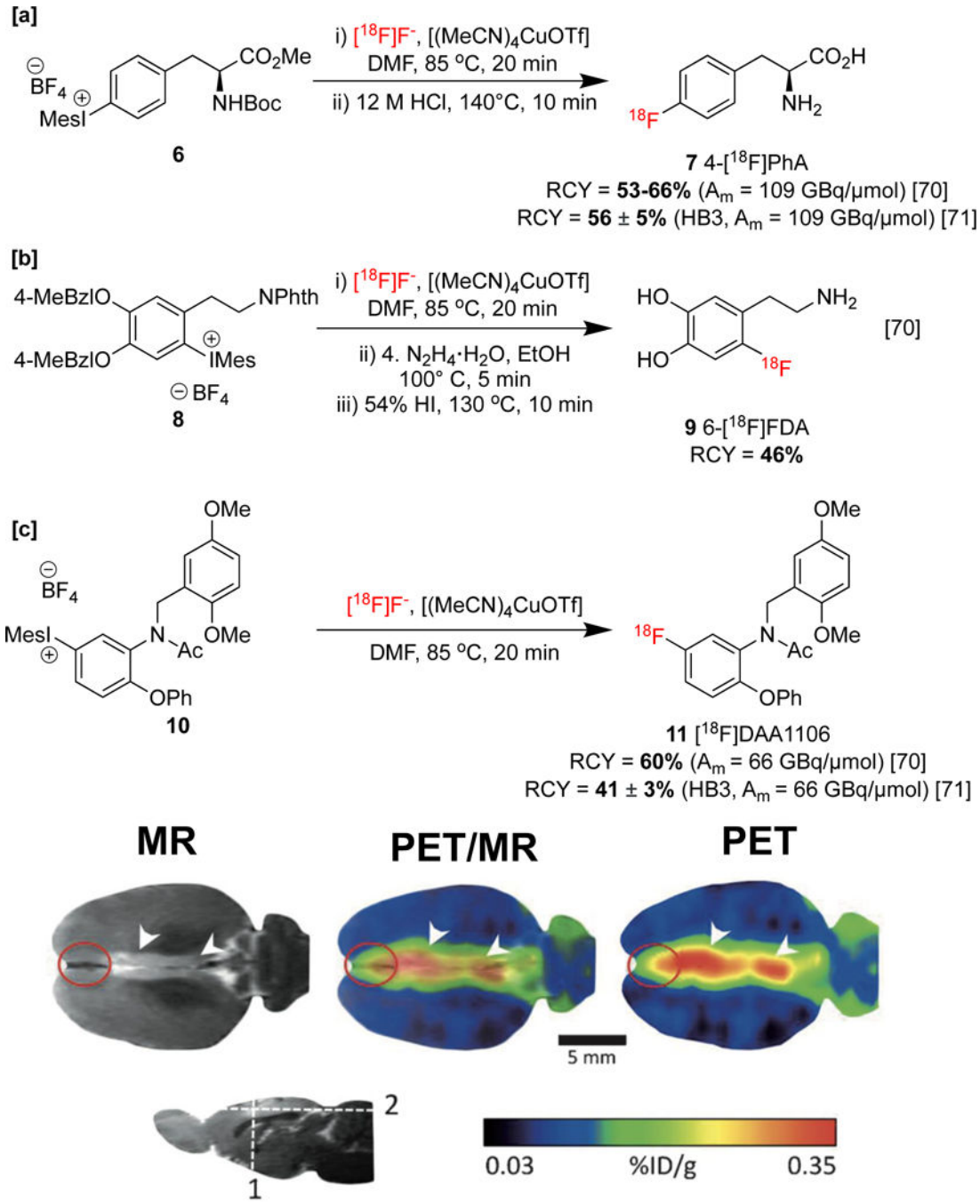

Scheme 2:

[a]: Synthesis of 4-[^{18}F]L-Phe **[b]**: Synthesis of 6-[^{18}F]DP **[c]**:Synthesis and preclinical evaluation of [^{18}F]DAA1106. Images were obtained six days after anterior cerebral artery occlusion, with the ischemic lesion in the anterior cingulate cortex visible as hyperintensity (white arrowheads). The peri-infarct zone is highlighted by red circles. PET-MR images republished from reference 70 with permission from John Wiley & Sons.

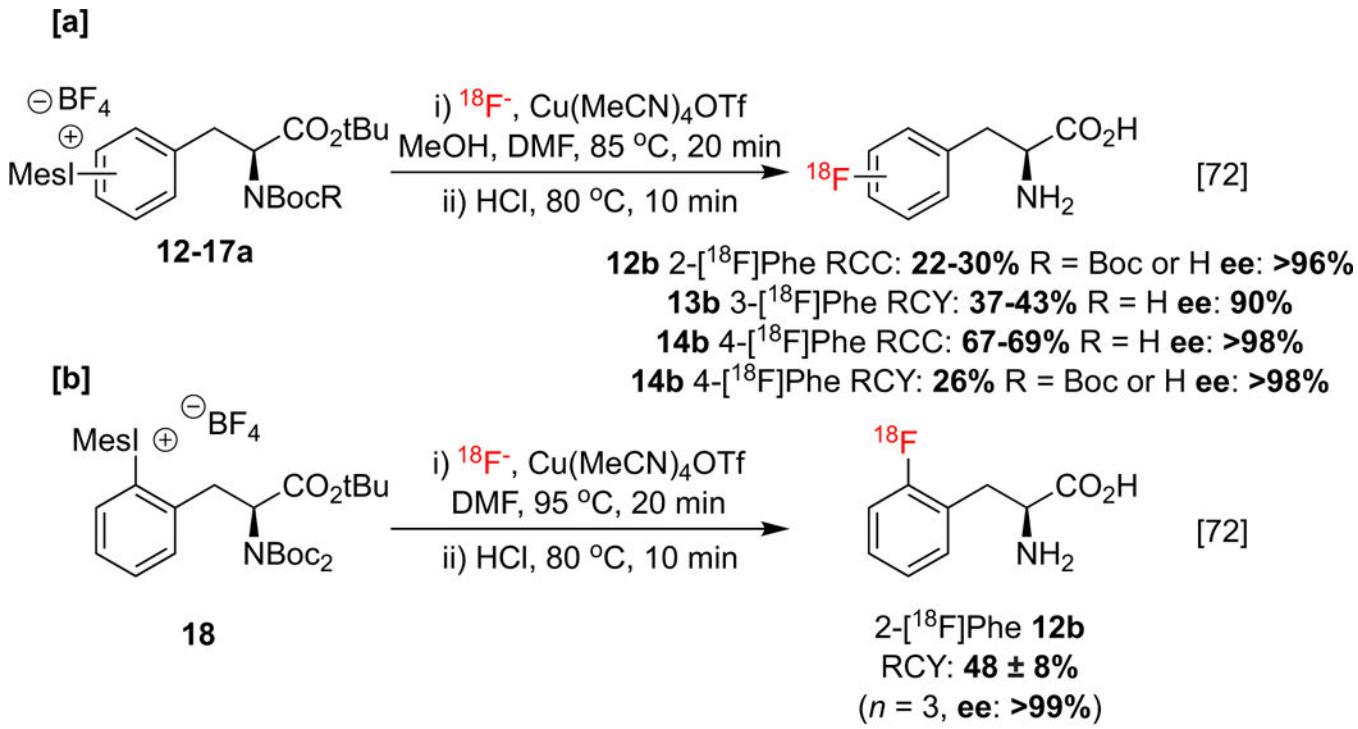

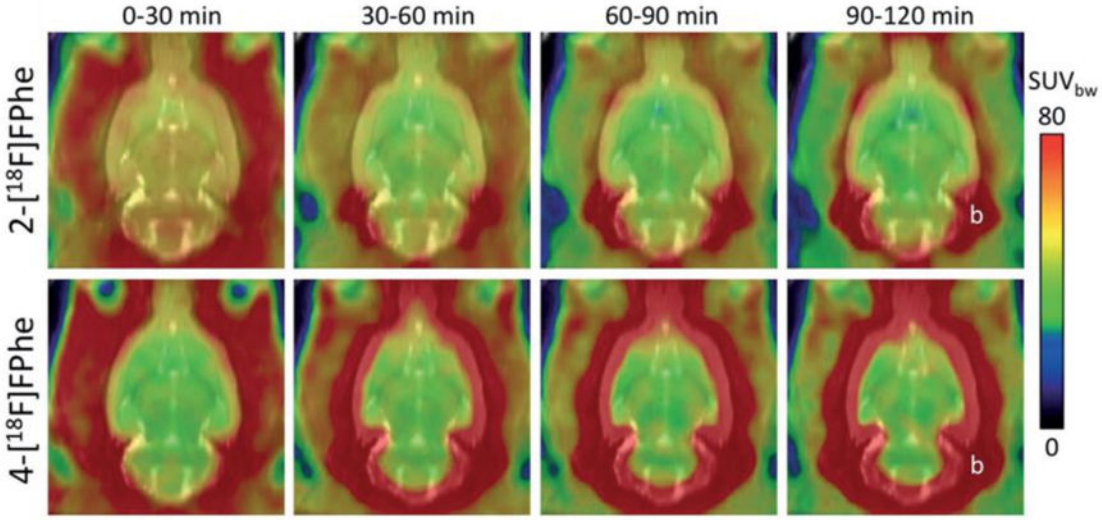

Scheme 3:

Radiosynthesis of fluorine-18 labeled phenylalanine derivatives. **[b]** PET images of 2- and 4-[^{18}F]Phe in healthy rat brains. Significant skull accumulation in the latter can be observed. PET images republished from reference 72 with permission from Thieme.

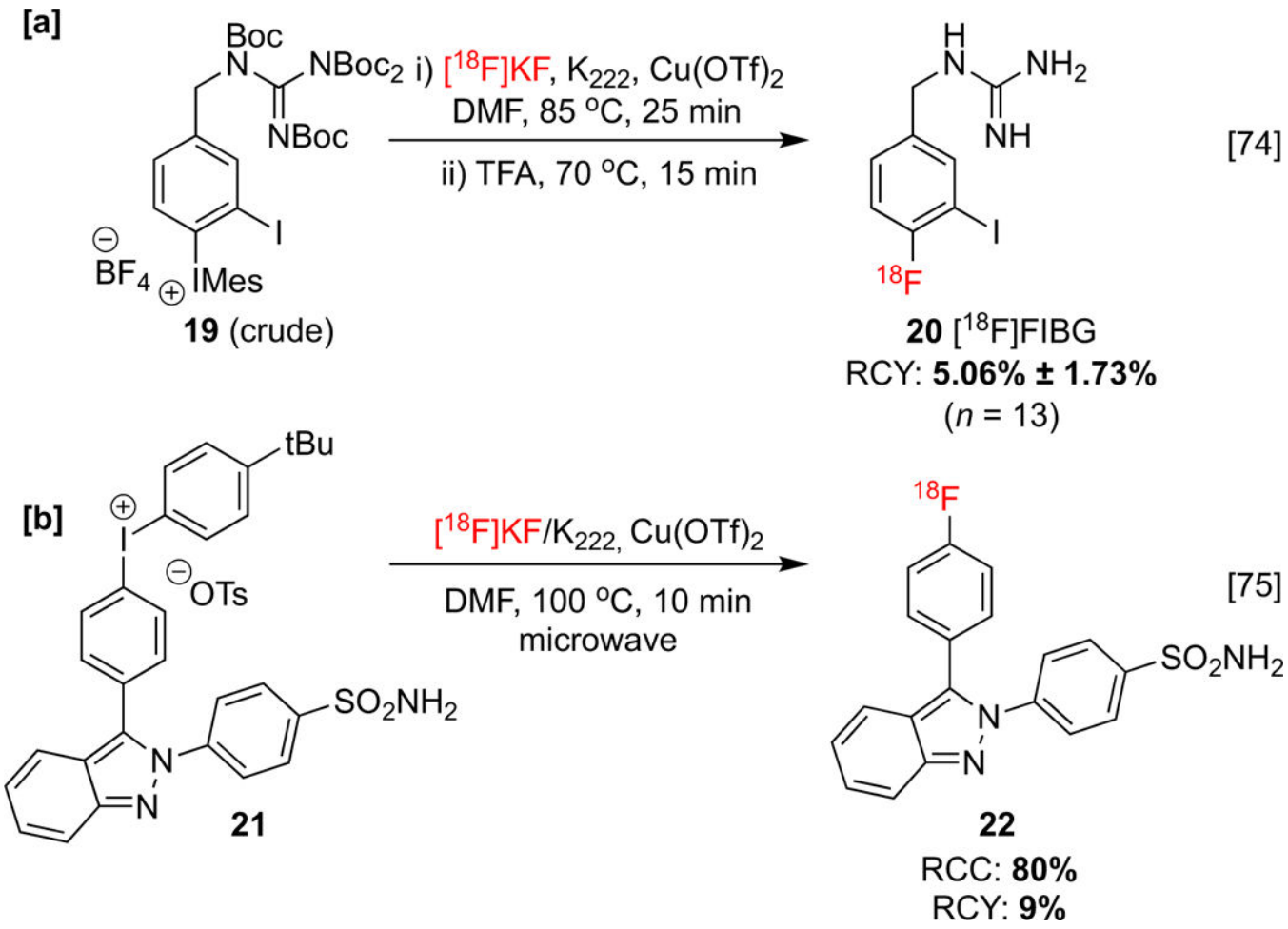

Scheme 4:

Radiosynthesis of **[a]**: [^{18}F]FIBG and **[b]**: indazole **22**.

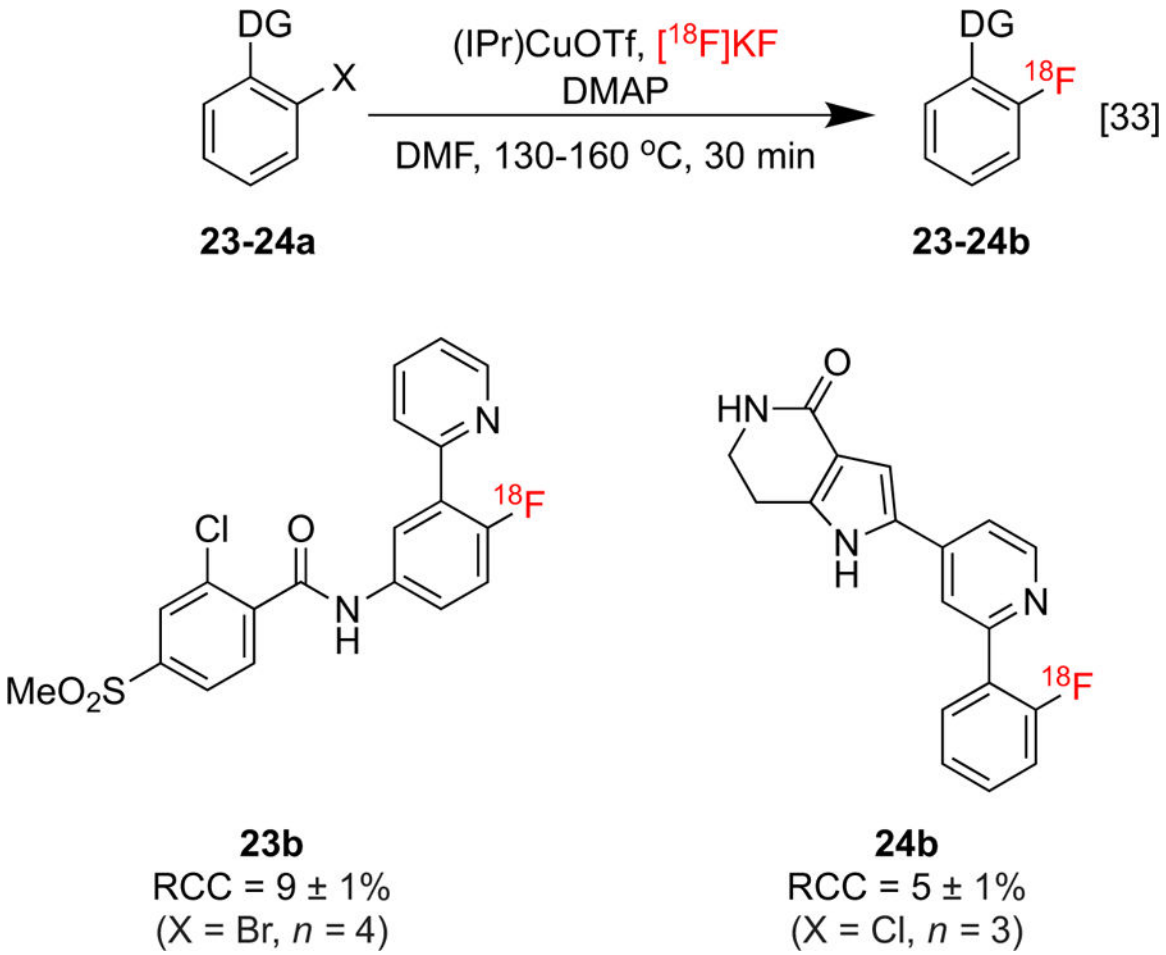

Scheme 5:
ortho-Directed radiofluorination of aryl halides.

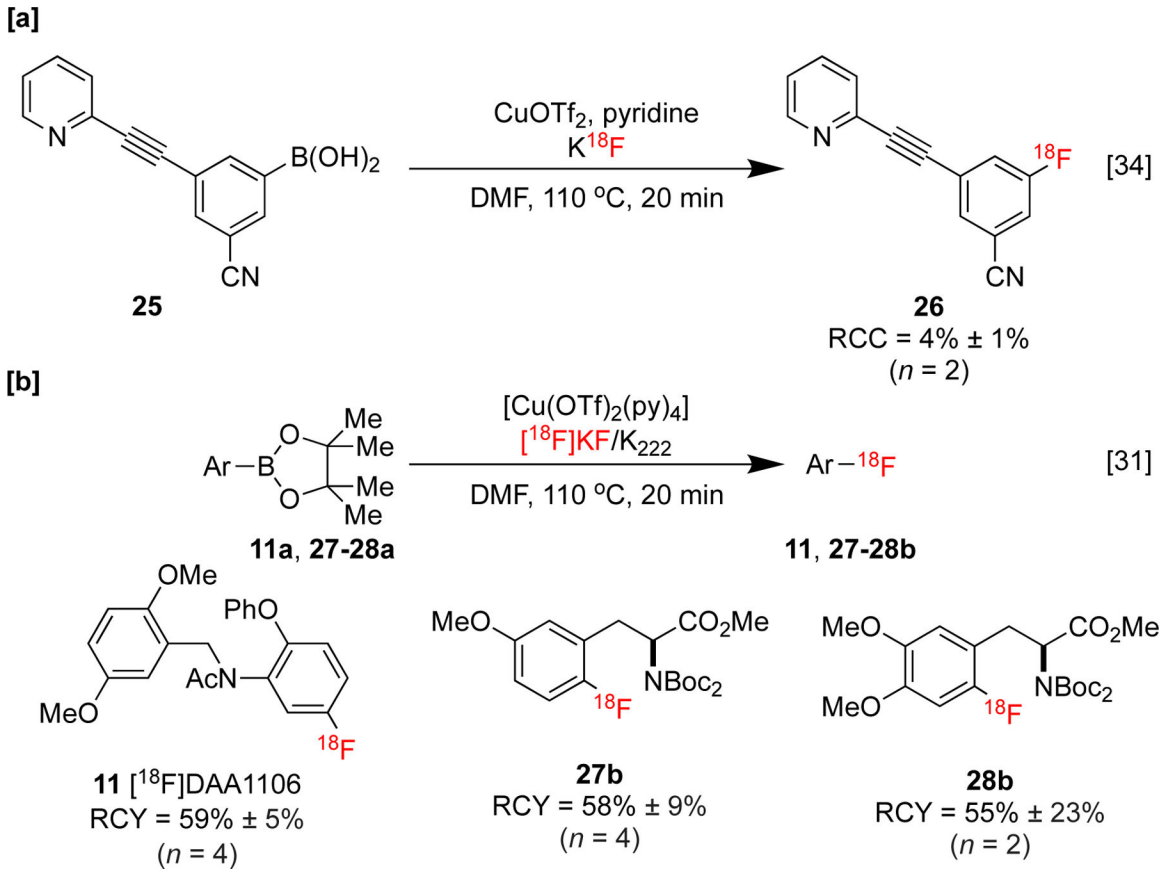

Scheme 6:
Seminal reports on the CMRF of organoborons.

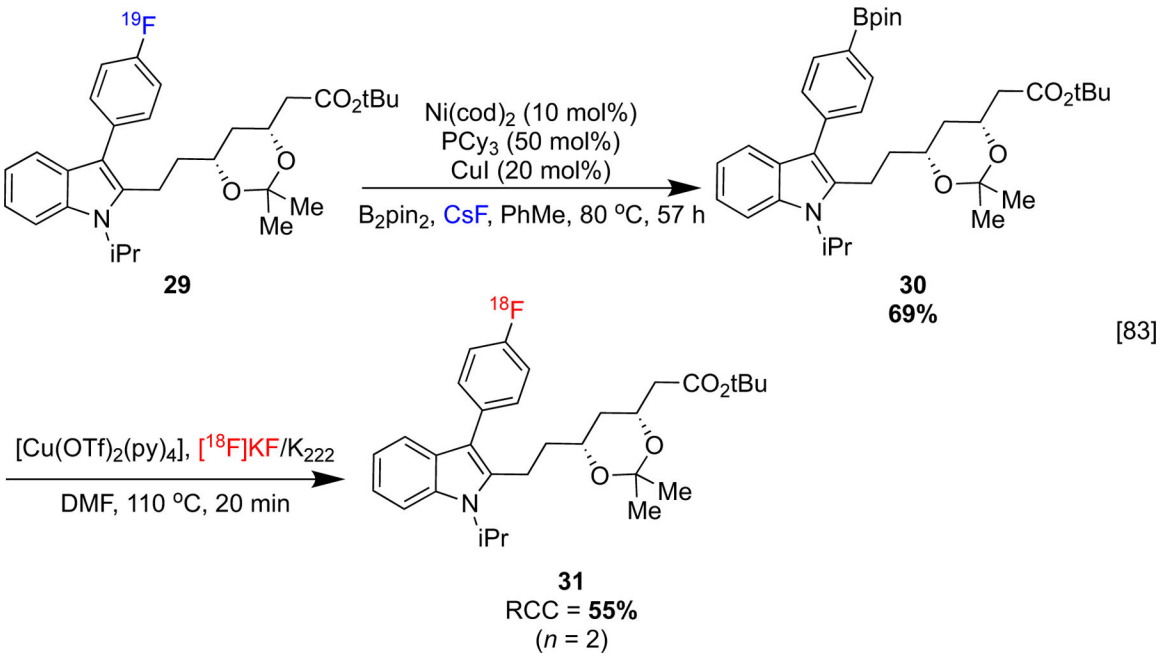

Scheme 7:
Ni-catalyzed fluorodeborylation and Cu-mediated radiofluorination sequence.

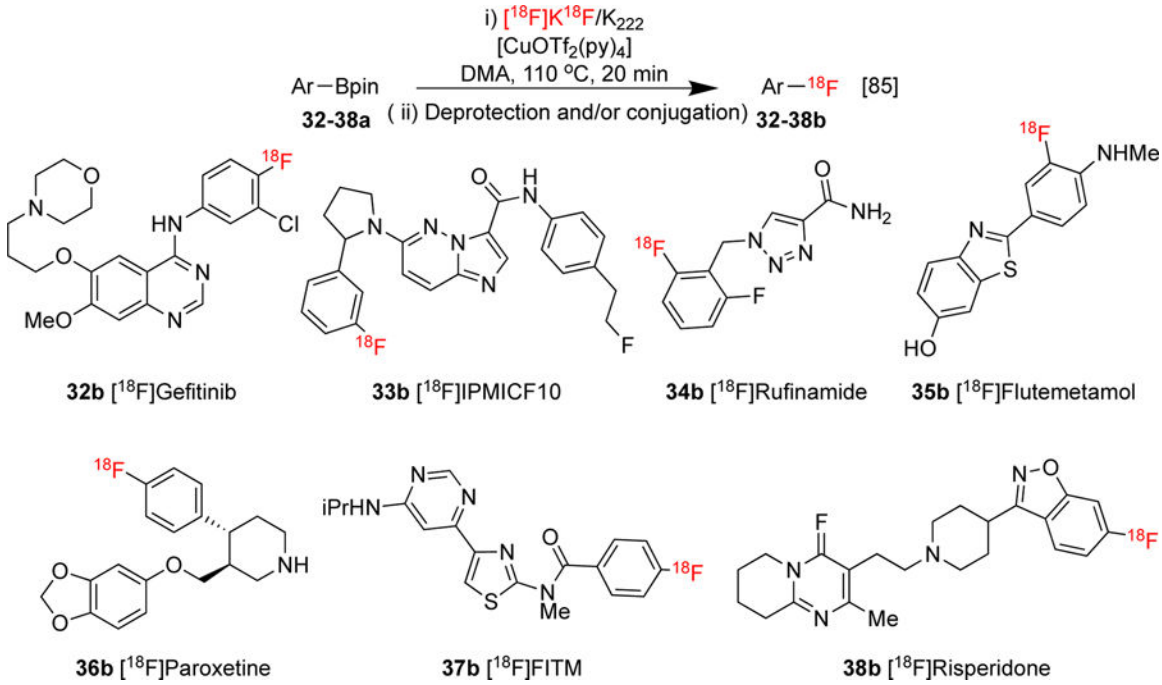

Scheme 8:

Derisked CMRF of organoborons. Multi-step labeling strategies (not shown) were used for the radiosynthesis of **34–38b**.

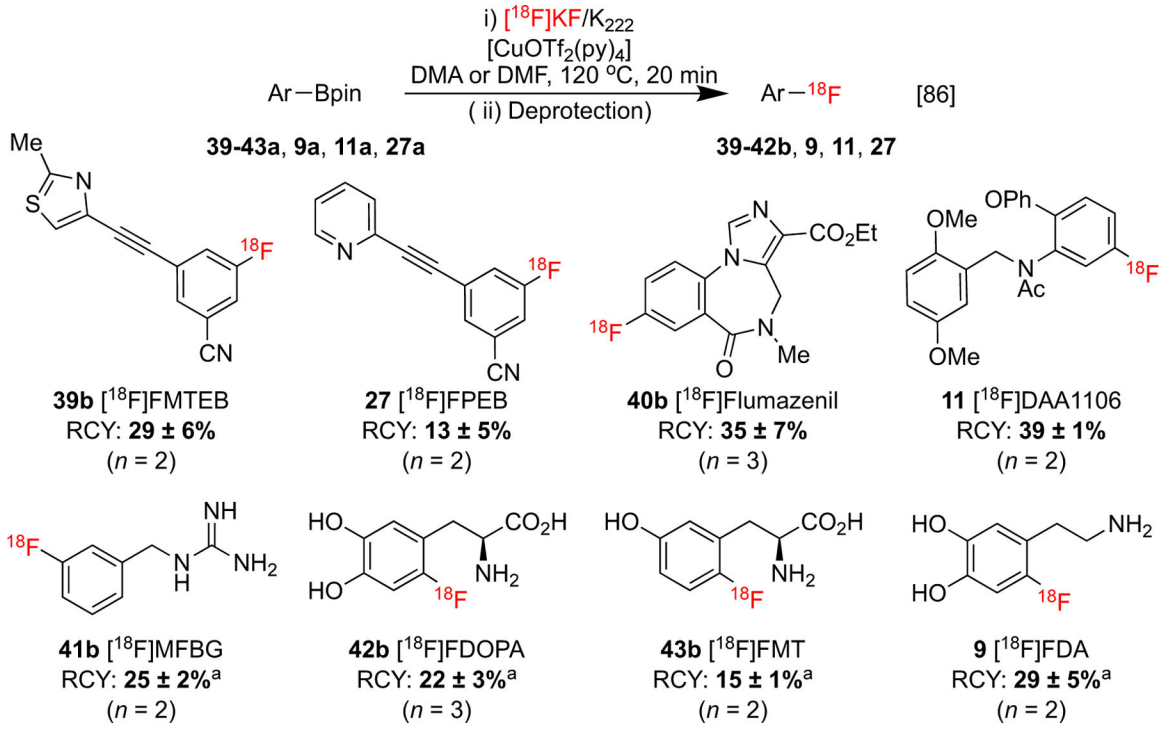

Scheme 9:

Enhanced CMRF of organoborons for the synthesis of imaging agents.

a RCY Reported From Protected Precursor Over Two (Radiofluorination and Deprotection) Steps. Product Obtained Following Deprotection with HI.

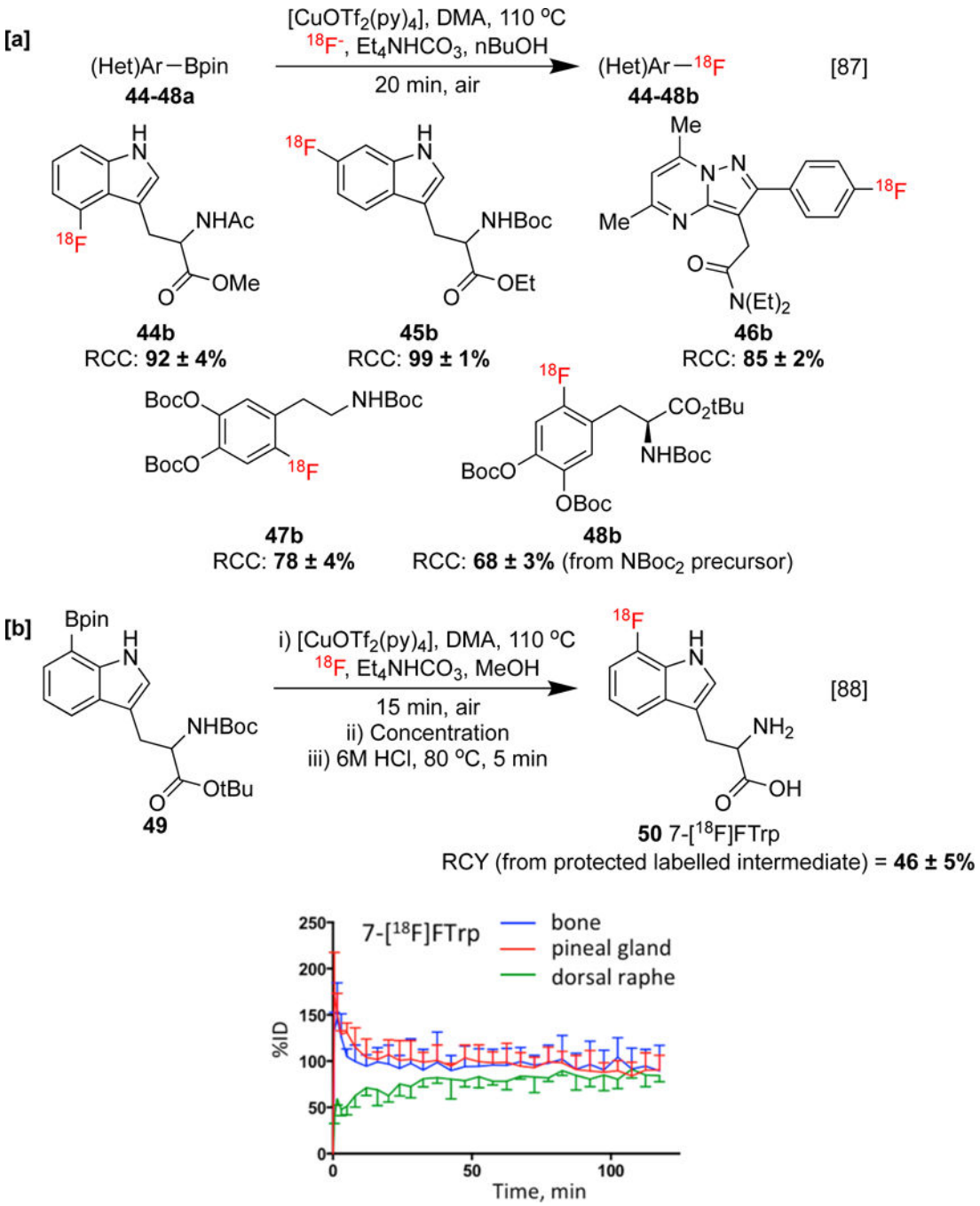

Scheme 10:

Synthesis of radiotracers via alcohol-promoted CMRF. **[b]** Pre-clinical evaluation of 7-[^{18}F]Trp and corresponding radioisomers, displaying regional-time activity curves for uptake of 7-[^{18}F]Trp in the skull (blue), pineal gland (red), and dorsal raphe (green) of rats (below). Metabolic stability data republished from Reference 88 with Permission from the ACS.

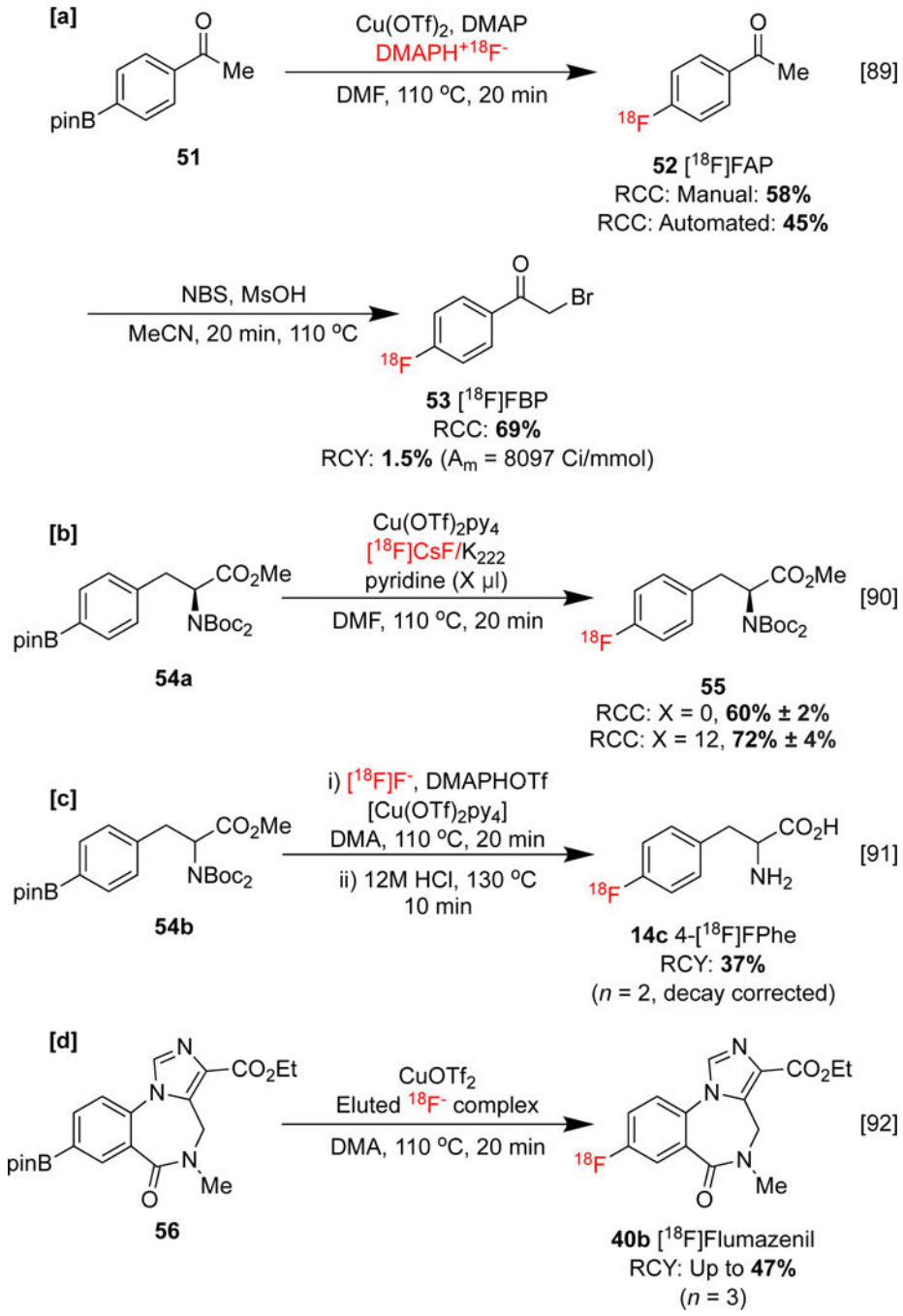

Scheme 11:
Effects of eluting with pyridine derivatives on CMRF.

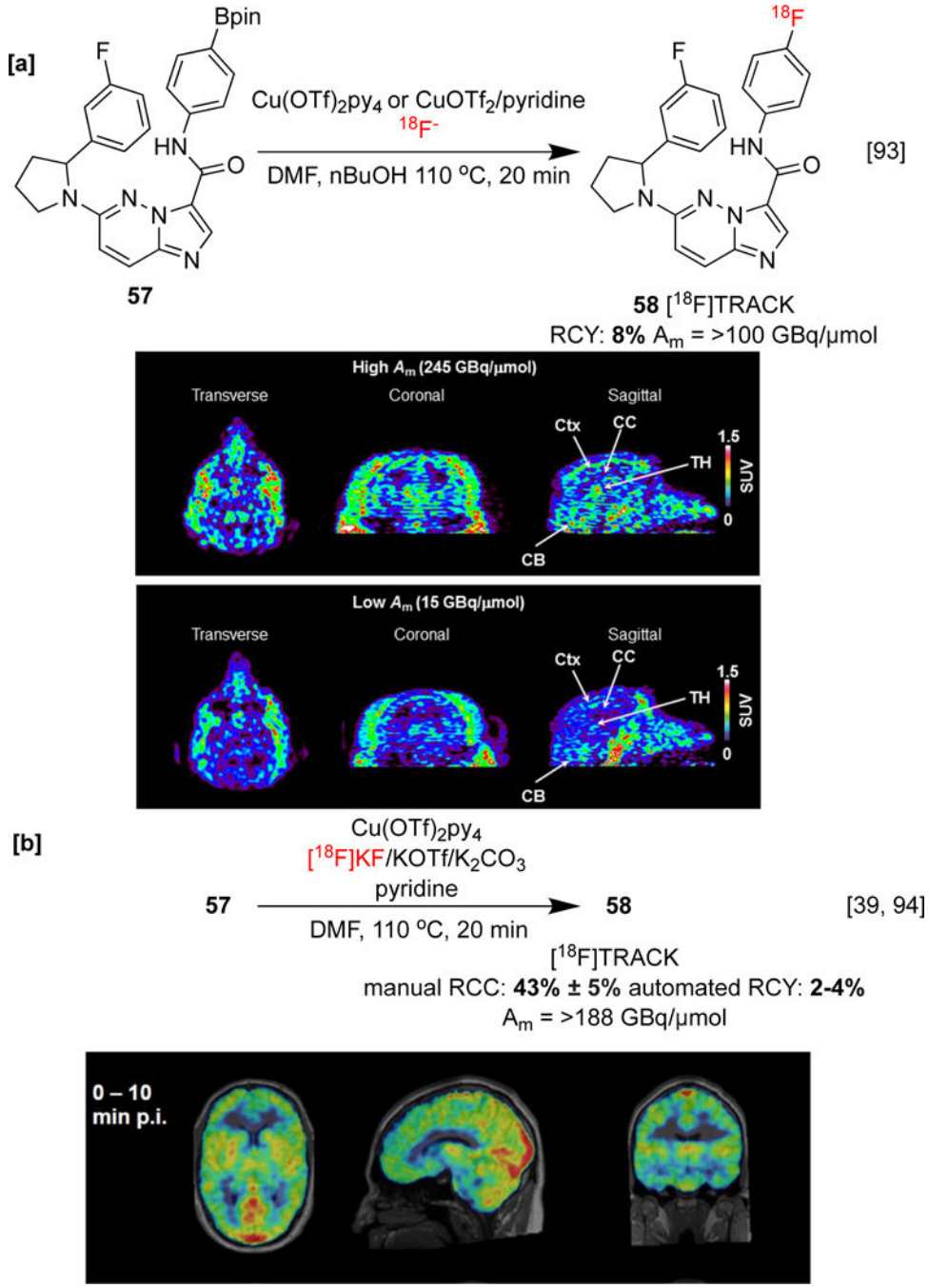

Scheme 12:

Radiochemical syntheses with preclinical and in-human evaluations of [^{18}F]TRACK. **[a]** *In vivo* imaging is displayed at high and low effective specific activity in NHP brain **[b]** Summed PET/MR SUV images at 0–10 min in a healthy human brain. PET images republished from references 93 and 94 with permission from the ACS.

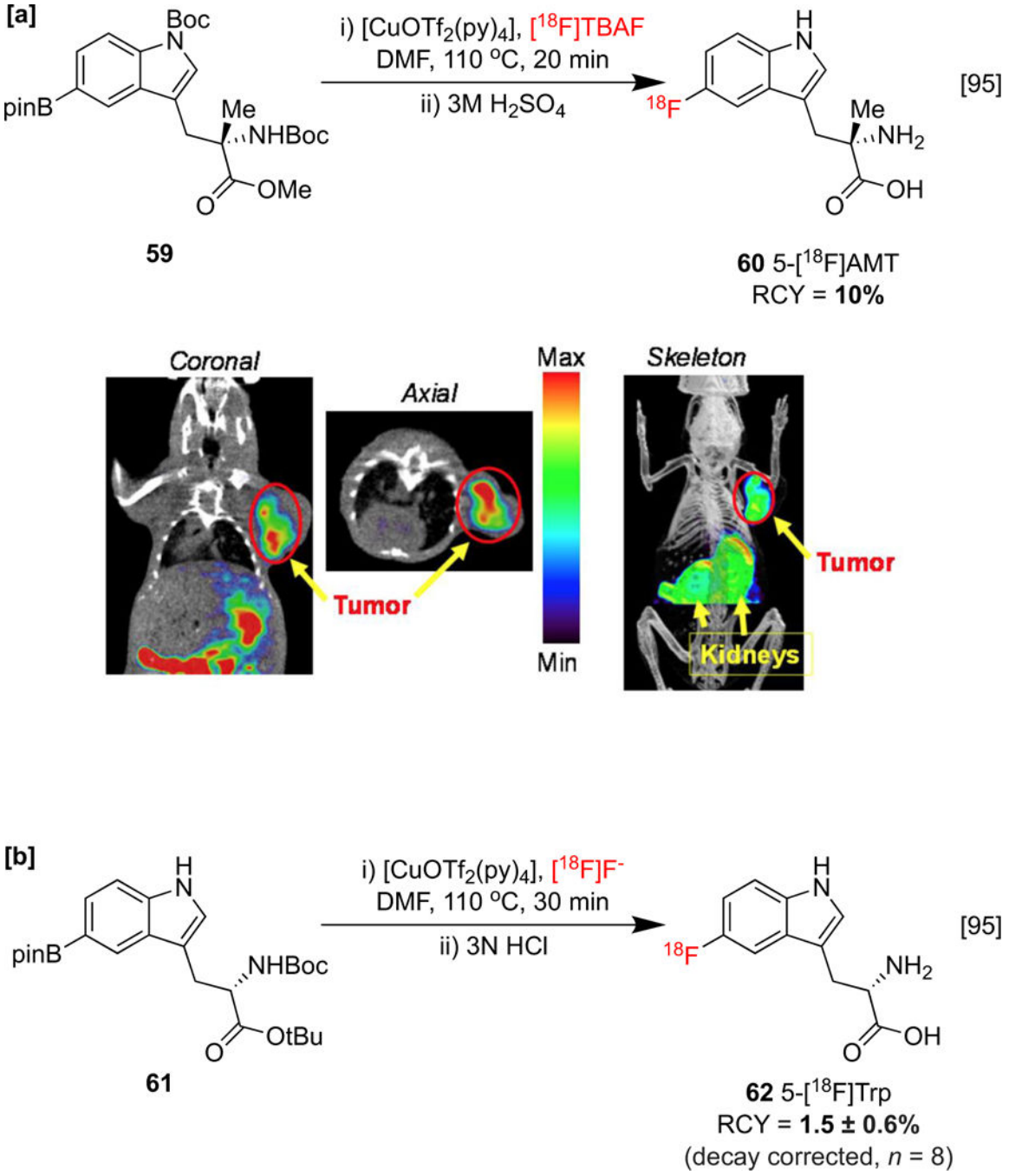

Scheme 13:

Radiosyntheses of [^{18}F]Tryptphan derivatives. **[a]**: Synthesis of 5-[^{18}F]AMT and Decay-corrected rodent PET-CT images of B16F10 melanoma after a 30 min injection of 5-[^{18}F]AMT. PET-CT images republished from reference 95 with permission from Ivyspring; **[b]**: Synthesis of 5-[^{18}F]Trp.

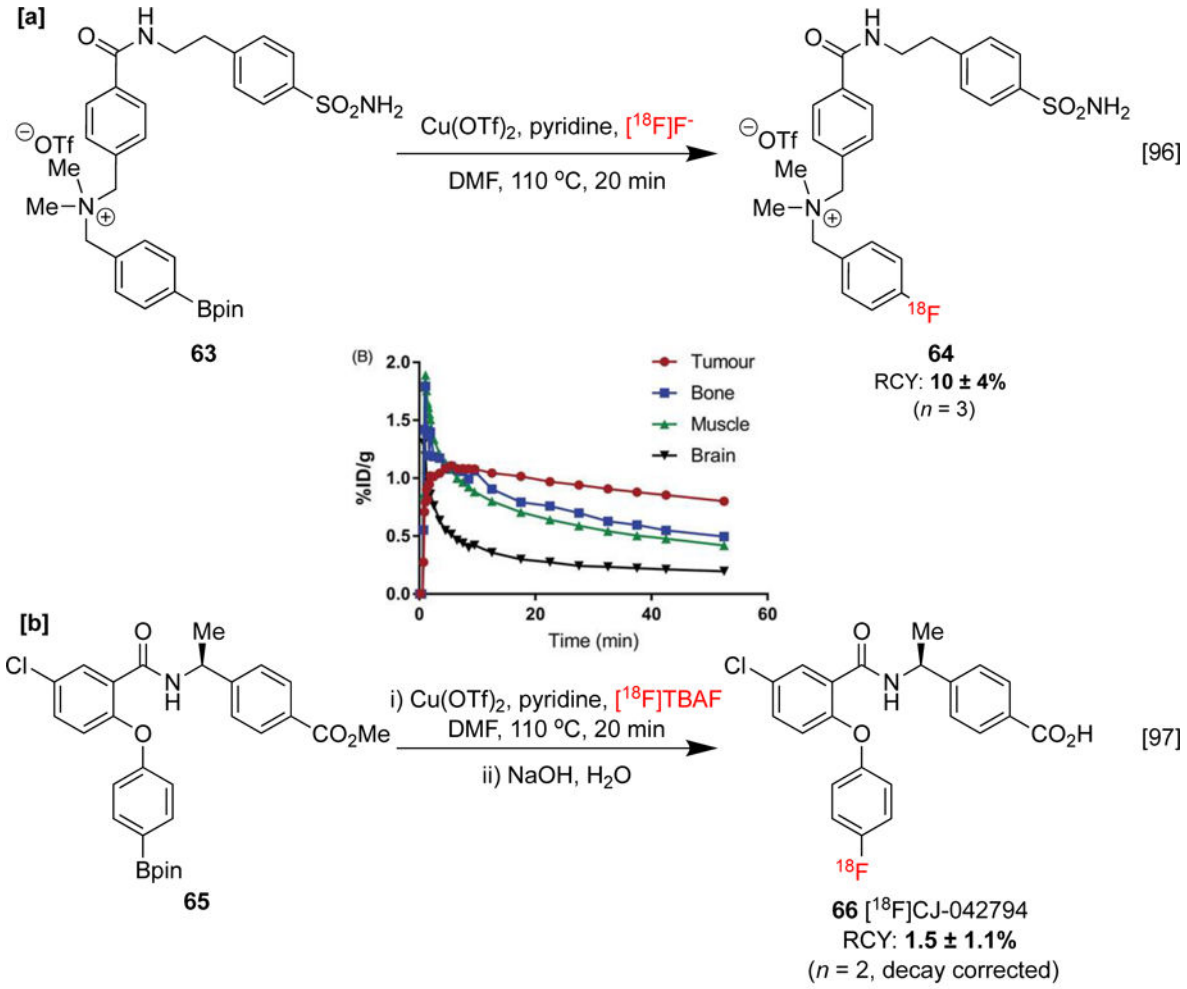

Scheme 14:

Radiosynthesis and preclinical evaluation of **64** and **66**. **[a]**: Biodistribution of **64** in the low activity organs of mice. **[b]**: PET-CT images of mice bearing LNCaP prostate cancer xenografts. Blocking was performed using non-radioactive CJ-042794. Biodistribution data and PET-CT images republished from references 96 and 97 with permission from Taylor & Francis (open access) and Elsevier, respectively.

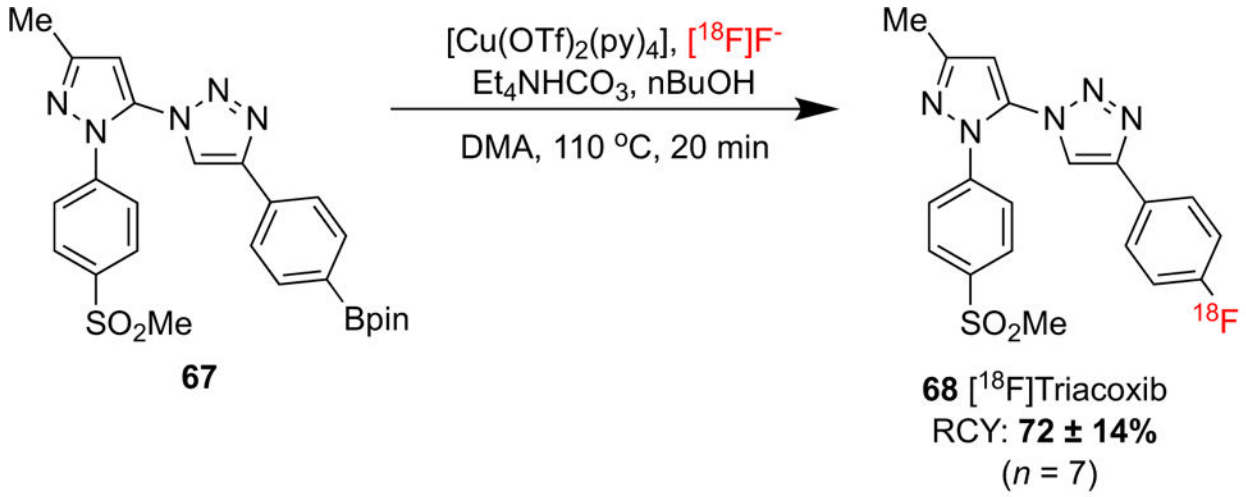

[98]

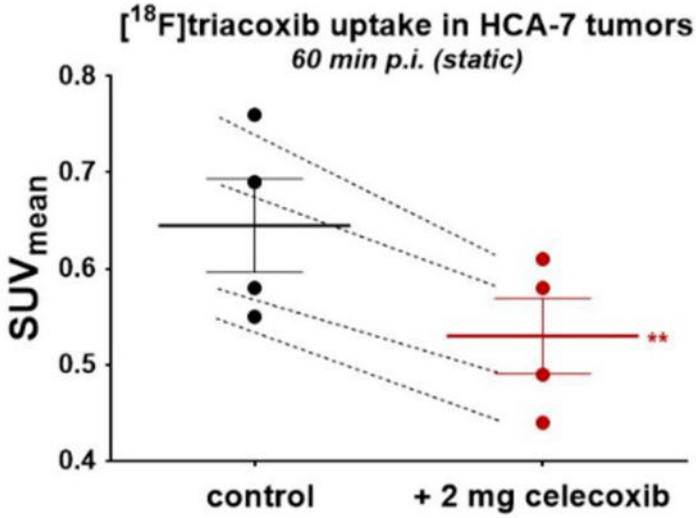

Scheme 15:

Synthesis of [^{18}F]Triacoxib. Statistical analysis displaying uptake in a control and with celecoxib as a blocking agent. SUV data republished from reference 98 with permission from the ACS.

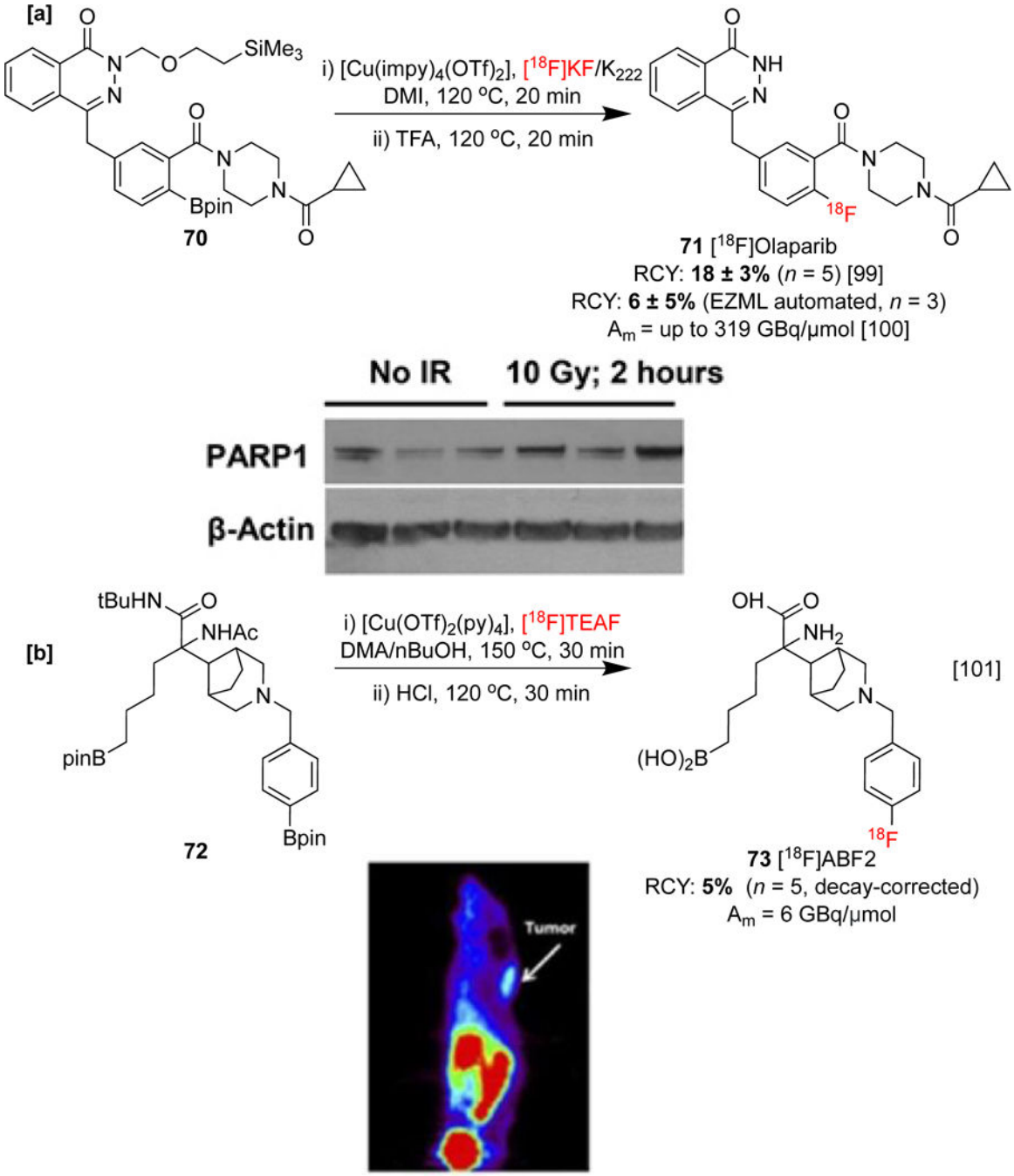

Scheme 16:

[a] Radiosynthesis and preclinical evaluation of **71**. Western blot study displaying PARP-1 and β-actin levels with/without irradiation in PSN-1 xenografts. **[b]** Radiosynthesis an preclinical evaluation of **73**. PET imaging in PC3 cell lines of immune-deficient mouse. Western blot study and PET image republished from references 99 and 101 with permission from SNMMI and John Wiley & Sons, respectively.

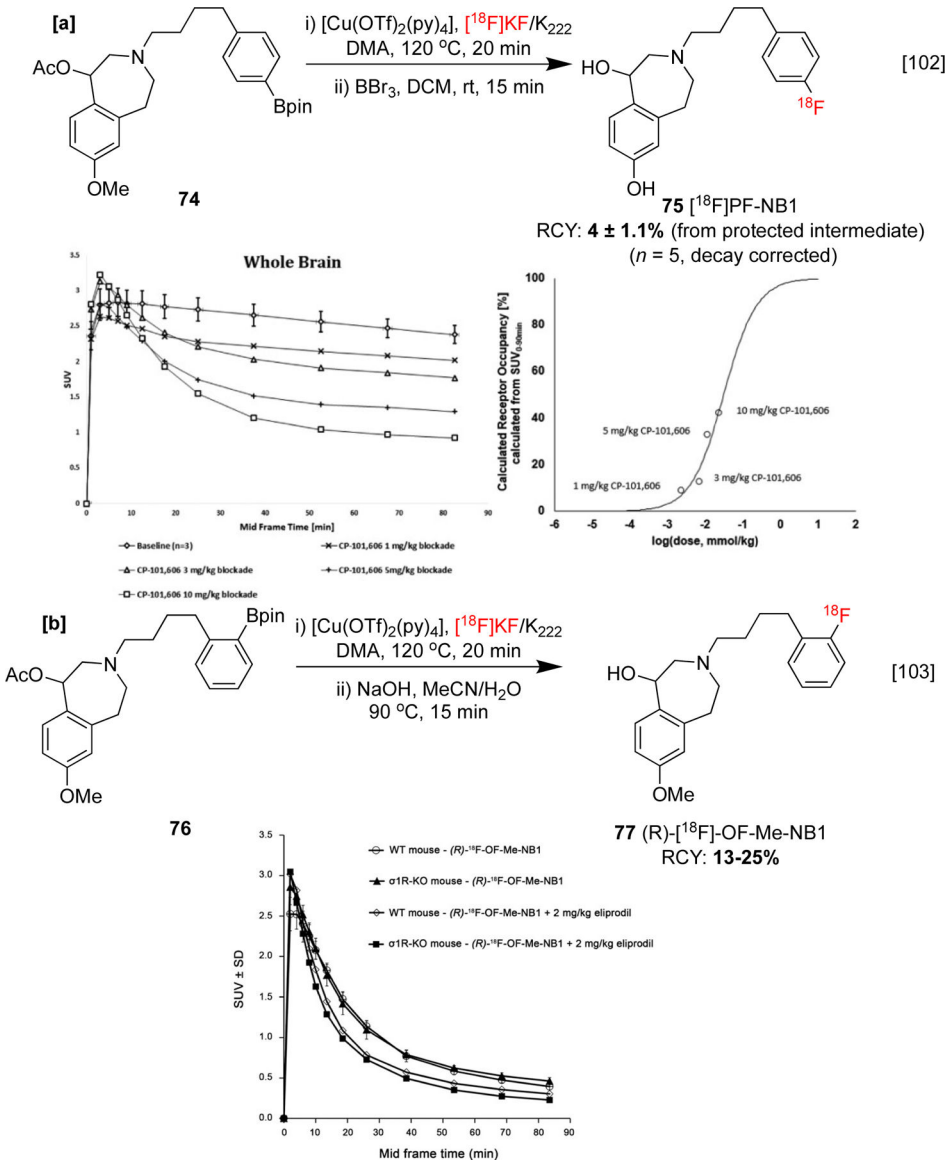

Scheme 17:

[a]: Synthesis and preclinical evaluation of **75**. Whole brain accumulation levels with varying quantities of GluN2B antagonist C-P101,606 **[b]** Synthesis and preclinical evaluation of **77**. Brain-time activity curves from PET study in σ1R-KO and wild-type mice. Eliprodil was used for the blockade study. Uptake data republished from references 102 and 103 with permission from SNMMI and the ACS, respectively.

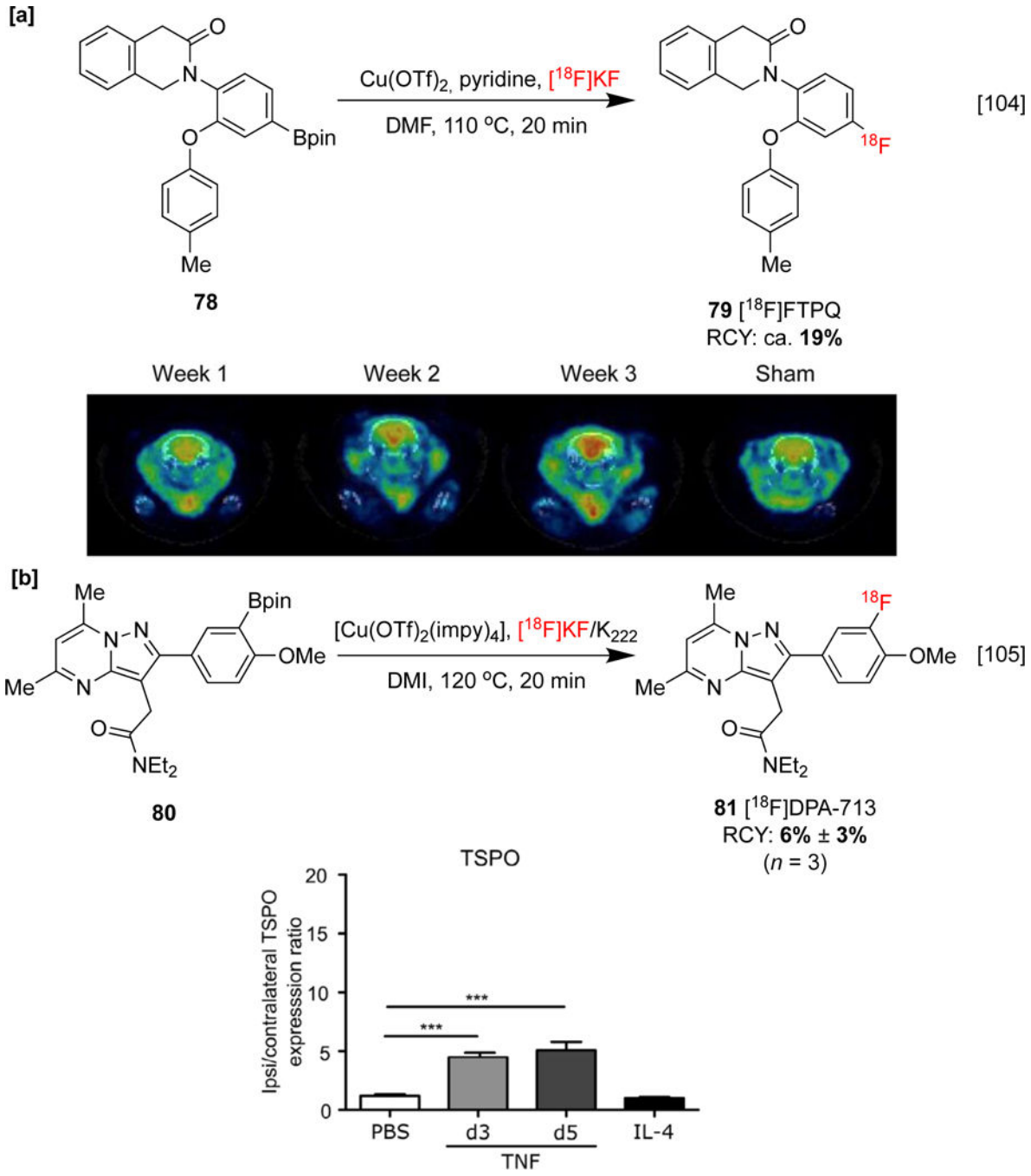

Scheme 18:

Synthesis and preclinical evaluation of [^{18}F]FTPQ and [^{18}F]DPA-713. **[a]**: MicroPET-CT images obtained following injection of ca. 18.5 MBq for 30 min. **[b]**: TSPO expression 3 and 5 days after intracerebral injection of AdTNF, and 24 h following PBS and IL-4 injection. PET-CT images and TSPO expression data republished from references 104 and 105 with permission from Springer Nature and John Wiley & Sons, respectively.

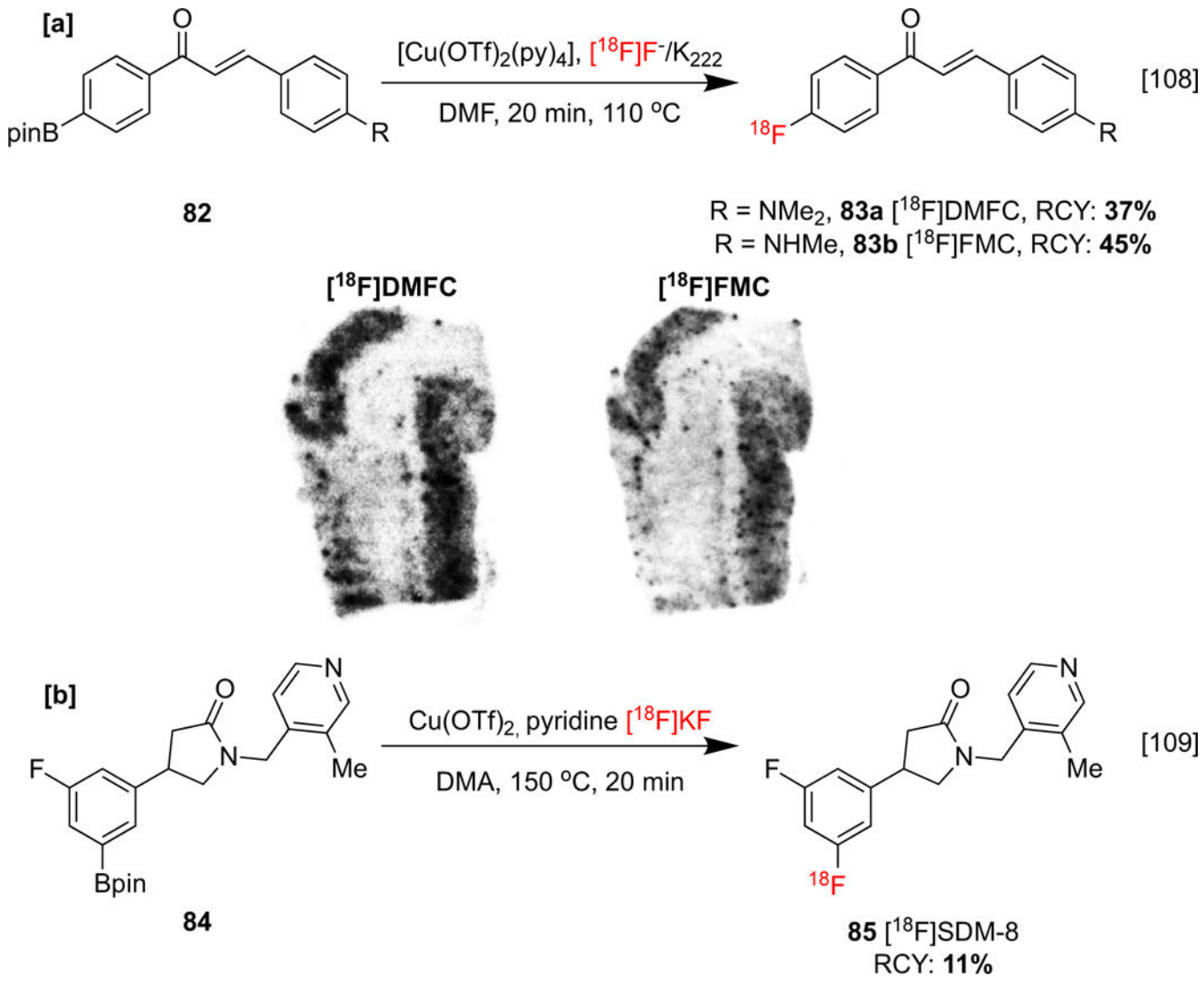

Scheme 19:

[a] Synthesis and preclinical evaluation of [^{18}F]DMFC, [^{18}F]FMC. In vitro ARG of AD brain sections labeled with [^{18}F]DMFC (left) and [^{18}F]FMC (right), depicting accumulation along the gray matter of the frontal lobe. **[b]**: Synthesis of [^{18}F]SDM-8. ARG image republished from reference 108 with permission from Elsevier.

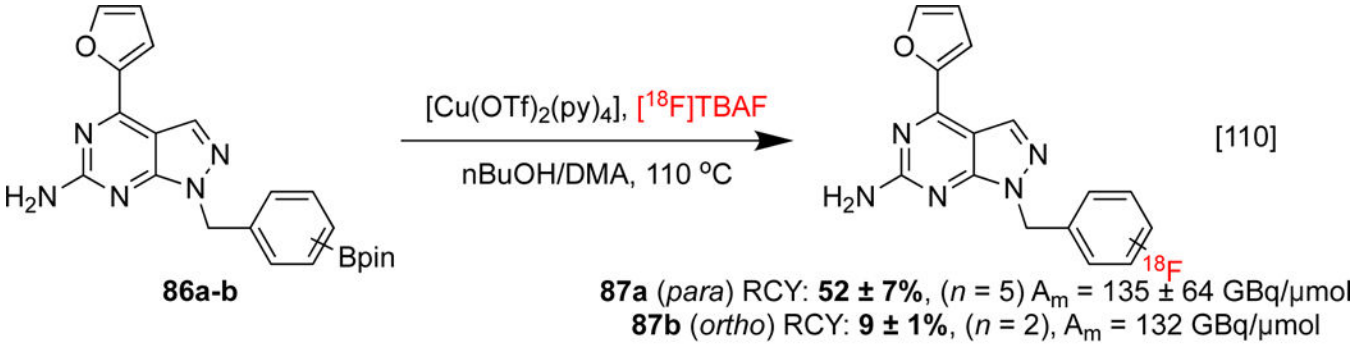

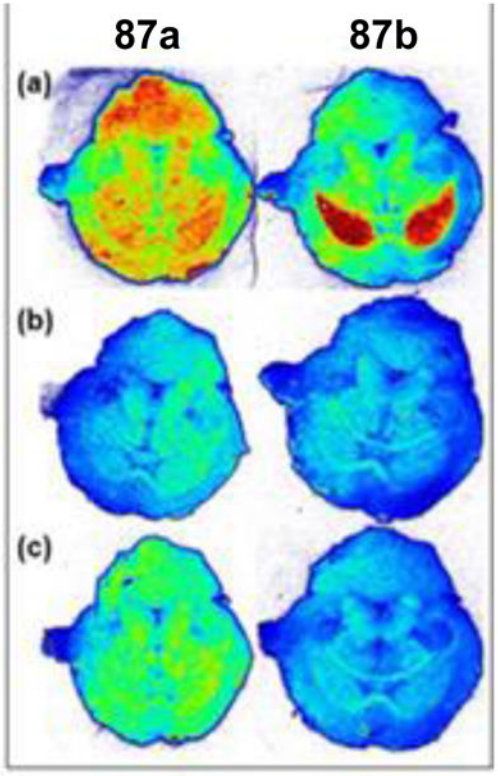

Scheme 20:

Synthesis and preclinical evaluation of **87a** and **87b**. PET images of a mice brain depicts (a) Total binding (b) Self-blocking (c) Blocking with ZM241385. PET images republished from reference 110 with permission from John Wiley & Sons.

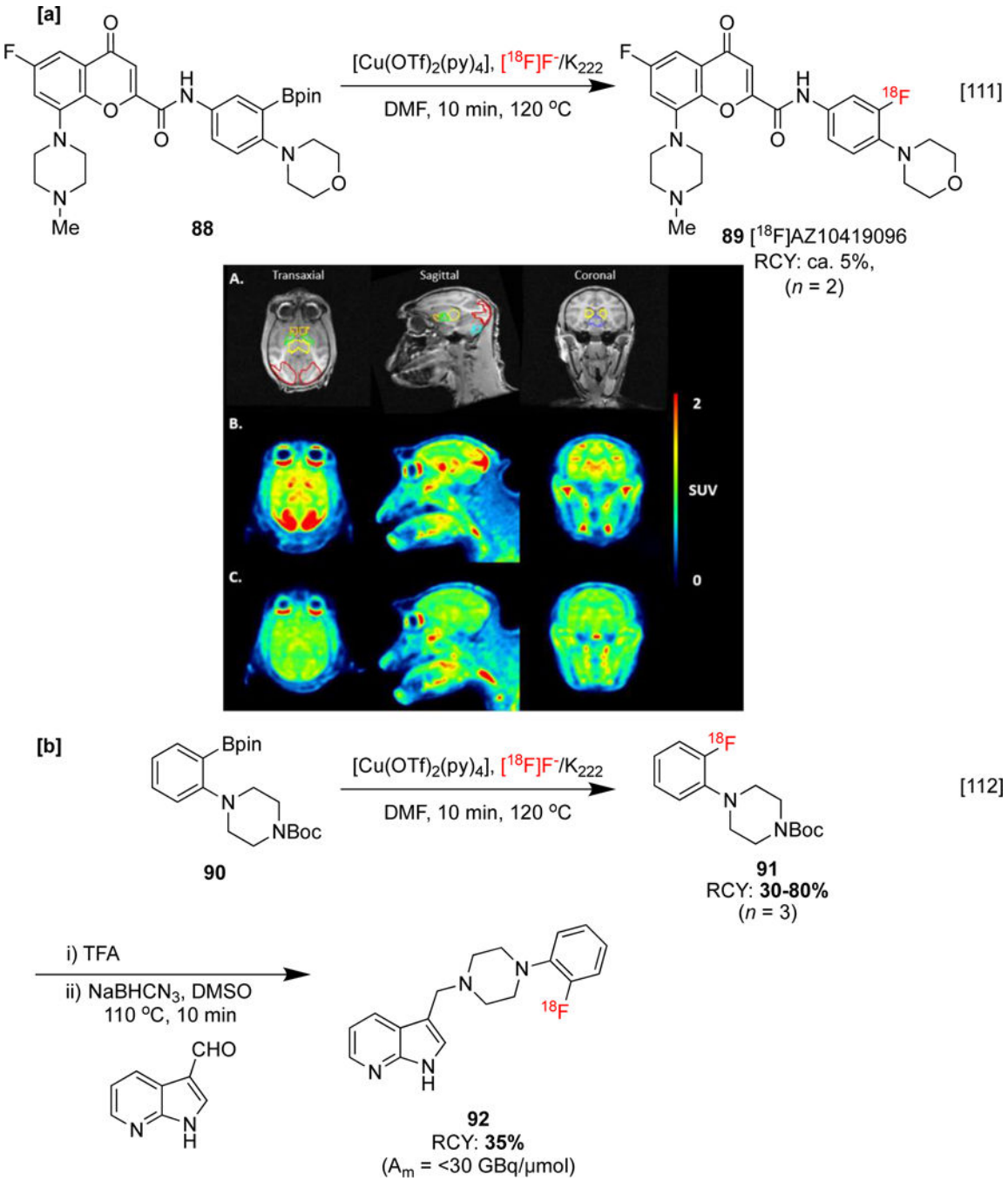

Scheme 21:

[a] Synthesis and preclinical evaluation of [^{18}F]AZ10419096 in NHP brain. A: MRI images. B: PET SUV baseline experiment. C: PET SUV blocking experiment using AR-A000002 (2.0 mg/kg) **[b]** Prosthetic group radiosynthesis of **92**. MRI and PET images republished from reference 111 with permission from Elsevier.

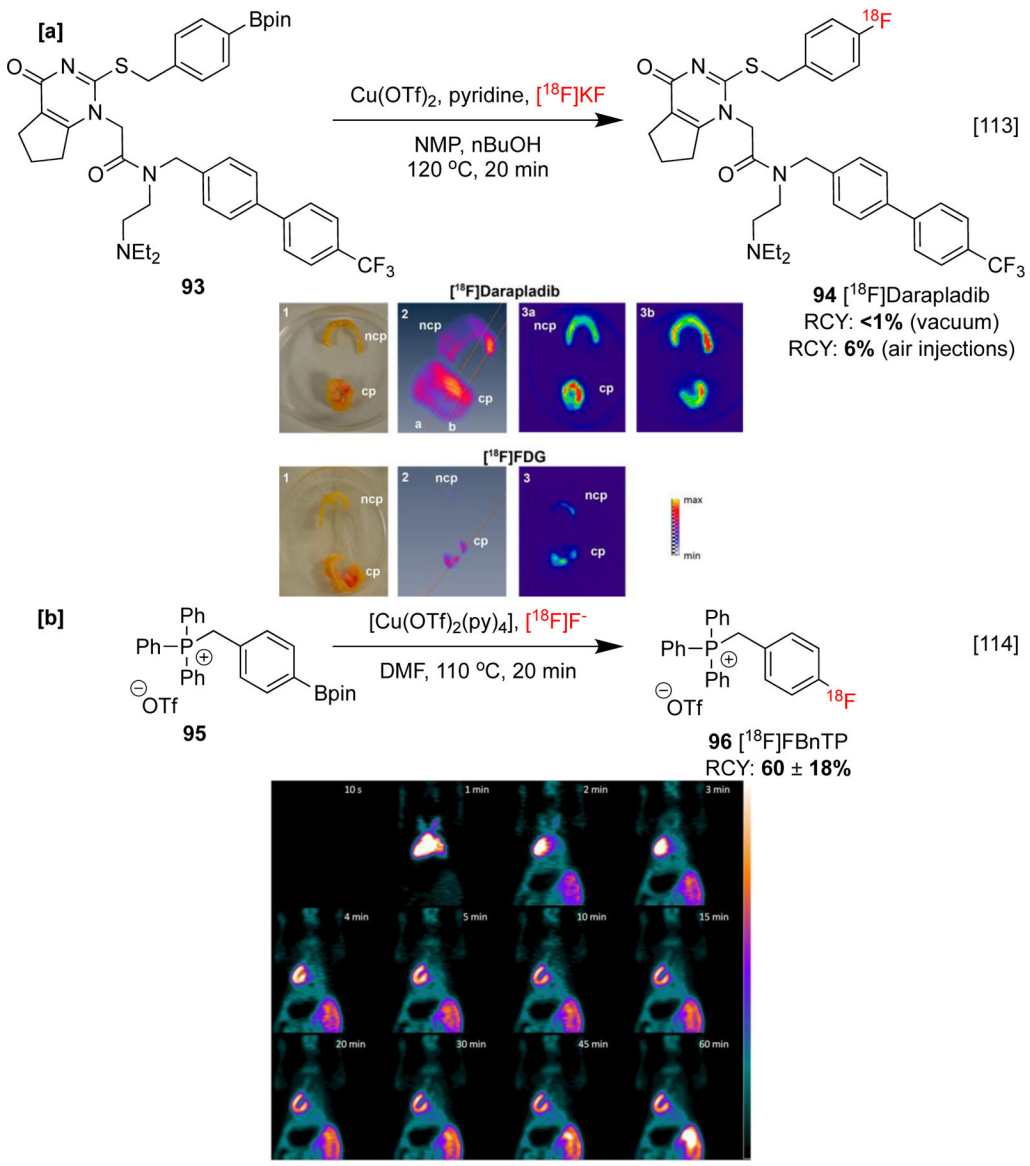

Scheme 22:

Synthesis and preclinical evaluation of [^{18}F]darapladib and [^{18}F]FBnTP. **[a]**: Ex vivo tracer accumulations. 1: Macroscopic view. 2: 3D PET imaging view. 3: Corresponding orthoslice of planes *a* and *b*. **[b]**: Dynamic PET images of [^{18}F]FBnTP in a female mouse, depicting myocardial uptake 1 min post-injection. Images republished from references 113 and 114 with permission from the ACS and John Wiley & Sons, respectively.

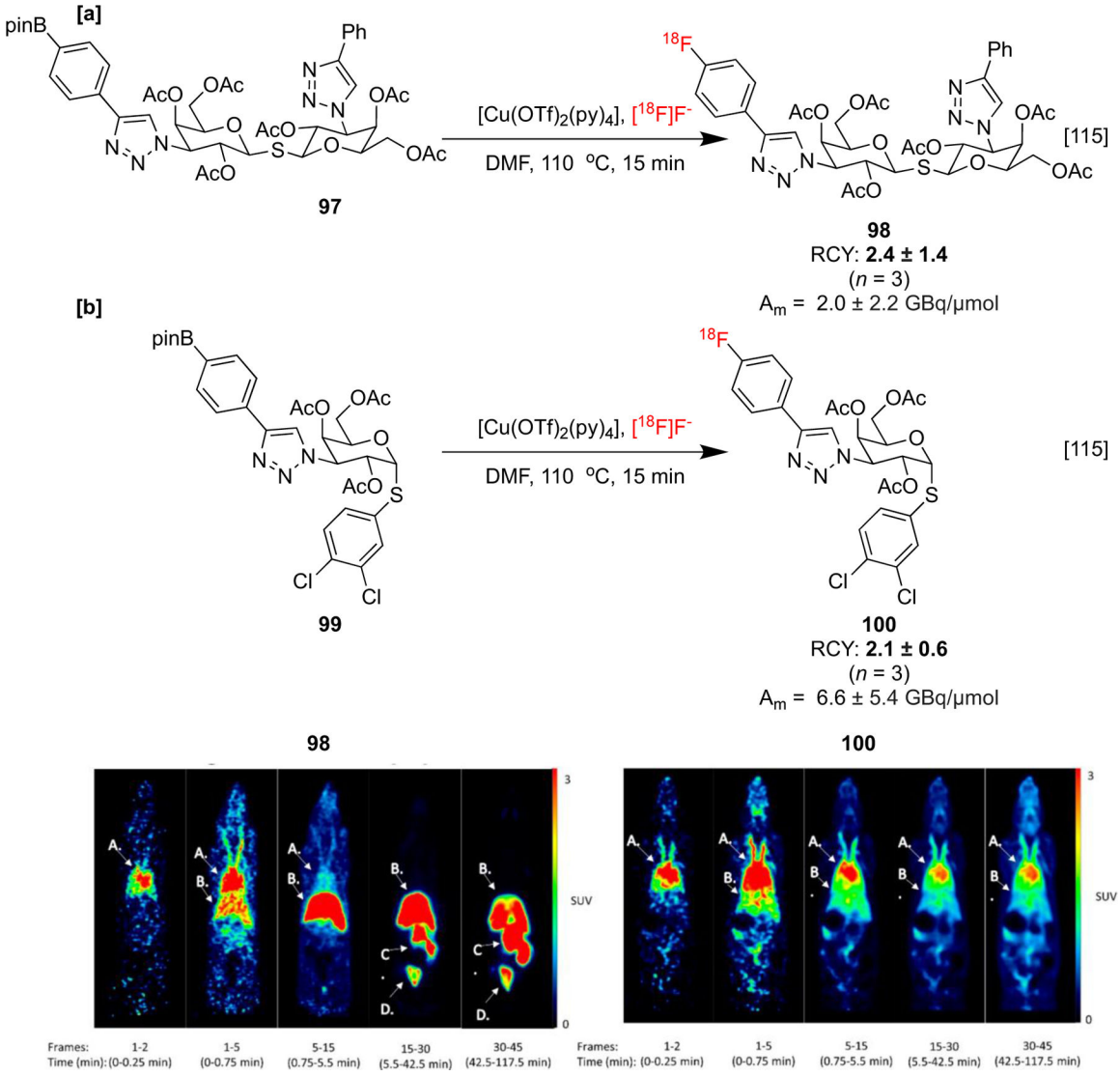

Scheme 23:

Radiosyntheses and preclinical evaluation of glycomimetic tracers **98** and **100**. PET images of the coronal plane at frames between 0 and 120 min. A: Heart, B: Liver, C: Intestine, D: Bladder. Images republished from reference 115 with permission from the ACS.

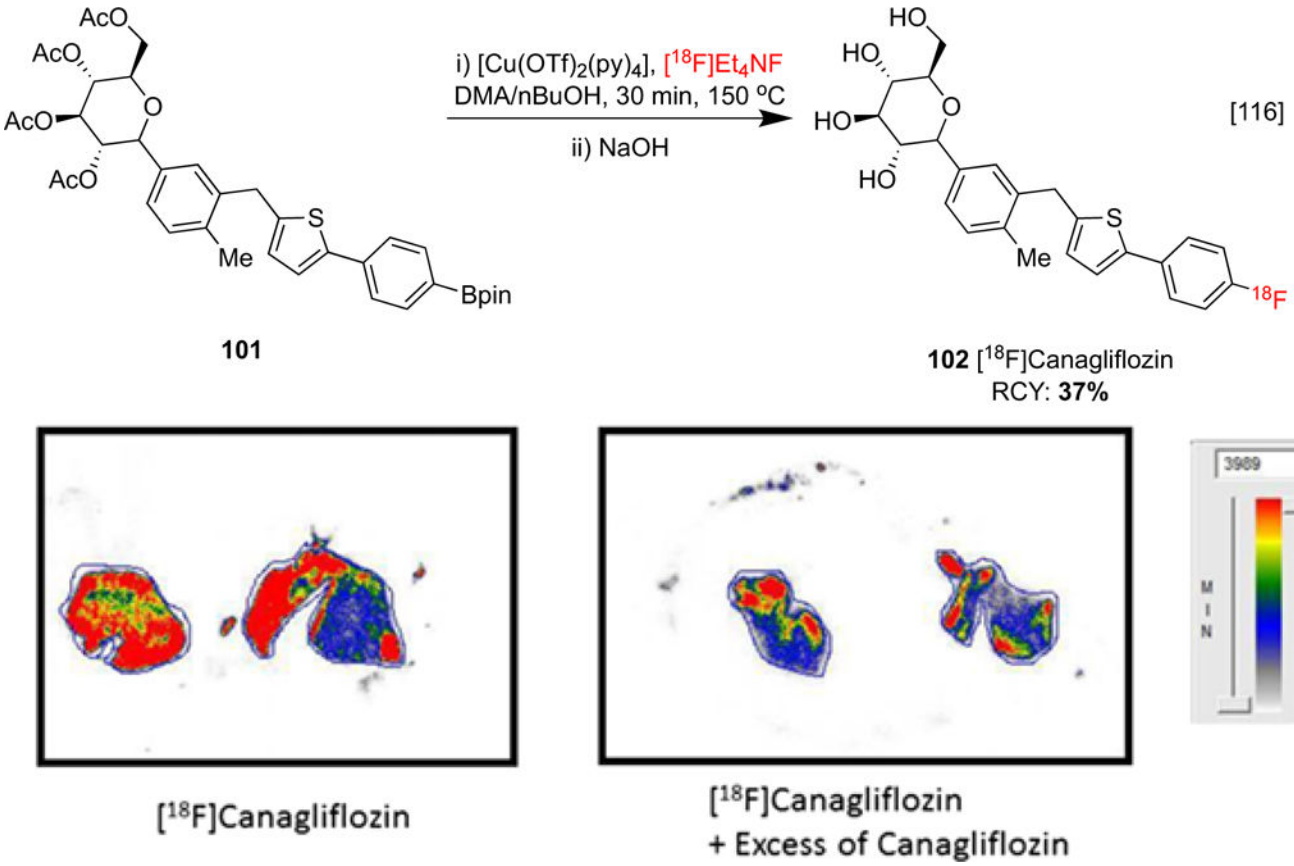

Scheme 24:

Radiosynthesis and ARG of [^{18}F]canagliflozin in a human liver. ARG images republished from reference 116 with permission from John Wiley & Sons.

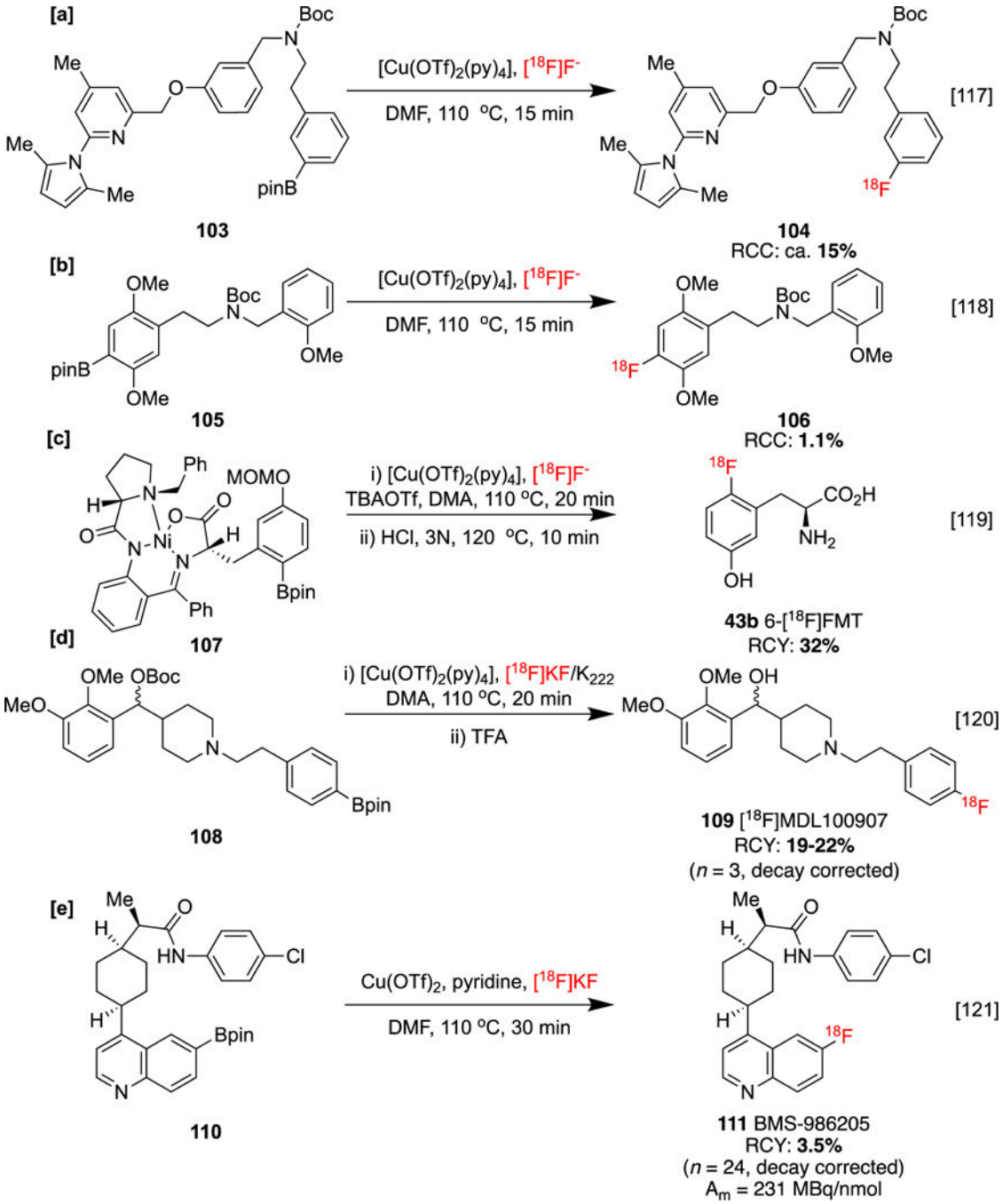

Scheme 25:

Radiosyntheses of other clinically relevant fluorine-18 labelled molecules via CMRF of organoborons.

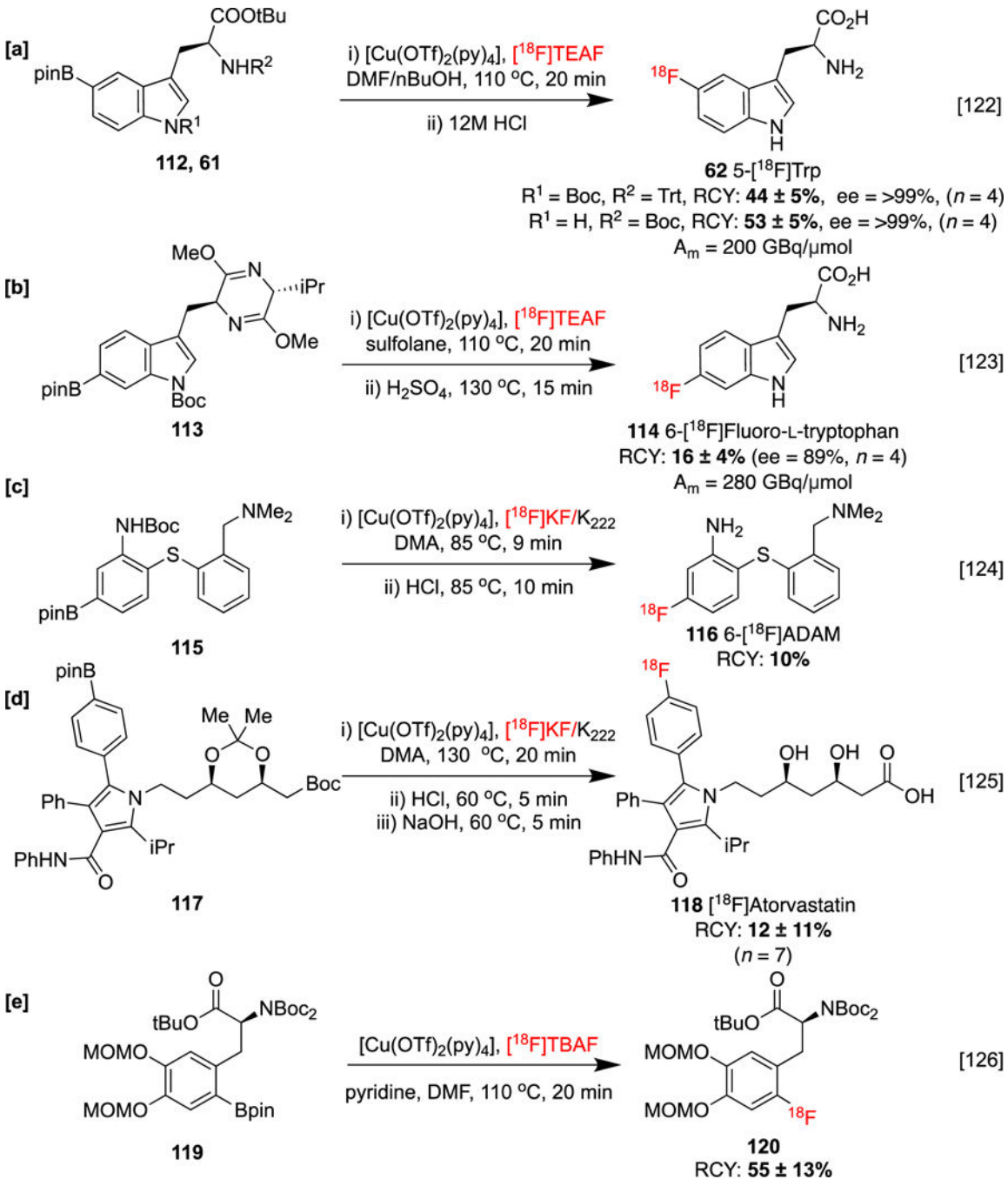

Scheme 26:

Radiosyntheses of other clinically relevant fluorine-18 labelled molecules via CMRF of organoborons.

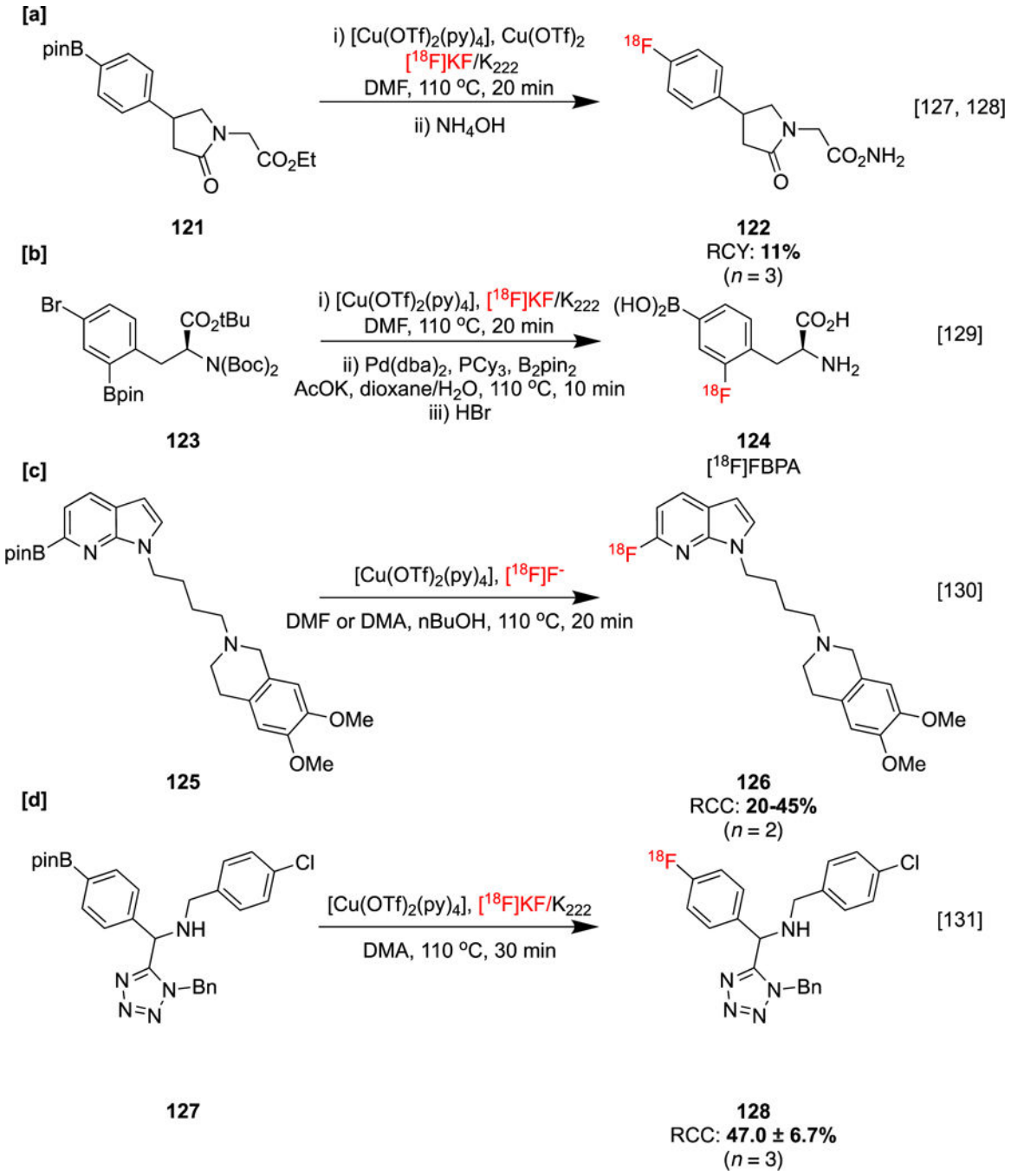

Scheme 27:

Radiosyntheses of other clinically relevant fluorine-18 labelled molecules via CMRF of organoborons.

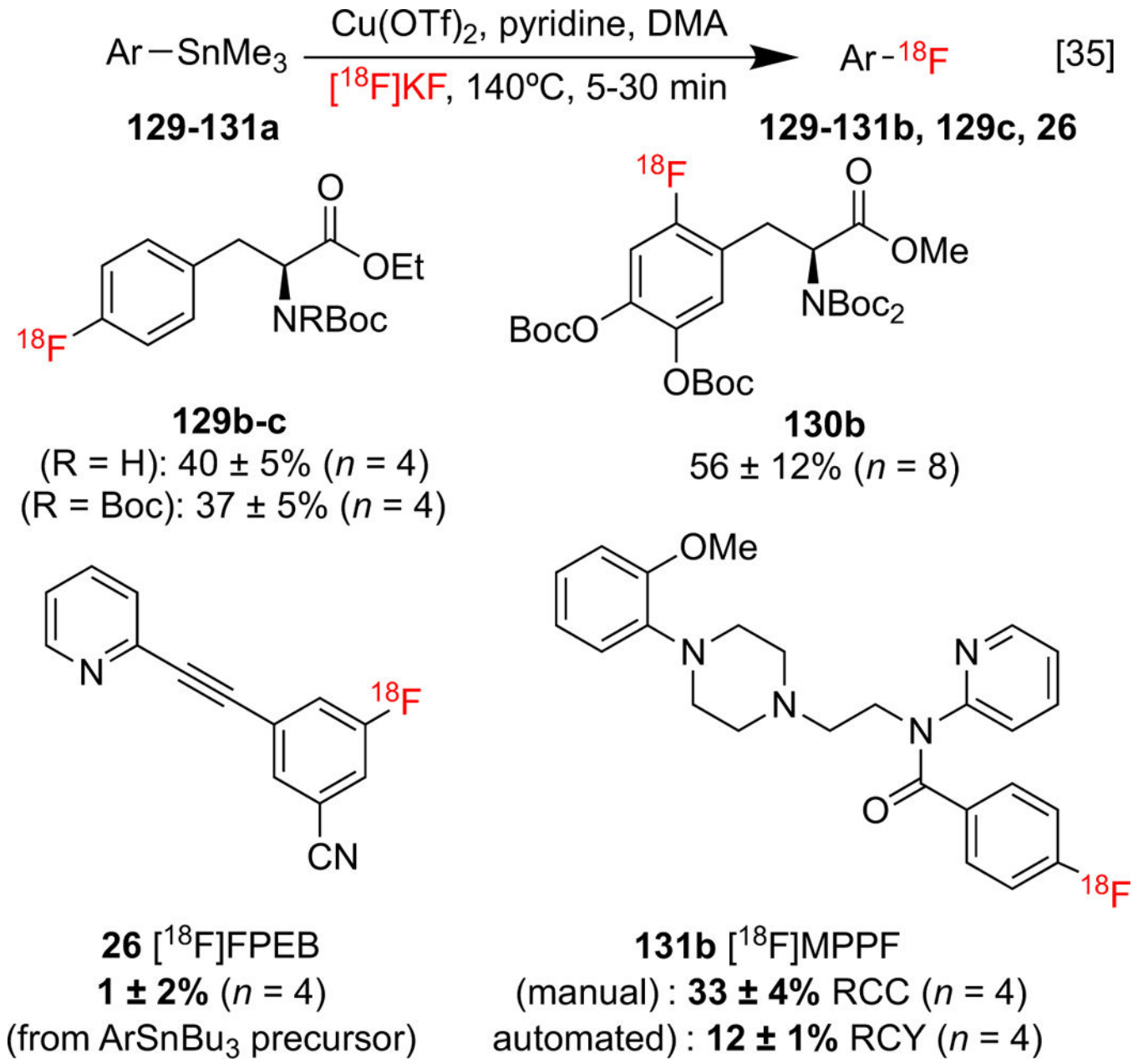

Scheme 28:
CMRF of arylstannanes for the synthesis of clinically relevant imaging agents.

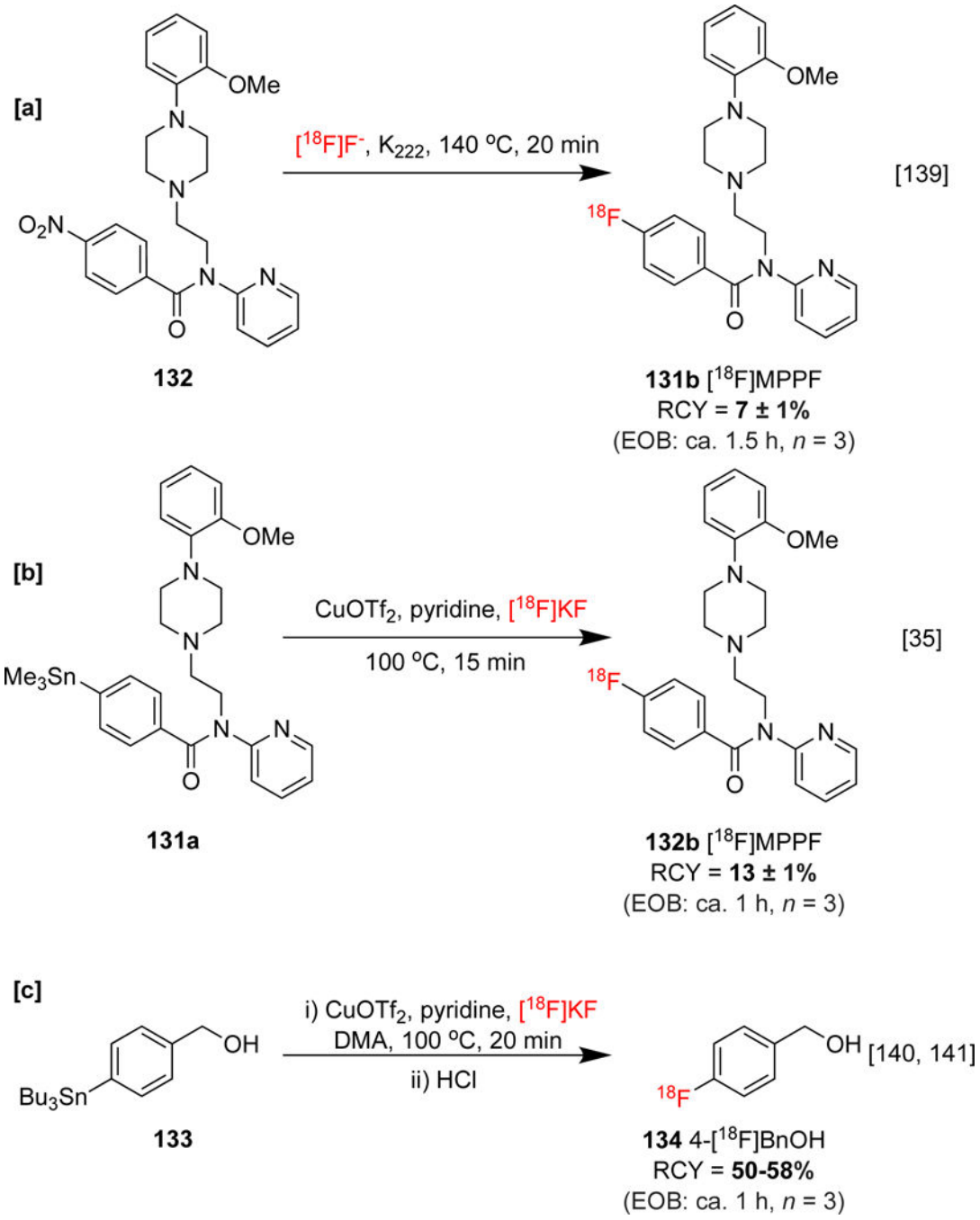

Scheme 29:

[a] [b] Radiosyntheses of [^{18}F]MPPF and **[c]** 4-[^{18}F]Fluorobenzylalcohol.

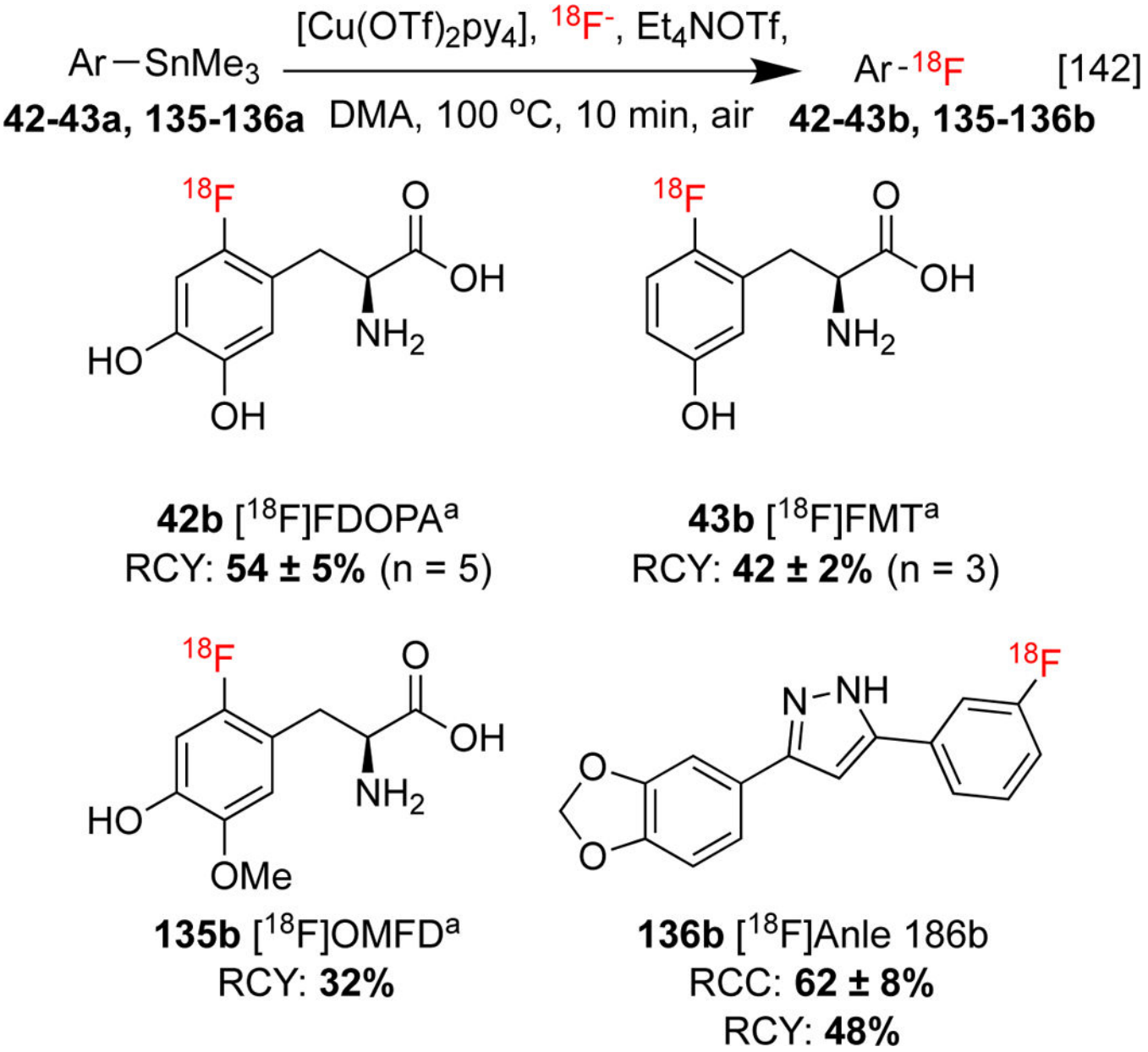

Scheme 30:

Modified radiofluorodestannylation protocol.

a From protected precursor, RCY reported over two (radiofluorination and HBr deprotection) steps

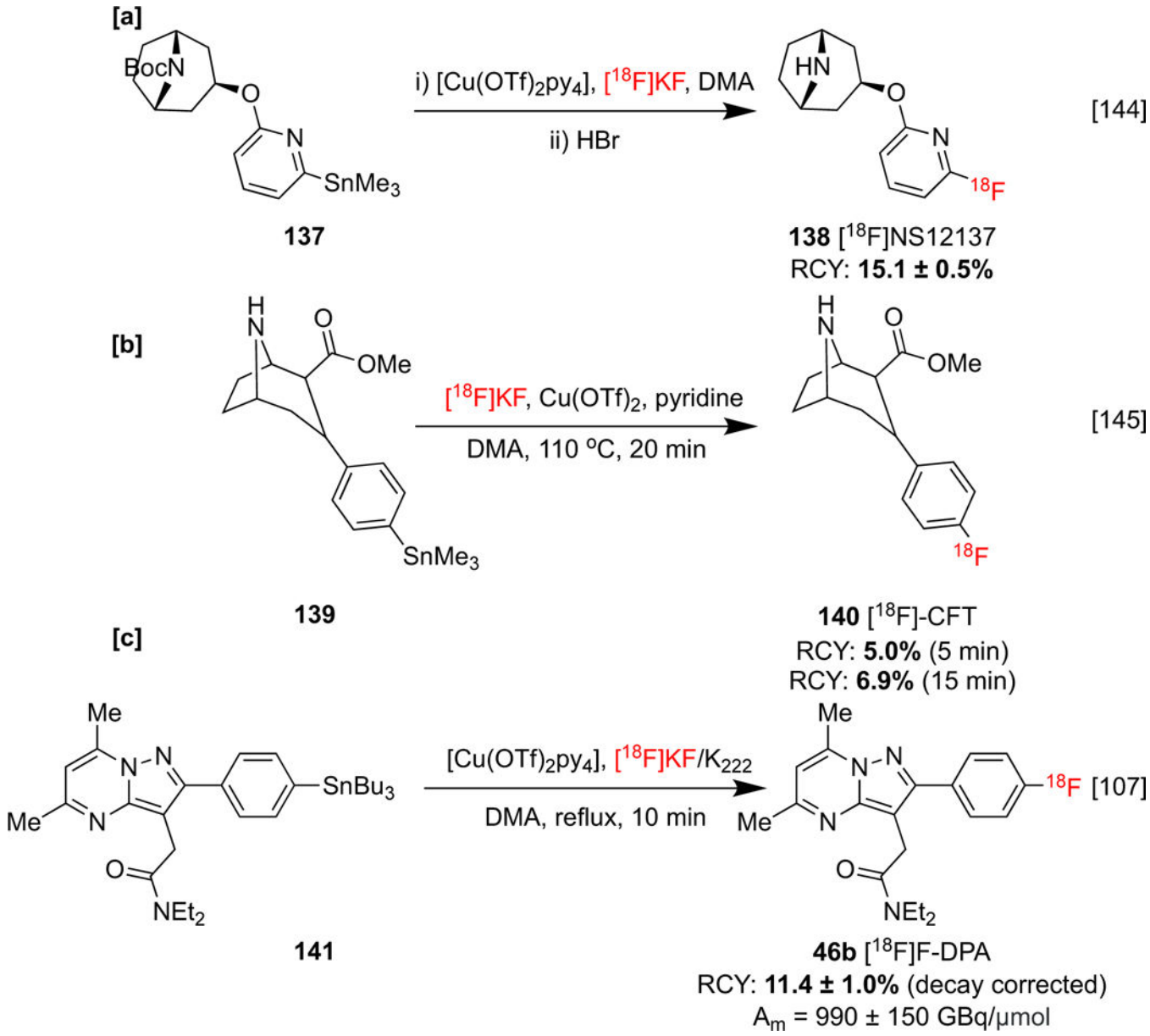

Scheme 31:

[b] Radiosynthesis of ^{18}F]NS12137 **[a]**, [^{18}F]-CFT **[b]** and [^{18}F]F-DPA **[c]**.

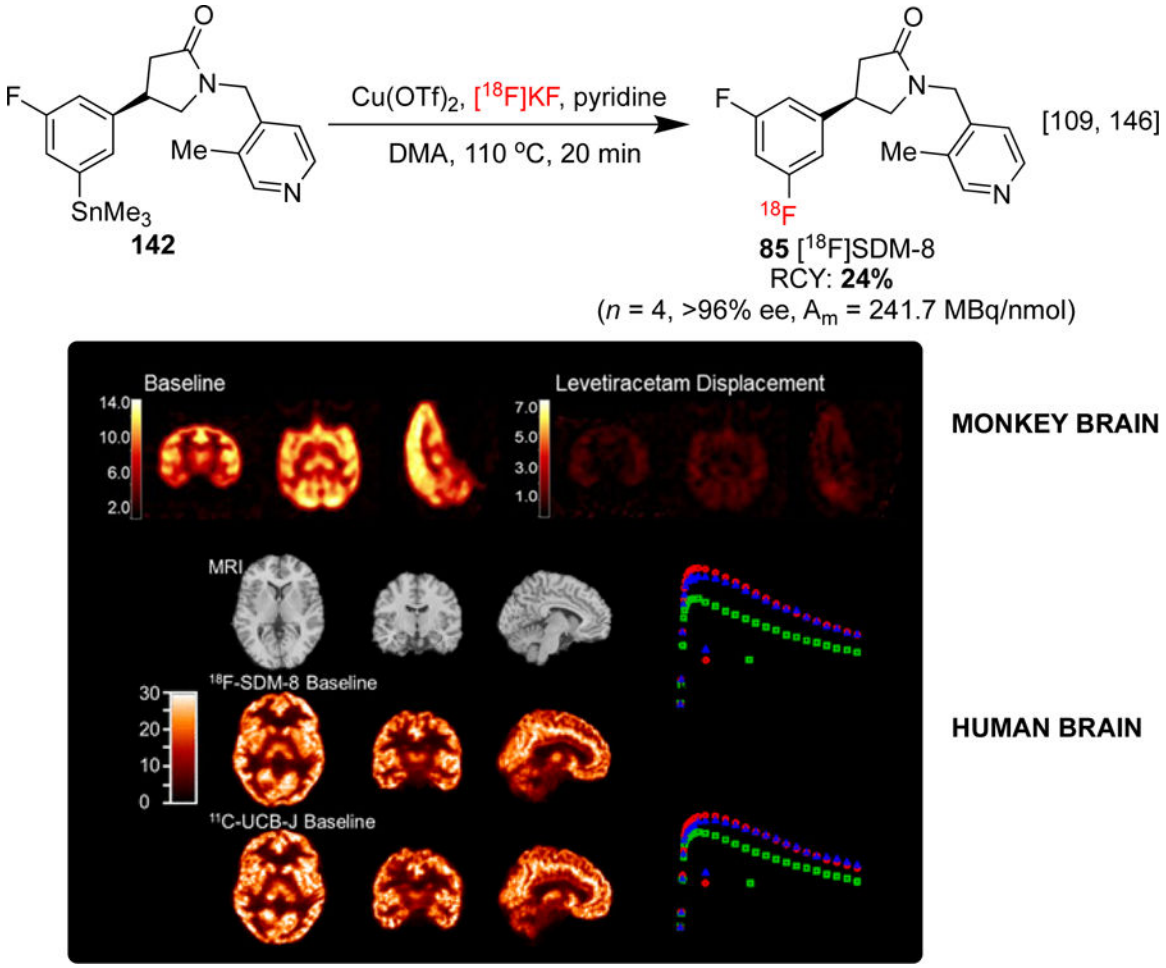

Scheme 32:

Radiosyntheses and preclinical evaluations of [^{18}F]-SDM-8. Summed PET SUV images in NHP brain depicting baseline and LEV displacement (30 mg/kg) scans (Above) MRI and PET images in a human brain depicting uptake of **85** and [^{11}C]UCB-J (Below) Images republished from references 109 and 146, with permission from the ACS and SNMMI, respectively.

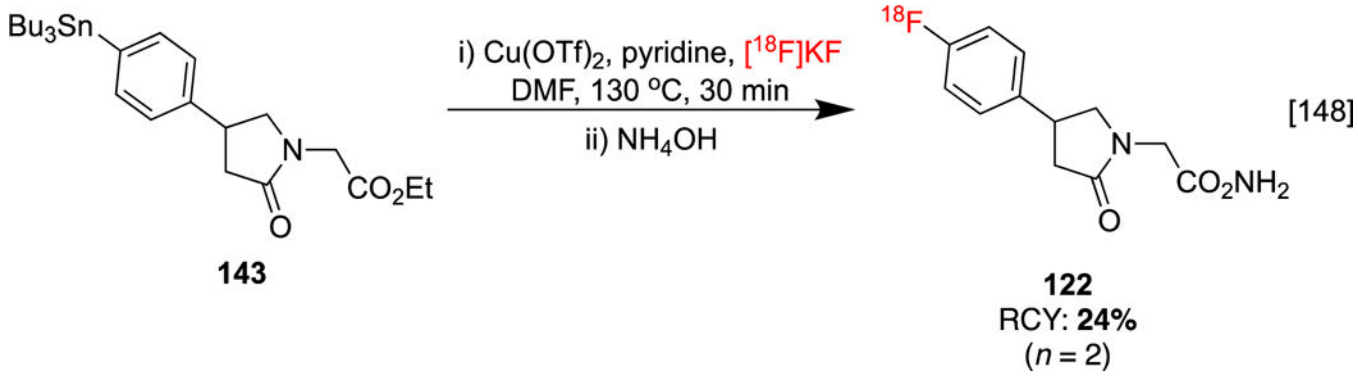

Scheme 33:
Improved radiosynthesis of 4(4-[^{18}F]fluorophenyl)piracetam.

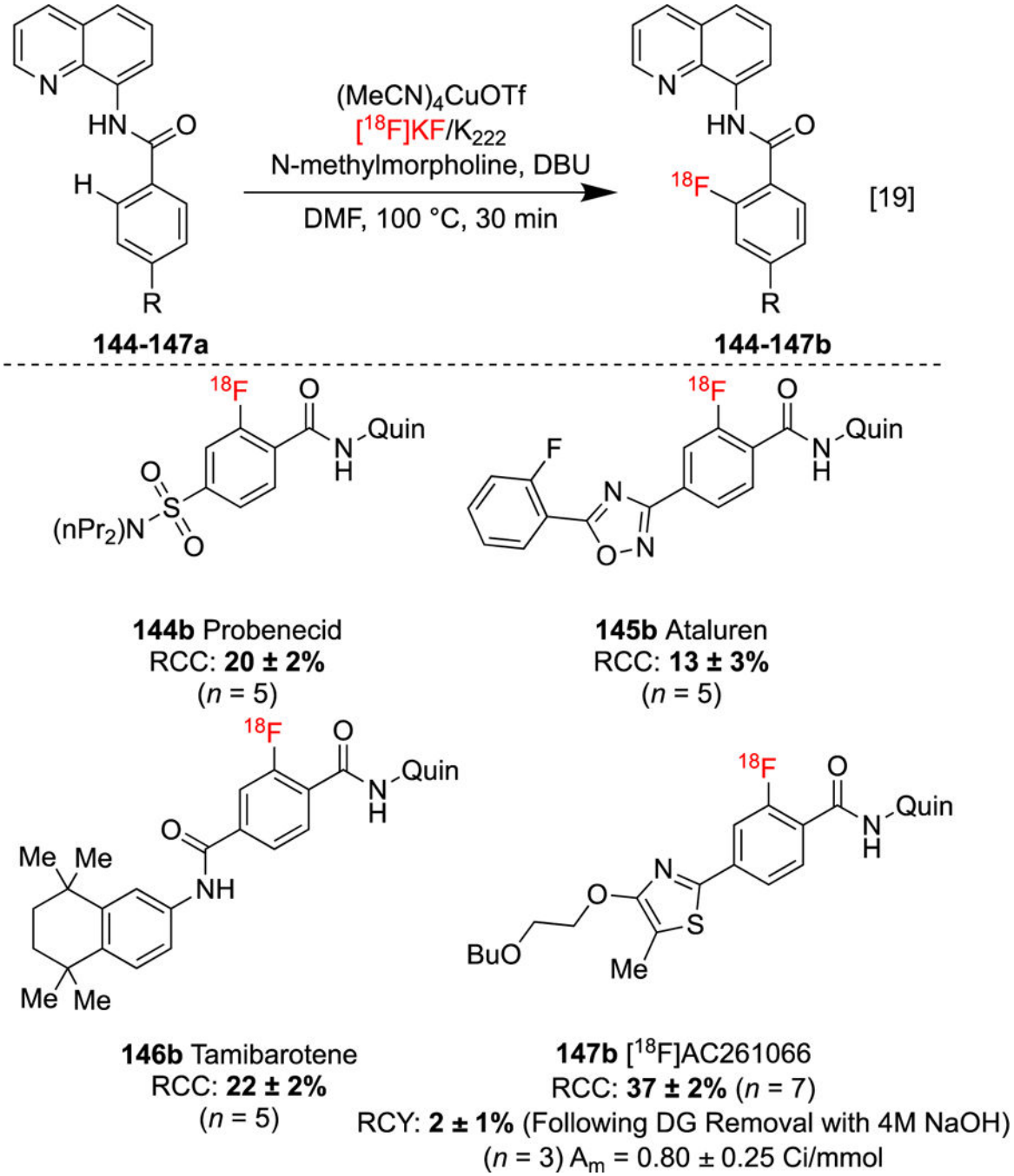

Scheme 34:
CMRF of aromatic C-H bonds.

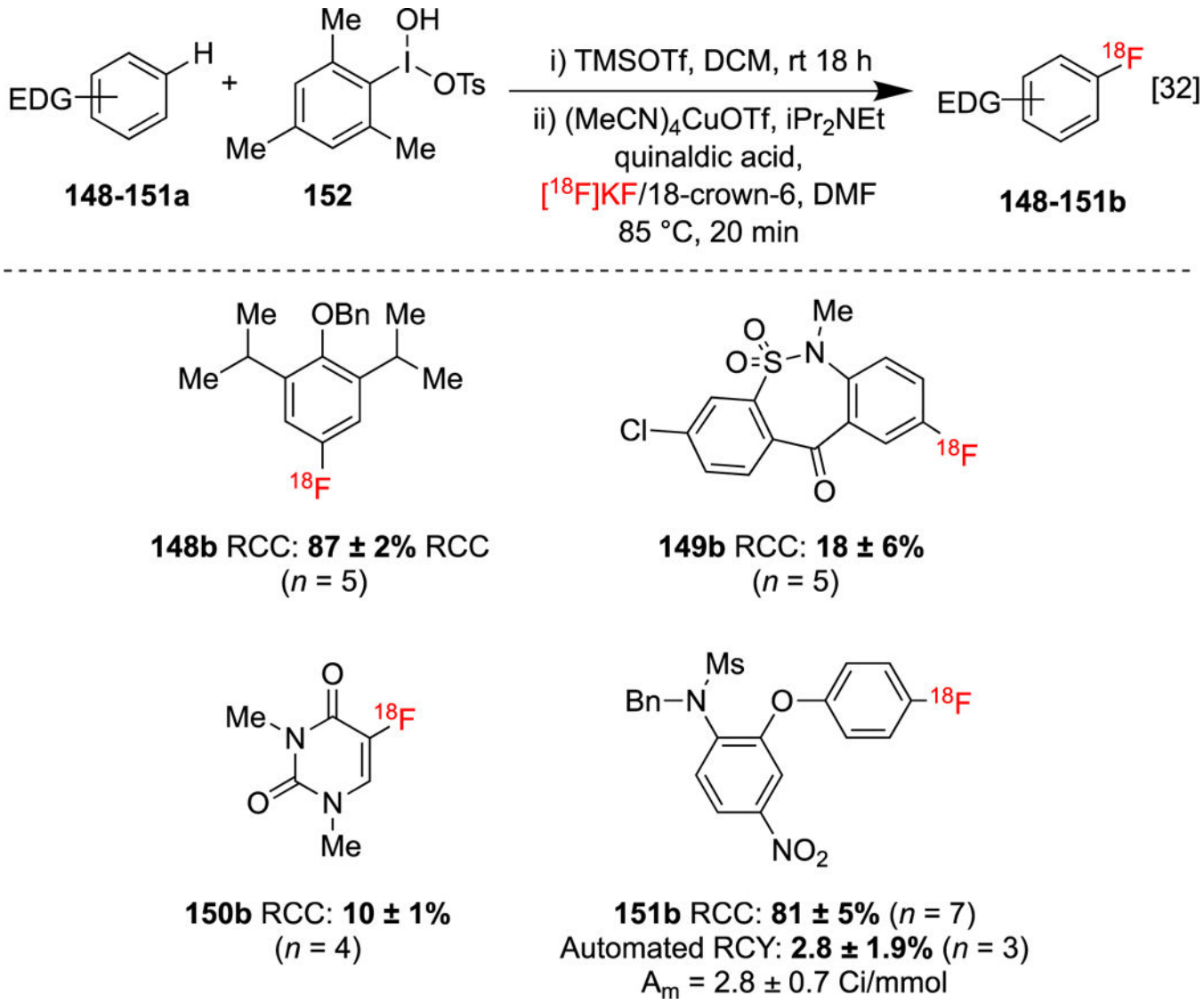

Scheme 35:
C-H radiofluorination using a hypervalent iodine reagent.